72-17,172

SEARS, Alan Roy, 1942-
ADSORPTION AT THE MERCURY-AQUEOUS SOLUTION
ELECTRICAL DOUBLE LAYER.

Yale University, Ph.D., 1971
Chemistry, physical

University Microfilms, A XEROX Company, Ann Arbor, Michigan

ADSORPTION AT THE MERCURY-AQUEOUS SOLUTION ELECTRICAL DOUBLE LAYER

Alan R. Sears

A Dissertation Presented to the Faculty
of the Graduate School of Yale University
in Candidacy for the Degree of
Doctor of Philosophy
1971

SUMMARY

The adsorption of KBr from xMKBr + (1-x)MKF and of xM6-amino-hexanoic + .5MKF at the mercury aqueous solution interface has been investigated. The necessary data were obtained by determining the differential capacity curve, the streaming electrode potential and the surface tension at the point of zero charge. The adsorption of KBr from KBr + KF has been shown to be similar to KCl from KCl + KF if the data in the same range of specifically adsorbed charge are compared. The results at larger values of specifically adsorbed charge have not previously been observed for halide systems. They can be explained by assuming a standard free energy with both linear and quadratic terms and variable isotherm parameters. The bromide and chloride results imply that the simpler picture for the iodide ion is due to the limited range of surface charge which has been studied. Within the range of surface charge available, 6 amino-hexanoic acid is maximally adsorbed when the surface charge density is -6, with a quadratic standard free energy of adsorption. The expectation that this system would show some of the characteristics of ionic adsorption proved to be incorrect. The quadratic standard free energy, which implies the adsorption of a point dipole, indicates that in this system adsorption should be considered to occur in the entire double layer rather than only in the inner layer. This assumption is necessitated by the dipole being significantly larger than the inner layer.

Glossary

The symbols occurring below are those which frequently are used in the text.

γ	surface tension
Γ_X	surface excess of X in Gibbs model
$\Gamma_{X,w}$	relative surface excess of X
Γ^d	surface concentration in the diffuse layer
Γ^i	surface concentration in the inner layer.
q, q^M	surface charge density on mercury
q^s	surface charge density in solution
q^d	surface charge density in diffuse layer
q^1	surface charge density of specifically adsorbed ions
$E^{\pm}$	potential of cell against a reversible electrode
E, E_{ref}	potential of cell against a reference electrode
Ez	potential of cell at the point of zero charge
ϕ^m	potential in the mercury electrode
ϕ^1	potential at the inner Helmholz layer
ϕ^2	potential at the outer Helmholz layer
ϕ^{m-2}	potential drop across the inner layer

C	capacity of the double layer
C^d	capacity of the diffuse layer
C^i	capacity of the inner layer
${}_{q}C^{i}$	differential capacity at constant amount adsorbed.
${}_{q}^{1}C^{i}$	differential capacity at constant charge
${}_{q}K^{i}$	integral capacity at constant amount adsorbed
${}_{q}^{1}K^{i}$	integral capacity at constant charge
X_1	position of the inner Helmholz layer
X_2	position of the outer Helmholz layer
ξ	$\xi = \gamma + qE$
E^b	value of E for base solution
C^b	value of C for base solution
ξ^b	value of ξ for base solution
$\Delta \frac{1}{C}$	$\frac{1}{C} - \frac{1}{C^b}$
ΔE	$E - E^b$
Φ	$\xi - \xi^b$ surface pressure
δ	$q - q_{max}$

TABLE OF CONTENTS

I. THEORY OF THE ELECTRICAL DOUBLE LAYER

The region of the electrode solution interface is known as the electrical double layer. The generally accepted model of this interface consists of the metallic phase, the compact or inner layer and the diffuse layer as is shown in Figure 1. The compact layer is divided into two parts. The inner Helmholz plane is the plane of closest approach of specifically adsorbed ions. An ion is specifically adsorbed if its adsorption can not be explained by diffuse layer theory. All adsorption of neutral molecules is therefore specific adsorption. The outer Helmholz plane is the plane of closest approach of completely solvated ions. The diffuse layer begins at the outer Helmholz plane and extends into the solution until the solution has its bulk concentration. The thermodynamic theory does not depend on the above model, but only on the existence of an interface and the absence of charge transfer across the interface. The Gouy-Chapman-Stern theory presupposes the model used and is applicable only to the diffuse layer. The thermodynamic derivation and that of the Guoy-Chapman-Stern theory are classical. The most complete discussion of both may be found in Mohilner's article.[1] The entire theory of the double layer is also discussed by Delahay.[2] The material discussed in Sections C and D is based on a method of analysis developed by Grahame and Parsons over the last twenty years. No single source is available in which the complete theory of the double layer is presented. A careful review of the theory was therefore considered advisable.

A. The Thermodynamic Derivation of the Electrocapillary Equation

The system which I will first describe is represented by the

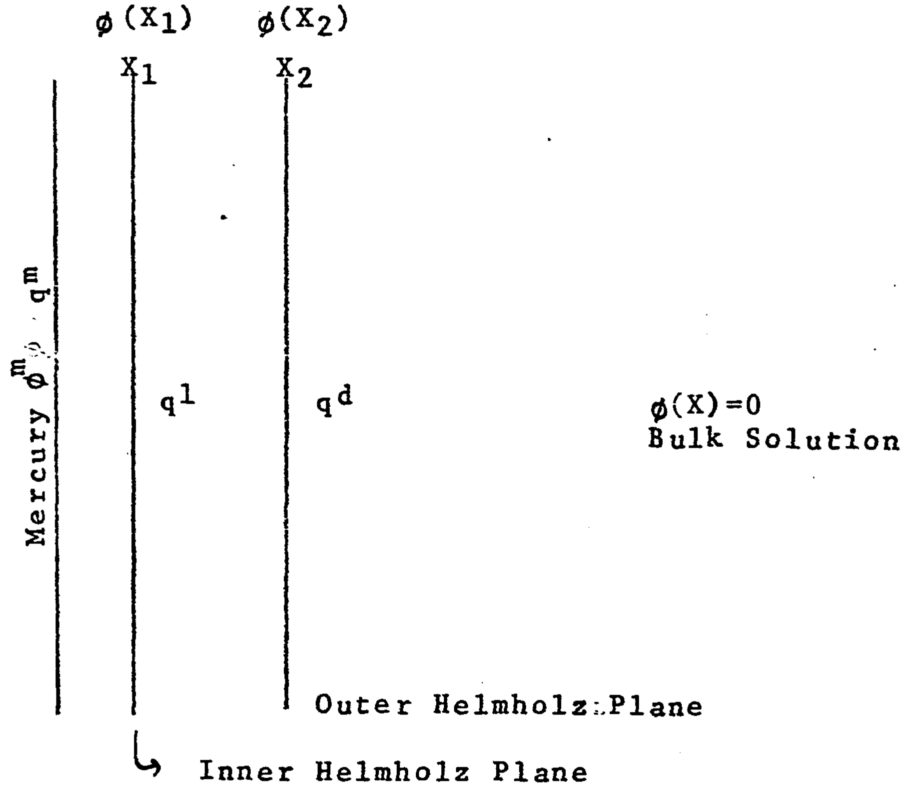

Figure 1. A Schematic Representation of The Electrical Double Layer

following cell:

$$Cu^2|In|KBr,KF,H_2O|Hg|Cu^1$$

The electrode In is a hypothetical K^+ reversible electrode in contact with the solution. A Br^- or F^- reversible electrode could also be used in the derivation. It will later be shown that a constant potential electrode may always be used instead of a reversible electrode. We assume that if a potential is imposed across the cell, equilibrium is reached, and that no charge transfer occurs across the interface. We then get the Gibbs absorption equation for this system:

$$d\gamma = - \Gamma_e d\bar{\mu}_e - \Gamma_{Hg^{+2}} d\bar{\mu}_{Hg^{+2}} - \Gamma_{K^+} d\bar{\mu}_{K^+} - \Gamma_{F^-} d\bar{\mu}_{F^-}$$

$$- \Gamma_{Br^-} d\bar{\mu}_{Br^-} - \Gamma_{H_2O} d\mu_{H_2O}$$

The μ are the electrochemical potentials in either mercury or the solution. The Γ are the surface excesses per unit area and will depend on the choice of the Gibbs plane. γ is the surface tension. In the metallic phase

$$\mu_{Hg} = \bar{\mu}_{Hg+2} + 2\bar{\mu}_{e^-}$$

and

$$\bar{\mu}_{e^-}^{Hg} = \bar{\mu}_{e^-}^{Cu^1}$$

therefore

$$- \Gamma_e d\bar{\mu}_e^{Hg} - \Gamma_{Hg+2} d\bar{\mu}_{Hg+2} = - (\Gamma_e - 2\Gamma_{Hg+2}) d\bar{\mu}_e^{Cu^1}$$

$$- \Gamma_{Hg+2} d\mu_{Hg}$$

Let q^M be the charge per unit area on the metal surface and $d\mu_{Hg} = 0$ since we are restricting ourselves to constant T and P.

$$q^M = - F(\Gamma_{e^-} - 2\Gamma_{Hg^{+2}})$$

and

$$d\gamma = \frac{q^M}{F} d\bar{\mu}_{e^-}^{Cu^1} - \Gamma_{K^+} d\bar{\mu}_{K^+} - \Gamma_{Br} - d\bar{\mu}_{Br^-}$$

$$- \Gamma_{F^-} d\bar{\mu}_{F^-} - \Gamma_{Br^-} d\bar{\mu}_{Br^-} - \Gamma_{H_2O} d\mu_{H_2O}$$

also

$$\mu_{KF} = \bar{\mu}_{K^+} + \bar{\mu}_{F^-}$$

$$\mu_{KBr} = \bar{\mu}_{K^+} + \bar{\mu}_{Br^-}$$

therefore

$$- \Gamma_{K^+} d\bar{\mu}_{K^+} - \Gamma_{F^-} d\bar{\mu}_{F^-} - \Gamma_{Br^-} d\bar{\mu}_{Br^-} =$$

$$-(\Gamma_{K^+} - \Gamma_{F^-} - \Gamma_{Br^-}) d\bar{\mu}_{K^+} - \Gamma_{F^-} d\mu_{KF} - \Gamma_{Br^-} d\mu_{KBr}$$

Let q^S be the charge per unit area in the solution:

$$q^S = F(\Gamma_{K^+} - \Gamma_{F^-} - \Gamma_{Br^-})$$

therefore

$$d\gamma = \frac{q^M}{F} d\bar{\mu}_{e}^{Cu^1} - \frac{q^S}{F} d\bar{\mu}_{K^+} - \Gamma_{F^-} d\mu_{KF}$$

$$- \Gamma_{Br^-} d\mu_{KBr} - \Gamma_{H_2O} d\mu_{H_2O}$$

The indicator electrode is reversible to the K^+ ion.

therefore

$$\bar{\mu}_{K^+}^{In} + \bar{\mu}_{e^-}^{In} = \mu_K$$

and

$$d\bar{\mu}_{e^-}^{In} = d\bar{\mu}_{K^+}^{In}$$

also

$$d\bar{\mu}_{K^+}^{In} = d\bar{\mu}_{K^+} \text{ (solution)}$$

$$d\bar{\mu}_{e^-}^{In} = d\bar{\mu}_{e^-}^{Cu^2}$$

and

$$q^M = - q^S$$

to preserve electroneutrality. Therefore

$$\frac{q^M}{F} d\bar{\mu}_e^{Cu^1} - \frac{q^S}{F} d\bar{\mu}_{K^+} = + \frac{q^M}{F} d(\bar{\mu}_e^{Cu^1} - \bar{\mu}_e^{Cu^2})$$

but

$$\bar{\mu}_e^{Cu^1} = \mu_e - F\phi^{Cu^1}$$

$$\bar{\mu}_e^{Cu^2} = \mu_e - F\phi^{Cu^2}$$

therefore

$$\frac{q^M}{F} d(\bar{\mu}_e^{Cu^1} - \bar{\mu}_e^{Cu^2}) = - q^M d(\phi^{Cu^1} - \phi^{Cu^2})$$

$$= - q^M dE^+$$

where E^+ is the potential of the cell with a cation reversible indicator electrode. The symbol q will now be used in place of q^M to designate the surface charge per unit area on the mercury surface.

We now have:

$$d\gamma = -\,qdE^{+} - \Gamma_{Br^-}d\mu_{KBr} - \Gamma_{F^-}d\mu_{KF} - \Gamma_{H_2O}d\mu_{H_2O}$$

The Gibbs-Duhem gives us

$$d\mu_{H_2O} = -\frac{x_{KBr}}{x_{H_2O}}\,d\mu_{KBr} - \frac{x_{KF}}{x_{H_2O}}\,d\mu_{KF}$$

therefore

$$d\gamma = -\,qdE^{+} - \left(\Gamma_{Br^-} - \frac{x_{KBr}}{x_{H_2O}}\,\Gamma_{H_2O}\right) d\mu_{KBr}$$
$$- \left(\Gamma_{F^-} - \frac{x_{KF}}{x_{H_2O}}\,\Gamma_{H_2O}\right) d\mu_{KF}$$

or

$$d\gamma = -\,qdE^{+} - \Gamma_{F^-,w}d\mu_{KF} - \Gamma_{Br^-,w}d\mu_{KBr}$$

The quantities $\Gamma_{F^-,w}$, $\Gamma_{Br^-,w}$ are called the relative surface excesses. They are the experimentally determined surface excesses and are independent of the position of the Gibbs surface. If we had used a fluoride reversible indicator electrode, we would get the equation:

$$d\gamma = -\,qdE^{-} - \Gamma_{K^+,w}d\mu_{KF} - \Gamma_{Br^-,w}d\mu_{KBr}$$

If neutral molecules were present, terms such as $-\Gamma_{N,w}d\mu_N$ must be added. The procedure could also be extended to include amalgam electrodes.

In interpreting a system we are actually interested in the quantities Γ^{OHP}, Γ^{d}, Γ^{i}. Γ^{OHP} is the surface excesses calculated at the outer Helmholz plane. Γ^{d} is that part of the surface excess which is in the diffuse layer. Γ^{i} is the surface concentration of specifically absorbed ions. As will be further discussed, compelling evidence indicates that KF is not specifically adsorbed, but is present only in the diffuse layer. $\Gamma_{K^+}^{OHP}$ and $\Gamma_{K^+}^{d}$ are equal and can be used to evaluate diffuse. layer parameters. To use this approach one must assume that $\Gamma_{F^-,w} = \Gamma_{F^-}^{OHP}$ which is equivalent to $\frac{x_{KF}}{x_{H_2O}} \Gamma_{H_2O}$ being negligible. The same situation arises in determining Γ^{i}. This approximation is only valid at low concentrations (1M and below).[3]

As was mentioned earlier, the use of a reversible electrode is not necessary. If a reference electrode, for example a calomel electrode,is used instead, the potential can be written:

$$E_{ref} = E_{Hg} - E_{cal}$$

$$E^{+} = E_{Hg} - E_{In}$$

therefore

$$E_{ref} = E^{+} + E_{In} - E_{cal}$$

For a K^+ reversible half cell E_{In}

$$K^{+} + 1e^{-} \rightarrow K$$

$$E_{In} = E^{o} + \frac{RT}{F} \ln a_{K^+}$$

therefore

$$E_{ref} = E^{+} + \frac{RT}{F} \ln a_{K^+} + \text{constant}$$

In evaluating data, only dE^{+} is used. If an experiment is run in which a_{K^+} varies, one simply calculates E^{+} from the above equation. The only questionable but necessary practice is using $a_{\pm}$ for a_{K^+}.

The general form for any system will be $d\gamma = - qdE - \Gamma_{x,w}d\mu_{MX} - \Gamma_{N,w}d\mu_N$ where MX is a salt and N a neutral molecule. The second derivative of γ, C

$$C = \left(\frac{\partial q}{\partial E}\right)_\mu = -\left(\frac{\partial^2 \gamma}{\partial E^2}\right)_\mu$$

is an experimentally available quantity known as the differential capacity. If C is measured as a function of E at constant μ, the integration of the C - E curves will give γ and q. Two integration constants are needed and can be obtained either directly or from the base solution values in a region where there is no specific absorption. The directly available constants are Ez, the potential at which $q = 0$, which is obtained by use of the streaming electrode and γ at Ez which is obtained by using the capillary electrometer. It then follows that

$$q = \int_{Ez}^{E} CdE$$

$$\gamma - \gamma(Ez) = - \int_{Ez}^{E} \int_{Ez}^{E} CdEdE$$

If alternatively, the curves of C versus E are identical in a given region for two solutions of the same ionic strength in neither of which specific absorption occurs in that region, the values of C, q, E, and γ at a point in this region for one solution may be used to integrate the other solution. To check this procedure, one compares the back integrated value of Ez to the streaming electrode value.

Let us assume that the curve has been integrated such that values of γ and E are known at integral values of q. We now define the function of $\xi = \gamma + qE$ which is a Legendre transformation of γ.

$$d\xi = Edq - \Gamma d\mu$$

If values of ξ at constant q are differentiated with respect to μ, Γ is obtained. Γ could also be found from the derivative of γ by μ at constant E. The choice depends on whether you wish to further evaluate your data at constant q or constant E. The surface charge density q is directly related to the field in the interface. The potential difference across the cell E is a more complicated quantity. The choice of constant q is both intuitively satisfactory and leads to a somewhat easier analysis. Theoretical and experimental attempts to resolve this problem have been inconclusive.[4,5]

B. The Gouy-Chapman-Stern Theory of the Diffuse Double Layer

The G.C.S. theory deals only with the diffuse layer. We assume that the closest approach of an ion to the mercury surface is the outer Helmholz plane, X_2. One assumes that the concentration at a distance X from the electrode surface is given by

$$C_i(X) = C_i^b \exp\left(-\frac{Z_i F \phi(X)}{RT}\right)$$

where Z_i is the charge, $\phi(X)$ the potential at X, and C_i^b the bulk concentration. In the equations below $\rho(X)$ is the charge density, $\vec{D}$ the displacement vector and $\vec{E}$ the electric field vector. It then follows from standard electromagnetic theory that

$$\nabla \cdot \vec{D} = \rho$$

$$\vec{D} = \epsilon\vec{E} = -\epsilon\nabla\phi$$

$$\nabla \cdot \epsilon\nabla\phi = -\rho(X)$$

$$\nabla^2\phi = -\frac{\rho(X)}{\epsilon}$$

or

$$\frac{d^2\phi(X)}{dX^2} = -\frac{1}{\epsilon}\sum_i z_i F C_i^{\,b} \exp\left(-\frac{z_i F\phi(X)}{RT}\right)$$

if ϕ is a function of X only and ϵ is a constant. We now multiply both sides by $2\frac{d\phi(x)}{dX}$.

$$2\frac{d\phi}{dX}\frac{d^2\phi}{dX^2} = \frac{d}{dX}\left(\frac{d\phi}{dX}\right)^2 = -\frac{2}{\epsilon}\sum_i z_i F C_i^{\,b}\frac{d\phi}{dX}\exp\left(\frac{-Z_i F\phi(X)}{RT}\right)$$

We now integrate and get the constant of integration from the fact that $\frac{d\phi(X)}{dX}$ goes to zero as X goes to infinity.

$$\left(\frac{d\phi}{dX}\right)^2 = \left(\frac{2RT}{\epsilon}\right)\sum_i C_i^{\,b}\left[\exp\left(\frac{-z_i F\phi}{RT} - 1\right)\right]$$

$$\vec{E} = -\frac{d\phi}{dX}\,\hat{i} = \pm\left(\frac{2RT}{\epsilon}\right)^{\frac{1}{2}}\left(\sum_i C_i^{\,b}\left[\exp - \frac{z_i F\phi}{RT} - 1\right]\right)^{\frac{1}{2}}\hat{i}$$

Let X_2 be the position of the outer Helmholz plane.

$$E(X_2) = -\left.\frac{d\phi(X)}{dX}\right|_{X=X_2}$$

and

$$D(X_2) = q^M + q^1$$

where q^M is the charge density on the metal and q^1 is the charge density of the specifically absorbed species. Therefore

$$q^M + q^1 = \pm (2RT\epsilon)^{\frac{1}{2}} \left(\Sigma C_i^b\left[\exp - \frac{z_iF\phi}{RT} - 1\right]\right)^{\frac{1}{2}}$$

For a 1-1 electrolyte or for a mixture of 1-1 electrolytes with one ion in common at constant ionic strength.

$$q^M + q^1 = (8RT\epsilon C^b)^{\frac{1}{2}} \sinh \frac{|z|F\phi^2}{2RT}$$

Since q^M and q^1 are experimentally available, the capacity due to the diffuse layer is easily found.

$$C^d = \frac{\partial\phi^2}{\partial(q^M+q^1)} = \left(\frac{2|z|^2F^2\epsilon C^b}{RT}\right)^{\frac{1}{2}} \cosh\left(\frac{F\phi^2}{2RT}\right)$$

also

$$\phi^2 = \frac{2RT}{|z|F} \ln \left\{\left(\frac{q^M+q^1}{2A}\right) + \left[\left(\frac{q^M+q^1}{2A}\right)^2 + 1\right]^{\frac{1}{2}}\right\}$$

where $A = (2RT\epsilon C^b)^{1/2}$ and ϕ^2 is the potential at the outer Helmholz plane. The surface excess due to the diffuse layer which is equivalent to the surface excess with the Gibbs surface at the outer Helmholz plane is given by

$$\Gamma_i^d = C_i^b \int_{X_2}^{\infty} \left[\exp\left(- \frac{z_iF\phi(X)}{RT}\right) - 1\right] dx$$

and for a 1-1 electrolyte

$$\Gamma_+^d = \frac{A}{|z|F} \left(\exp\left(- \frac{|z|F\phi^2}{2RT}\right) -1\right)$$

$$\Gamma_-^d = \frac{A}{|z|F} \left(\exp\left(\frac{|z|F\phi^2}{2RT}\right) -1\right)$$

$$q_+^d = |z|F\,\Gamma_+^d \quad \text{and} \quad q_-^d = |z|F\,\Gamma_-^d$$

The general approach when dealing with absorption from a single salt solution is to find $\Gamma_{+,w}$ from $\left(\frac{\partial\xi}{\partial\mu}\right)_q$. Unless the cation is one of the few which is absorbed, q_+ can be completely assigned to the diffuse layer. Using the equation for q_+^d, one finds ϕ^2 and from it q_-^d. The amount of specifically adsorbed anion q^1 then follows from

$$q^M = -q^S = -(q^1 + q_-^d + q_+^d)$$

It has already been pointed out that at high concentrations an error can result from equating $\Gamma_{+,w}$ to Γ_+^{OHP}. Another source of error arises when there is weak specific adsorption. At positive surface charges Γ_+ has the limiting value of -A, but ϕ^2 goes to infinity. It follows that a small error in $\Gamma_{+,w}$ when $\Gamma_{+,w} \approx -A$ will cause a large error in ϕ^2. This makes the calculation of q_-^d and q^1 suspect when $\Gamma_{+,w}$ is near -A.[6]

C. The Components of the Capacity

1. No specific absorption

The potential drop across the cell with or without specific absorption may be written

$$E = (\phi^M - \phi^2) + \phi^2 - \phi^{ref}$$

In the absence of specific adsorption, ϕ^2 is a function of q only at constant μ. Therefore

$$\left(\frac{\partial E}{\partial q}\right)_\mu = \left(\frac{\partial(\phi^M - \phi^2)}{\partial q}\right)_\mu + \left(\frac{\partial\phi^2}{\partial q}\right)_\mu$$

or

$$\frac{1}{C} = \frac{1}{C^i} + \frac{1}{C^d}$$

C^i, which is the capacity of the inner layer, may be obtained from measured values of C and computed values of C^d. With fluoride salts of unadsorbed cations C^i, Figure 2, is a function of charge only. The total capacity measured for any concentration, and that calculated using C^i values measured at another concentration and computed C^d values are in agreement.[7] Furthermore, plots of $\frac{1}{C}$ versus $\frac{1}{C^d}$ at constant q are linear. This affords strong support for the validity of G.C.S. theory and the assumption that fluoride ions are not adsorbed. No theory at present can satisfactorily predict the dependence of C^i on q even in the simplest case of fluoride salts. One point of particular controversy is the anodic peak in the C^i curve which is most evident with specific adsorption. In 1MKF at 25°C it is almost a plateau.[8] These peaks have been ascribed to specific adsorption peaks and to the reorientation of the solvent layer. The anodic rise which follows the peak has been associated with electrostriction and with specific adsorption. The situation is at present unresolved.

Another support for our assumption of no fluoride ion specific adsorption comes from the Esin-Markov effect. We begin with the function ξ.

$$d\xi = E^{+}dq - \Gamma_{F^-,w}d\mu_{KF}$$

$$\left(\frac{\partial E^{+}}{\partial \mu}\right)_q = -\left(\frac{\partial \Gamma_{F^-,w}}{\partial q}\right)_\mu$$

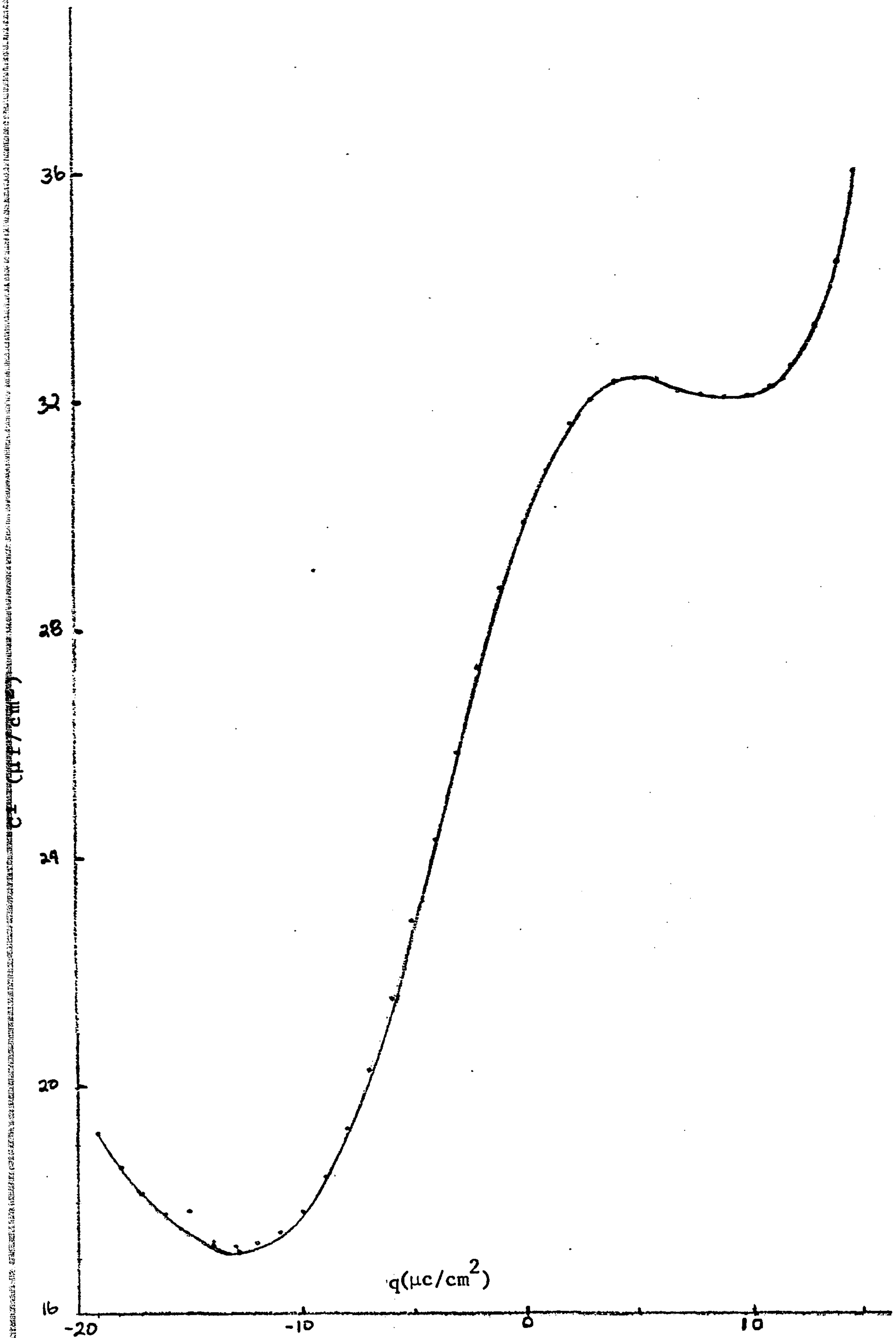

Figure 2. The Inner Layer Capacity of 1MKF Plotted as a Function of the Surface Charge Density

for a cation reversible electrode

$$E^{+} = E_{ref} - \frac{RT}{2F} \ln a_{\pm}^{2}$$

and

$$q_{F^-} = - F\Gamma_{F^-,w}$$

therefore

$$\left(\frac{\partial E_{ref}}{2\ln a_{\pm}^{2}}\right)_q = \frac{RT}{F}\left[\left(\frac{\partial q_-}{\partial q}\right)_\mu + \frac{1}{2}\right]$$

where we have assumed that $q_{F^-} = q_-^d$.

Also

$$q_-^d =. - A(\exp(\frac{RT\phi^2}{2F}) -1)$$

$$\phi^2 = \frac{2RT}{F} \sinh^{-1} q/2A$$

therefore

$$\left(\frac{\partial q_-^d}{\partial q}\right)_\mu = -\frac{1}{2} - \frac{1}{2}\left\{\frac{q/2A}{[1 + (q/2A)^2]^{1/2}}\right\}$$

For $q = 0$, we find that

$$\left(\frac{\partial E_{ref}}{\partial \ln a_{\pm}^{2}}\right)_q$$

should equal zero. In other words Ez measured against a reference electrode is independent of concentration. Parsons found this to be the case with NaF solutions. Furthermore, he compared the experimental and theoretical values of $\left(\frac{\partial E_{ref}}{\partial \ln a_{\pm}}\right)_q$ at different values of q and also found agreement.[9]

2. Specific adsorption present

In the presence of specific adsorption we may still write[10,11]

$$E = \phi^{m-2} + \phi^{2} - \phi^{ref}$$

where ϕ^{m-2} is the potential drop across the inner layer.

Also

$$\left(\frac{\partial E}{\partial q}\right)_\mu = \left(\frac{\partial \phi^{m-2}}{\partial q}\right)_\mu + \left(\frac{\partial \phi^{2}}{\partial q}\right)_\mu$$

but ϕ^2 is now a function of both q and q^1

therefore

$$\left(\frac{\partial \phi^{2}}{\partial q}\right)_\mu = \left(\frac{\partial \phi^{2}}{\partial q^d}\right)_\mu \left(\frac{\partial q^{d}}{\partial q}\right)_\mu$$

$$q = - q^1 - q^d$$

$$\left(\frac{\partial \phi^{2}}{\partial q}\right)_\mu = \frac{1}{C^d}\left[1 + \left(\frac{\partial q^{1}}{\partial q}\right)_\mu\right]$$

so that

$$\frac{1}{C} = \frac{1}{C^i} + \frac{1}{C^d}\left[1 + \left(\frac{\partial q^{1}}{\partial q}\right)_\mu\right]$$

C, C^d, and $\left(\frac{\partial q^{1}}{\partial q}\right)_\mu$ are known, which allows the computation of C^i. ϕ^{m-2} may be expressed as

$$\phi^{m-2} = E - \phi^2 - Ez$$

where Ez is the potential at point of zero charge for KF in the same cell. This is essentially a method of putting all of the systems on the same scale independent of the experimental design. ϕ^{m-2} may be considered a function of q and q^1. Therefore

$$d\phi^{m-2} = \left(\frac{\partial\phi^{m-2}}{\partial q}\right)_{q^1} dq + \left(\frac{\partial\phi^{m-2}}{\partial q^1}\right)_q dq^1$$

$$\frac{1}{C^i} = \left(\frac{\partial\phi^{m-2}}{\partial q}\right)_\mu = \left(\frac{\partial\phi^{m-2}}{\partial q}\right)_{q^1} + \left(\frac{\partial\phi^{m-2}}{\partial q^1}\right)_q \left(\frac{\partial q^1}{\partial q}\right)_\mu$$

or

$$\frac{1}{C^i} = \frac{1}{{}_qC^i} + \frac{1}{{}_{q^1}C^i} \left(\frac{\partial q^1}{\partial q}\right)_\mu$$

$${}_qC^i = \left(\frac{\partial q}{\partial\phi^{m-2}}\right)_{q^1} \qquad {}_{q^1}C^i = \left(\frac{\partial q^1}{\partial\phi^{m-2}}\right)_q$$

${}_qC^i$ and ${}_{q^1}C^i$ both have the dimensions of capacity. ${}_{q^1}C^i$ can be obtained from the slope of a plot of ϕ^{m-2} versus q^1 at constant q. Two other integral capacities can be obtained from this plot.

$${}_{q^1}K^i = \frac{\Delta q^1}{\Delta\phi^{m-2}} \qquad \text{at constant } q$$

$${}_qK^i = \frac{\Delta q}{\Delta\phi^{m-2}} \qquad \text{at constant } q^1$$

${}_{q^1}K^i$ will equal ${}_{q^1}C^i$ if the plots are linear. ${}_qK^i$ is equal to the difference Δq between a q and q = 0 curve divided by $\Delta\phi^{m-2}$ for the same value of q^1. For q = 0, ${}_qK^i = {}_qC^i$. ${}_qC^i$ is obtained by solving the equation for $1/C^i$. ${}_qK^i$ and ${}_{q^1}K^i$ have both been interpreted as the capacities of two parallel plate capacitors.

$$ {}_{q}K^{i} = \frac{\epsilon}{4\pi X_2} = \frac{q}{{}_{q}\phi^{m-2}} $$

$$ {}_{q^1}K^{i} = \frac{\epsilon}{4\pi(X_2 - X_1)} = \frac{q^1}{{}_{q^1}\phi^{m-2}} $$

where X_1 is the position of the inner Helmholz layer, ${}_{q}\phi^{m-2}$ is the part of ϕ^{m-2} due to the surface charges and ${}_{q^1}\phi^{m-2}$ is the part of ϕ^{m-2} due to the absorbed charges. The ratio

$$ \frac{{}_{q}K^{i}}{{}_{q^1}K^{i}} = \frac{X_2 - X_1}{X_2} $$

is known as the distance ratio. If the field in the inner layer is constant then we may write

$$ \phi_1 = \phi^m - \sigma X $$

$$ \phi_2 = \phi^m - \sigma X_1 $$

$$ \phi = \phi^m - \sigma X_2 $$

$$ \phi^{m-2} = \phi^m - \phi^2 = \sigma X_2 $$

where ϕ^1 is the potential at the inner Helmholz plane. A latter modification of this equation is

$$ \phi^1 - \phi^2 = [(X_2 - X_1)/X_2]\ {}_{q}\phi^{m-2} + \left[\frac{\gamma}{\gamma+\beta}\right] {}_{q^1}\phi^{m-2} $$

$\gamma/\gamma+\beta$ will approach unity when q^1 is large and most of the potential drop across the inner layer occurs between the inner and outer Helmholz planes. At low values of q^1,

$$\frac{\gamma}{\gamma+\beta} = \frac{X_2 - X_1}{X_2}$$

in order that

$$\phi^1 - \phi^2 = \frac{X_2 - X_1}{X_2} \quad \phi^{m-2}$$

An adsorption isotherm may be used to obtain the value of $\frac{X_2 - X_1}{X_2}$. For example, for KI + KCl, Parsons assumed the following:[12]

$$q^1 = K^1 a_{\pm} \exp(\phi^1 F/RT)$$

where $q^1 = |q^1|$ and K^1 is a function of q only. Then

$$\ln q^1/a_{\pm} - \frac{\phi^2 F}{RT} = \ln K^1 + \frac{\phi^{m-2} F}{RT}\left(\frac{X_2 - X_1}{X_2}\right)$$

If we plot ϕ^{m-2} versus the left side of the equation, the slope gives the distance ratio. More complicated isotherms and the modified expression for $\phi^1 - \phi^2$ can also be used. The capacity ratio method was used for a number of systems, but recently situations where ${}_q{}_1K^1$ is negative were found.[13,14] Since X_2 must be greater than X_1, the interpretation cannot be meaningful for these systems. The earlier success was fortuitous since the physical situation in the inner layer does not correspond to two capacitors in series. The above equations are based on the assumption that

$$\phi^{m-2} = {}_q\phi^{m-2} + {}_{q^1}\phi^{m-2}$$

or

$$\phi^{m-2} = \frac{q}{{}_qK^i} + \frac{q^1}{{}_{q^1}K^i}$$

This is not the equation for two capacitors in series or in parallel and its physical meaning is obscure. Values of the distance ratio determined by the isotherm method and those determined by the capacity ratio method have generally not been in agreement.

${}_qC^i$ is theoretically an experimentally determinable quantity. We return to the equation

$$\frac{1}{C^i} = \frac{1}{{}_qC^i} + \frac{1}{{}_{q^1}C^i}\left(\frac{\partial q^1}{\partial q}\right)_\mu$$

At infinite frequency, the second term is zero and we are measuring ${}_qC^i$. This assumes that diffuse layer theory is still valid at infinite frequency. ${}_qC^i$ is of particular importance in explaining the peaks in C^i versus charge curves. If the peak is due solely to specific adsorption, then ${}_qC^i$ which is measured at constant q^1 should not contribute to it. The fact that there are peaks in ${}_qC^i$ suggests that solvent reorientation plays a part in peak formation.

D. Adsorption Isotherms and the Shape of the Capacity Curve.

Theoretically, the shape of the capacity versus charge curve can, under certain conditions, be directly predicted from the adsorption isotherm.[15,16,17] The determination of the isotherm also provides information on the charge or potential dependence of the free energy of adsorption. The constants of the isotherm give information concerning the interaction of adsorbed ions. The two isotherms which are most frequently used are the Frumkin and virial. The isotherms and equations of state are given below.

Frumkin:

isotherm $$\ln \frac{a\beta}{\Gamma_S} = \ln \frac{\theta}{1-\theta} + A\theta$$

equation of state $$\frac{\Phi}{k T\Gamma_S} = -\ln (1-\theta) + \frac{A}{2} \theta^2$$

Virial:

isotherm $$\ln \Gamma + 2B\Gamma = \ln a\beta$$

equation of state $$\Phi = kT(\Gamma + B\Gamma^2)$$

Φ is the surface pressure and for constant q, $\Phi = \xi - \xi^b$ where ξ is the base solution value of ξ. β equals $\exp(-\Delta G/R\Gamma)$, Γ_S is the saturation concentration, a the activity, $\theta = \Gamma/\Gamma_S$, and A and B are isotherm constants. The problem of whether to study adsorption at constant q or E arises again at this point. As previously mentioned, it is unresolved.

The method of testing the Frumkin isotherm is to pick a value of A, allow θ to vary from $0 < \theta < 1$ and get a universal curve of ln $(\Phi/KT\Gamma_S)$ versus ln $(a\beta/\Gamma_S)$. This curve is compared with an experimental curve of ln Φ versus ln a. If the data fit a Frumkin isotherm, the two curves are superimpossible if the scale of ln Φ and ln a are changed to ln $\Phi + C_1$ and ln a + C_2. Obviously $C_1 = -\ln kT\Gamma_S$ and $C_2 = \ln \beta/\Gamma_S$. The values of A and Γ_S can be adjusted to get the best fit of the experimental data. The virial isotherm is much easier to handle. One rearranges the isotherm into the form

$$\Gamma = \frac{1}{2B} \ln \frac{a}{\Gamma} + \frac{1}{2B} \ln \beta$$

The experimental values of Γ are plotted against $\ln a/\Gamma$ and the slope gives $\frac{1}{2B}$, the intercept $\ln \beta$. The method used for the Frumkin isotherm can be used for any isotherm where $K\Phi$, K a constant, and β are functions only of θ and any number of isotherm constants. In studying the adsorption of a single ion, the question arises whether to use the salt activity $(a_{\pm}^{2})$ or the ion activity $a_{\pm}$ in the isotherm. It seems logical to use $a_{\pm}$, but this question is also unresolved.

The assumption which is necessary in order to relate the isotherm to the capacity curves is that $\Gamma = \Gamma(\beta a)$. This means that all isotherm constants are independent of the surface charge and the amount of specific adsorption. We begin with the differential form of ξ.

$$d\xi = Edq - \Gamma d\mu$$

$$\left(\frac{\partial E}{\partial \mu}\right)_q = -\left(\frac{\partial \Gamma}{\partial q}\right)_\mu$$

$$dE = -\int\left(\frac{\partial \Gamma}{\partial q}\right)_\mu d\mu \qquad q = \text{constant}$$

but since

$$\Gamma = \Gamma(\beta a)$$

$$\frac{1}{\beta}\left(\frac{\partial \Gamma}{\partial a}\right)_\beta = \frac{1}{a}\left(\frac{\partial \Gamma}{\partial \beta}\right)_a$$

and

$$\left(\frac{\partial \Gamma}{\partial q}\right)_\mu = \left(\frac{\partial \Gamma}{\partial \beta}\right)_\mu \left(\frac{\partial \beta}{\partial q}\right)_\mu$$

therefore

$$dE = -\int \frac{a}{\beta}\left(\frac{\partial \Gamma}{\partial a}\right)_\beta \frac{\partial \beta}{\partial q} \, d\mu$$

and

$$\Delta E = E - E^b = - RT \left(\frac{\partial \ln \beta}{\partial q}\right) \Gamma \quad \text{at constant } q$$

E^b is the value of E for the base solution at the same value of q. If ln β is linear in q, then plots of $E - E^b$ versus ln a should be part of the same curve if ln β is added to ln a. The isotherm and $\frac{d \ln\beta}{dq}$ can be obtained directly from this type of plot.

More generally, we can now take the derivative of the equation for ΔE by q at constant μ.

$$\left(\frac{\partial E}{\partial q}\right)_\mu - \left(\frac{\partial E^b}{\partial q}\right)_\mu = - kT \frac{\partial}{\partial q} \left[\frac{\partial \ln \beta}{\partial q} \cdot \Gamma\right]$$

or

$$\frac{1}{C} - \frac{1}{C^b} = - kT\left[\left(\frac{\partial \ln \beta}{\partial q}\right)^2 \left(\frac{\partial \Gamma}{\partial \ln \beta}\right)_\mu + \Gamma \frac{\partial^2 \ln \beta}{\partial q^2}\right]$$

at any given value of q. Let us first assume that

$$\frac{d \ln \beta}{dq} = K$$

$$\frac{d^2 \ln \beta}{dq^2} = 0$$

Then

$$\Delta \frac{1}{C} = \frac{1}{C} - \frac{1}{C^b} = - kTK^2 \left(\frac{\partial \Gamma}{\partial \ln \beta}\right)_\mu$$

$\left(\frac{\partial \Gamma}{\partial \ln \beta}\right)_\mu$ is obtained from the isotherm. For a Frumkin isotherm

$$\frac{\partial \Gamma}{\partial \ln \beta} = \Gamma_S \left\{ \frac{1}{\theta(1-\theta)} + A \right\}^{-1}$$

and is symmetrical about $\theta = .5$ where it is a maximum. A plot of $-\Delta\frac{1}{C}$ versus Γ at constant charge should give a maximum at $\theta = .5$. When $-\Delta\frac{1}{C}$ is a maximum C is also a maximum. Alternatively let us assume that a virial isotherm is obeyed.

$$\frac{1}{C} - \frac{1}{C^b} = - kTK^2 \left(\frac{\Gamma}{1+2B\Gamma} \right)$$

For large values of Γ, $-\Delta\frac{1}{C}$ reaches the limiting value of $\frac{kTK^2}{2B}$ and this would be evident in plots of $-\Delta\frac{1}{C}$ versus Γ at constant q. Plots of $-\Delta\frac{1}{C}$ versus q at constant μ will have the same characteristics if $\frac{d^2 \ln \beta}{dq^2} = 0$.

If we assume that $\ln \beta$ is a quadratic function of q, we may write it as follows

$$\ln \beta = \ln \beta_{max} - \frac{b}{2} \delta^2$$

where

$$\delta = q - q_{max}$$

also

$$\frac{d \ln \beta}{dq} = - b\delta$$

$$\frac{d^2 \ln \beta}{dq^2} = - b$$

A quadratic standard free energy is based on the assumption that ΔG is given by:

$$\Delta G = \Delta G^o + \frac{1}{2} q^2 \left[\frac{1}{C^S} - \frac{1}{C^b} \right] + q \left[\frac{\mu^b}{\epsilon^b} - \frac{\mu^S}{\epsilon^S} \right]$$

μ^S, C^S and ϵ^S are the dipole moment per unit volume, the capacity per unit area and the dielectric constant when the surface is saturated with absorbate; μ^b, C^b, and ϵ^b are for the base solution. ΔG^o is the non-electrical part of ΔG. This equation may be rearranged to the form

$$\Delta G = \Delta G_{max} + \frac{1}{2} b^1 \delta^2$$

by finding ΔG_{max} from the derivative $\partial \Delta G/\partial q$ when it equals zero. ΔG and ΔG_{max} are negative, b^1 is positive. Since $\beta = \exp(-\Delta G/RT)$

$$\ln \beta = \ln \beta_{max} - \frac{1}{2} b\delta^2$$

We then have for Δ 1/C the following equation.

$$\Delta\frac{1}{C} = kT\left[\Gamma b - b^2\delta^2\left(\frac{\partial \Gamma}{\partial \ln \beta}\right)_\mu\right]$$

If we take the derivative of $\Delta\frac{1}{C}$ by δ at constant μ and set it equal to zero, we find the values at which $\Delta\frac{1}{C}$ is an extreme. This expression is

$$b\delta^2 = \frac{3(\partial\Gamma/\partial \ln \beta)_\mu}{(\partial^2\Gamma/\partial \ln \beta^2)_\mu}$$

There are three values of δ which satisfy this equation. One is $\delta = 0$, independent of the isotherm chosen. This point corresponds to maximum adsorption since ln β is a maximum at $\delta = 0$. $\Delta \frac{1}{C}$ will be a maximum and C will have its minimum value. The other two values of δ correspond to maxima in C and minima in $\Delta \frac{1}{C}$. They depend on the particular isotherm obeyed. As δ goes to plus or minus infinity, $\Delta \frac{1}{C}$ goes to zero for any isotherm. C is then equal to C^b and there is complete desorption. Quadratic dependence is easily demonstrated by a plot of $\Delta \frac{1}{C}$ versus q at constant μ. Plots of Δ 1/C versus Γ at constant q may be used as an alternative method of finding q_{max}. The curve for $q = q_{max}$ should be linear and have the largest slope which will equal kTb.

This analysis has been used to explain the shape of capacity curves with adsorption. It is truly rigorous only for the adsorption of neutral molecules. With ionic absorption one must decide whether to use $\Delta\frac{1}{C}$ or $\Delta\frac{1}{C^i}$. The derivation necessitates the use of $\Delta\frac{1}{C}$, but unlike neutral adsorption the value of C^d for the base solution will not be the same as that for the solution with adsorption. Using Δ $1/C^i$ solves this problem and is intuitively appealing, but without rigorous justification. Another problem arises with adsorption from a single salt solution, what do we use for the base solution values of C^b? The values used in the literature are the C values for KF at the same concentration. Actually, the derivation indicates that the base solution is the solvent, and that the use of KF values needs further justification. These problems can be alleviated by working with a mixed electrolyte system at constant ionic strength such as xMKBr + (1 - x)MKF. C^d is then always large and makes a minor contribution to C. Equating the base solution to 1M KF is also justified in this type of system.

With single salt adsorption, the use of the surface pressure also becomes ambiguous.[11,18] We begin with

$$d\xi^{+} = Edq - (\Gamma^{d}_{Br^-} + \Gamma^{i}_{Br^-})\, d\mu_{KBr}$$

We then assume that the surface pressure can be written as

$$\Phi = \xi^{+} + I - \xi_{o}^{+}$$

where

$$I = \int_{-\infty}^{\mu} \Gamma_{Br^-}^{d} \, d\mu_{KBr}$$

and ξ_{o}^{+} is the value of ξ when $\mu = -\infty$ or

$$\Phi' = \xi^{+} + I$$

$$I' = \int_{\mu_1}^{\mu_2} \Gamma_{Br^-}^{d} \, d\mu_{KBr}$$

The magnitude of Φ' will differ from Φ by a constant at constant q. A significant problem in this approach is whether the surface pressure due to the anion is Φ or $\Phi/2$. It is essentially the same problem of whether to use $a_{\pm}$ or $a_{\pm}^{2}$ in the isotherm.[19] Using Φ implies that all of the effect is due to the anion, whereas $\Phi/2$ implies that only half of the change is caused by the anion. Since the cation is also adsorbed, though not specifically, it must also have an effect on the surface pressure. A more basic difficulty, is whether the entire concept is valid in single salt solutions with varying ionic strength. This again reduces to the identification of the base solution. With organic adsorption, or adsorption from a solution of fixed ionic strength, this problem does not exist. Let us assume we have system governed by the equation:

$$d\xi = E dq - \Gamma_{N,w} d\mu_{N} - \Gamma_{F,w} d\mu_{KF}$$

$$d\mu_{KF} = 0$$

Then the surface pressure is given by

$$\bar{\Phi} = \xi - \xi_o$$

where ξ_o is the value of the KF solution in the absence of N and there is no ambiguity.

II. EXPERIMENTAL PROCEDURE

Three separate experiments are needed in order to obtain the data required to interpret the structure of the electrical double layer. These are the determination of the potential (Ez), and the interfacial tension (γ_{Ez}) at the point of zero charge ($q = 0$), and the determination of the differential capacity curve for each concentration of adsorbate studied. The potential and interfacial tension at the point of zero charge are the two constants needed to integrate the differential capacity curve.

A. The Determination of Ez

Let us assume that we have the following cell:

$$\mathrm{Cu}\,|\mathrm{CAL}\,|\mathrm{KBr},\mathrm{KF},\mathrm{H_2O}\,|\mathrm{Hg}\,|\mathrm{Cu}$$

CAL is a calomel reference electrode. A potentiometer is connected between the two copper leads. The mercury electrode consists of a capillary with its top in the solution connected to a mercury reservoir. The reservoir is in turn connnected to a tank of nitrogen so that the pressure in the reservoir may be varied at will. The pressure on the mercury is then increased until a rate of flow is reached at which a stable potential exists between the reservoir and the calomel electrode. The pressure is then varied and the potential recorded as a function of pressure. As the pressure increases, the potential will become more negative, reach a plateau and then increase slightly. The potential in the plateau region is the potential of zero charge. The concept behind this experiment is that once an adequate rate of flow is reached, any excess charge on the mercury will be carried off and furthermore the area of the electrode is effectively infinite. Therefore the surface charge density is zero. The slight rise in potential which occurs at large pressures was unexpected and remains unexplained. It has been observed in a sufficient number of systems that the nature of the adsorbate cannot be the cause. Grahame did an extensive amount of work on the determination of Ez, and found that this is the most reliable method.[20] Ez is reproducible to 1 mv or less and even this variation could be due to variations in the liquid junction potential. This method assumes that equilibrium has been reached at the electrode surface. If this is not the case, Ez must be determined by finding the maximum in the electrocapillary curve.

B. The Determination of γ_{Ez}

The capillary electrometer and its use for determining the electrocapillary curve were developed by Gouy early in this century. The same cell used to determine Ez, is used in this experiment, except that a much finer capillary is needed. A potential is applied across the cell. The capillary is connected to a mercury reservoir which can be varied in height above the capillary tip. The criterion for choosing a capillary is that it be able to support a column of mercury at least 60 cm high when Ez is the applied potential. The capillary is calibrated by using a solution whose electrocapillary curve is known. We apply a potential and measure the position of the mercury meniscus in the capillary. At the interface,

$$\Delta P = \frac{2\gamma}{r}$$

ΔP is computed from the height of the mercury and corrected for the solution height above the tip. Since γ is known, the radius of the capillary at a fixed position is also known. We now may use the capillary for any other solution. At each value of the imposed potential, the mercury reservoir is adjusted until the meniscus is at the calibrated position. We then compute γ using the known value of the radius. There are several possible sources of error in this experiment. We assume that the contact angle between the solution and the mercury in zero, and that we may accurately return the meniscus to the calibrated position. We have no choice concerning the contact angle since it cannot be measured, but the agreement of Ez values obtained from the electrocapillary curve and those obtained from the streaming electrode supports the zero contact angle assumption. The other problem depends on the capillary. If the radius is changing rapidly, then large errors will be made in positioning the meniscus, but if the radius changes too slowly, a definite equilibrium position is not easily achieved. If the results are reproducible, one may assume the taper of the capillary curve is correct. The potential at which the electrocapillary curve is a maximum is Ez. Unfortunately, the curve is quite flat in this region. This allows an accurate measurement of γ_{Ez}, but a poor measurement of Ez. The best procedure is to obtain Ez from the streaming electrode and γ_{Ez} from the electrocapillary curve.

C. The Differential Capacity Curve

The procedure for measuring the differential capacity was first developed by Grahame and improved by Hills and Payne.[21] A schematic of the apparatus is shown in Figure 3. The cell consists of three

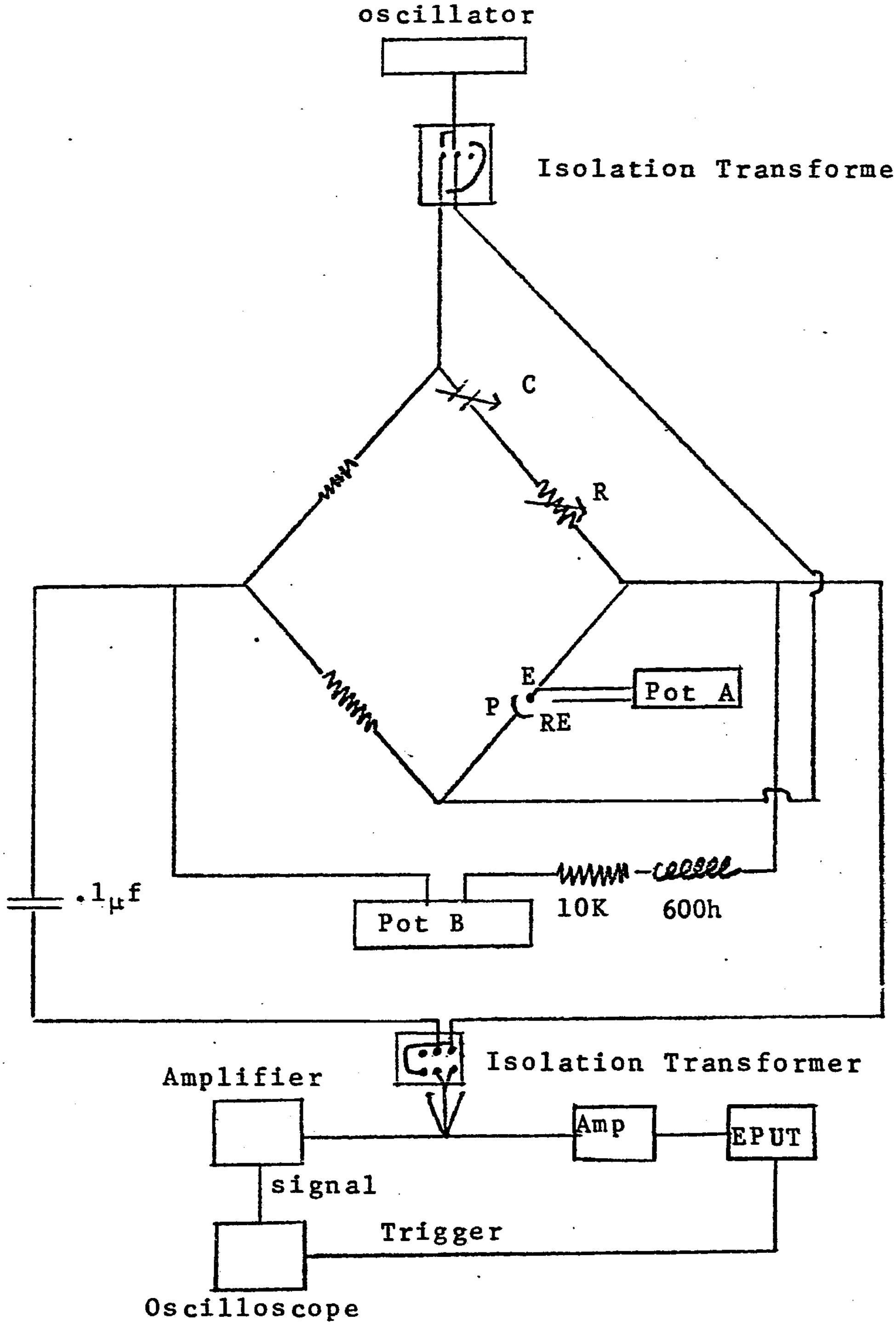

Figure 3. A Schematic Representation of the Apparatus Used to Determine The Differential Capacity

electrodes. A dropping mercury electrode (E) is attached to one terminal of the bridge. Its tip is inside a platinum mesh basket (P) which is attached to another terminal. Together they form one of the four bridge arms. The third electrode is a reference electrode (RE) which is separated by two stopcocks from the solution being measured. The closed stopcocks are ungreased allowing electrical contact but preventing the diffusion of chloride ions from the reference electrode into the solution. Potentiometer A measures the potential between the dropping electrode and the reference electrode. Potentiometer B imposes a constant potential across the entire bridge. The only direct current which flows is that to charge the capacitors. An alternating voltage of 10 mv is impressed across the bridge and the bridge output fed into two amplifiers. The first amplifier feeds the signal to the vertical plates of an oscilloscope. The second amplifier takes the signal to a modified Beckman EPUT meter. The maximum output of the bridge occurs when a drop falls off. At this point the bridge is completely out of balance. The EPUT meter has been modified in such a way that in the TIM mode it can be used both as a timer and as trigger pulse. One adjusts the EPUT meter so that it will not begin counting until a drop has fallen off. It then counts for 10 sec and provides a pulse which is used to trigger the scope. The scope is also calibrated so that the time it takes for a signal to get to the 5 cm line is known. The oscillator frequency is 1000 Hz and the scope sweep time about 1 sec/cm. The individual waves are therefore not resolved, rather they appear as a wedge shaped image on the screen. One adjusts the variable capacitor (C) and resistor (R) until the wedge goes to a minimum at the center of the screen. This means that at the time represented by the 5 cm line the bridge is in balance. Since the electrical double layer is a pure capacity, the value of the variable capacitor is the capacity of the drop. The EPUT meter and scope repeat this sequence for each drop. The surface area of the drop is determined by measuring the flow rate of the mercury. From the flow rate we get:

$$V = \frac{4}{3}\pi r^3 = \frac{mt}{d}$$

where m is the flow rate, t the time in the life of the drop and d the density of mercury. If follows that

$$A = 4\pi r^2 = 4\pi\ ^{2/}{}_{3} \sqrt{\frac{3}{4\pi}\frac{mt}{d}}$$

The capacity per unit area is now determinable for each value of potential set by potentiometer B and read on potentiometer A.

The main source of error in this experiment lies in the improper choice and preparation of capillaries. The capillary must be thoroughly cleaned and then coated with dimethyl-dichloro-silane. This prevents the solution from getting inside the capillary. The tip of the capillary must be even. A sliver of glass projecting from the tip will effectively decrease the surface area of the drop. The flow rate must also vary during the course of the experiment since the interfacial tension is a function of potential and the actual pressure causing flow is $(P - \frac{2\gamma}{r})$. The variation in the rate of flow is not significant. It is also assumed in this experiment that the mercury surface is at equilibrium. At very low concentrations where this is not the case, an extrapolation must be made to the zero frequency value of the capacity.

III. The Adsorption of Halide Ions

A. Review of Previous Work

The halide systems have received particular attention in the study of the electrical double layer. They exhibit a continuous variation between the non-specifically adsorbed fluoride ion and the strongly adsorbed iodide ion. Compared with most other anions studied, the halides have a simple structure which can, to a first approximation, be represented by a point charge. This removes the complication introduced by permanent dipole moments, and the further difficulty with polynuclear anions of several possible orientations relative to the mercury surface. The halide systems are then obviously the first place to begin looking for a coherent explanation of anionic specific adsorption.

1. The fluoride ion

Grahame's work, which has been previously discussed, clearly shows that the fluoride ion is not specifically adsorbed.[7,8] It should be mentioned that the identity of the cation has a slight quantitative effect, but no qualitative significance. The remaining question is to explain the shape of the C^i versus q curve. Unfortunately an adequate theory is still not in existence. On Figure 2, the C^i versus q curve for 1MKF is plotted. The slight anodic peak is clearly evident. For NaF, Grahame found that this peak disappears with increasing temperature and that the capacity at 85°C rises continuously as q becomes more positive. The shape of the curve was independent of concentration at constant charge and temperature. These results lend support to the belief that the peak is due to a local maximum in the dielectric constant of the inner layer. The maximum could be caused by the reorientation of the water dipole. If one assumes that the dipole is preferentially oriented with its positive side to the mercury, then reorinetation would occur at positive surface charges. In the region where reorientation is occurring, the dipole should be freer to rotate with the alternating field. This results in a larger dielectric constant. One could also explain the peak by a variation in the thickness of the inner layer, which in fact was Grahame's choice. Peaks which can not be ascribed to specific adsorption also occur in other solvents at both positive and negative surface charge densities.[22] This tends to support the dipole reorientation interpretation as opposed to a change in thickness. The remainder of the curve can be explained by a combination of electrostriction and dielectric saturation.

2. The chloride ion.

The adsorption of KCl was studied by Grahame and Parsons.[12] The isotherms at constant charge are definitely curved and would give a value of $q^1 = -q$ at infinite dilution if the linearity at low concentration was maintained. This effect has been observed in the adsorption of the I^-, Cl^-, Br^-, NO_3^- ions from single salt solutions.[23] At infinite dilution one would expect q^1 to equal zero rather than $-q$. There is at present no reasonable explanation for this effect. The variation of q^1 with q at constant concentration is similar to that for KI and KBr, and the linear portions have the same slope. The components of the capacity were obtained from plots of ϕ^{m-2} versus q^1 at constant surface charge. The points at constant surface charge were considered to lie on a straight line. Therefore ${}_{q}1C^{i} = {}_{q}1K^{i}$ and ${}_{q}1\,K^{i}$ is a function of surface charge.only. There are large systematic leviations from a straight line which cast doubt on the constancy of ${}_{q}1K^{i}$. In any case, using the constant values, the other components of the capacity were derived. ${}_{q}1K^{i}$ decreases with increasing surface charge and ${}_{q}K^{i}$ must therefore also vary with q^1. Parsons compared

${}_qK^i$ at $q^1 = 0$ to the integral capacity of the inner layer in a KF solution and found reasonable agreement. The integral capacity is given be

$$K = \frac{1}{\phi^{m-2}} \int_0^{\phi^{m-2}} C^i \, d\, q$$

The distance ratio was calculated by both the isotherm and capacity ratio methods. The values obtained from the two methods are different, but in each case they are lower than those obtained for KI. On this basis it is assumed that X_1 is larger for the chloride ion than for the iodide ion.

Payne has studied the adsorption of KCl from constant ionic strength solutions of KCl and KF.[24] The capacity curves have a distinct peak which becomes more prominent with increasing concentration. The peak remains when the inner layer capacity is determined and C^i is almost independent of concentration except at low concentrations. As in the pure KCl system, ${}_q^1C^i = {}_q^1K^i$ and is a function of charge only. In contrast to pure KCl, ${}_q^1K^i$ increases with increasing surface charge. The fact that C^i is almost independent of concentration is due to a simultaneous decrease in ${}_qC^i$ and increase in $\left|\frac{1}{{}_q^1K^1}\left(\frac{\partial q^1}{\partial q}\right)_\mu\right|$ as $|q^1|$ increases. The adsorption was found to fit a virial isotherm with $\ln\beta$ a non-linear function of the surface charge. Both the virial isotherm and the non-linear dependence of $\ln\beta$ on q are supported by Payne's plots of $-\Delta\frac{1}{C}$ versus q^1 at constant surface charge. These plots approach a limiting value for each charge. The limiting values are different due to the second term in $-\Delta\frac{1}{C}$. When $-\Delta\frac{1}{C}$ is plotted versus q at constant concentration, a peak occurred near q=6, and was followed by a decrease and approach to a limiting value. This is not true quadratic behavior in which the peak would be followed by a minimum and then another peak. Payne found that his isotherms could not be superimposed on the pure KCl isotherms whether he used $a_{\pm}$ or $a_{\pm}^{2}$ for the activity.

3. The bromide ion.

Recently, the adsorption of the bromide ion has been studied as part of an experiement whose primary purpose was to compare the two distinct methods of investigating the electrical double layer.[25] These are the electrocapillary curve and the differential capacity curve. It was determined that neither a virial or Frumkin isotherm fit the data. A complete analysis of specific adsorption was not presented.

4. The iodide ion

Grahame performed the most complete study of the adsorption of KI in water.[26] He found that q^{1} was an approximately linear function of q at constant concentration except at quite negative values of q. The isotherms at constant charge were linear except at low concentrations where they begin to approach $q^{1} = -q$. Grahame assumed this was due to experimental error and he used values of q^{1} obtained by extrapolating the linear part of the curve. In a latter paper, Parsons, using Grahame's data, found that iodide adsorption fits a virial isotherm with $\ln\beta$ a linear function of the surface charge. It is not clear whether Parsons used Grahame's experimental data or his "corrected" data. The compounds of the capacity were then analyzed and ${}_{q}^{1}C^{i}$ was found to be a function of charge only. ${}_{q}^{1}C^{i}$ changes from $83\mu f/cm^{2}$ at $q = -12$ to $70\ \mu f/cm^{2}$ at $q = 16$. There are systematic deviations from these constant values which he assumed to be within experimental error. The intercept for the $q = 0$ line gave a value of Ez for KF which was 16 mv too cathodic. There must therefore be some curvature at low concentrations. Using his values of ${}_{q}^{1}C^{i}$, he determined ${}_{q}C^{i}$. The value of ${}_{q}C^{i}$ was independent of q^{1} and approximately equal to

C^i for KF at the same value of q. The equivalence of C^i and ${}_qC^i$ implies that the adsorbed ions do not have the same effect as the surface charges.

Dutkiewicz and Parsons studied the adsorption of KI from constant ionic strength solutions of KI in KF.[28] Parsons was able to fit the ΔE versus $\ln x$ curves to a single composite curve and found the $\ln\beta$ was a linear function of the surface charge. The highest value of the surface charge used in this work appears to be $q = -4$ and the largest value of q^1 was -12. Presumably the rapid rise in the capacity at more positive charge did not allow accurate data to be obtained. Plots of $\Delta \frac{1}{C}$ versus concentration indicate a Henry's low isotherm with $\frac{\partial \ln\beta}{\partial q}$ a constant. Plots of ϕ^{m-2} versus q^1 at constant charge were linear and parallel within experimental error. ${}_q1\,K^i$ was equal to $89 \mu f/cm^2$. The intercept found from these plots is quite different than that found from the pure KI data which should not be the case. The distance ratio is larger in KI+KF than in pure KI implying that X_1 is smaller in KI+KF. The constant value of $\partial\ln\beta/\partial q$ is supported by the ΔE versus $\ln x$ curves which can be fit to a single composite curve. If the adsorption isotherms at constant charge are plotted against the salt activity, the curves for KI and KF +KI can be superimposed. This can not be done if the anion activity is used. At the time this result appeared to resolve the question of which activity to use in the isotherm, but further work has shown it to be limited to the iodide system.

B. The adsorption of KBr from a constant ionic strength solution of KBr in KF.

Introduction

As should be obvious from the discussion of previous research, the adsorption of halide ions is not as simple as one would first expect. One of the main problems is to explain the different behavior of KCl and KI when they are adsorbed from constant ionic strength solutions with KF. The difference between the iodide and chloride ion is much more pronounced in the mixed electrolyte systems than in the single salt systems. One possible explanation is that there are no qualitative differences, and that this would be apparent if iodide adsorption could be studied at positive surface charge densities. The bromide ion is intermediate in its strength of adsorption between the chloride and iodide, and the purpose of this experiment was to study its adsorption as compared to the other halides. The mixed electrolyte system was chosen for two main reasons: 1) The analysis can be more rigorously justified than that for a single salt. 2) The data for KI+KF and KCl+KF is more complete and probably more reliable than the earlier work on the single salt systems.

One of the benefits of chosing the mixed electrolyte system is a simplification which occurs in the electrocapillary equation and allows the specifically adsorbed charge to the determined without first determining the diffuse layer charge. We begin with the previously derived equation:

$$d\gamma = -q\ d\ E - \Gamma_{F^-,w}\ d\ \mu_{KF} - \Gamma_{Br^-,w}\ d\mu_{KBr}$$

We assume that the activity coefficients of KBr and KF are dependent only on the total ionic strength.

Therefore

$$d\ \mu_{KF} = R\ T\ d\ \ln m_{KF} = k\ T\ d\ \ln(1-x)$$

$$d\ \mu_{KBr} = R\ T\ d\ \ln m_{KI} = k\ T\ d\ \ln x$$

where x is the molarity of KBr, the total molarity being 1M. Substituting in the electrocapillary equation gives

$$d\gamma = -q\ d\ E - \left[\Gamma_{Br^-,w} - \left(\frac{x}{1-x}\right)\Gamma_{F^-,w}\right] k\ T\ d\ \ln x$$

From diffuse layer theory and the assumption that the fluoride ion is not specifically adsorbed, one gets the relationship:

$$\frac{\Gamma^d_{Br^-}}{\Gamma^d_{F^-}} = \frac{x}{1 - x}$$

also

$$\Gamma_{Br^-} = \Gamma^i_{Br^-} + \Gamma^d_{Br^-}$$

Therefore

$$d\gamma = - q\, d E - \Gamma^i_{Br^-}\, k T\, d \ln x$$

and

$$d\xi = E\, d q - \Gamma^i_{Br^-}\, k T\, d \ln x$$

The specifically adsorbed charge is determined directly from the differentiation of ξ and γ. The assumptions used here are more general than those needed for adsorption form a single salt. We are assuming that $\Gamma^d_{Br^-}$ is proportional to x, whereas in the single salt system we would have to derive $\Gamma^d_{Br^-}$ from a specific equation. The determination of the amount specifically adsorbed is therefore more reliable. Another simplification arises when isotherms are considered. In the mixed electrolyte system the choice of activity does not arise since the assumption that the activity coefficients are constant is equivalent to setting $d \ln a_{K^+} = 0$ in the following equation.

$$d \ln a_{KBr} = d \ln a_{K^+} + d \ln a_{Br^-} = d \ln m \cdot$$

but

$$d \ln a_{Br^-} = d \ln m.$$

Either assumption leads to using x for the activity.

Experimental

All experiments were performed with the previously discussed equipment. Reagent grade chemicals were used without further purification, but the water used was distilled from alkaline potassium permanganate. The reliability of the equipment and the absence of adsorbable impurities in the salts was confirmed by comparing our results for 1 MKF and 1MKBr with those previously reported in the literature. The capacity was measured at 50 mv intervals from at least -1.4v to the most positive voltage obtainable. This is usually -.2 volts. In the region where the capacity peak occurs, smaller voltage intervals were used. Five capacitance decades from 1µf to .0001µf were available and balance was reproducible to ± .0002µf, which represents .1% in the measured capacity. Streaming electrode potentials were as previously stated reproducible to within 1 mv.

Results

The capacity of eleven solutions of xMKBr + (1 - x) MKF were measured at 25°C and are shown in Figure 4. These curves are qualitatively similar to those found in KCl + KF in that a distinct peak occurs at higher concentrations. The peak in the KBr curves occurs at a higher value of the capacity and a more negative value of the potential than in KCl. It is also less pronounced. This shift in the peak height and position is due to the stronger adsorption of the bromide ion. The capacity curves are equivalent when the potential is less than -1.3 volts. This fact was used in integrating the curves. The capacity curve is integrated by fitting each successive set of three points to a parabola. The first integral gives q and the second γ and ξ. The values of q, C, E, γ, and ξ are then

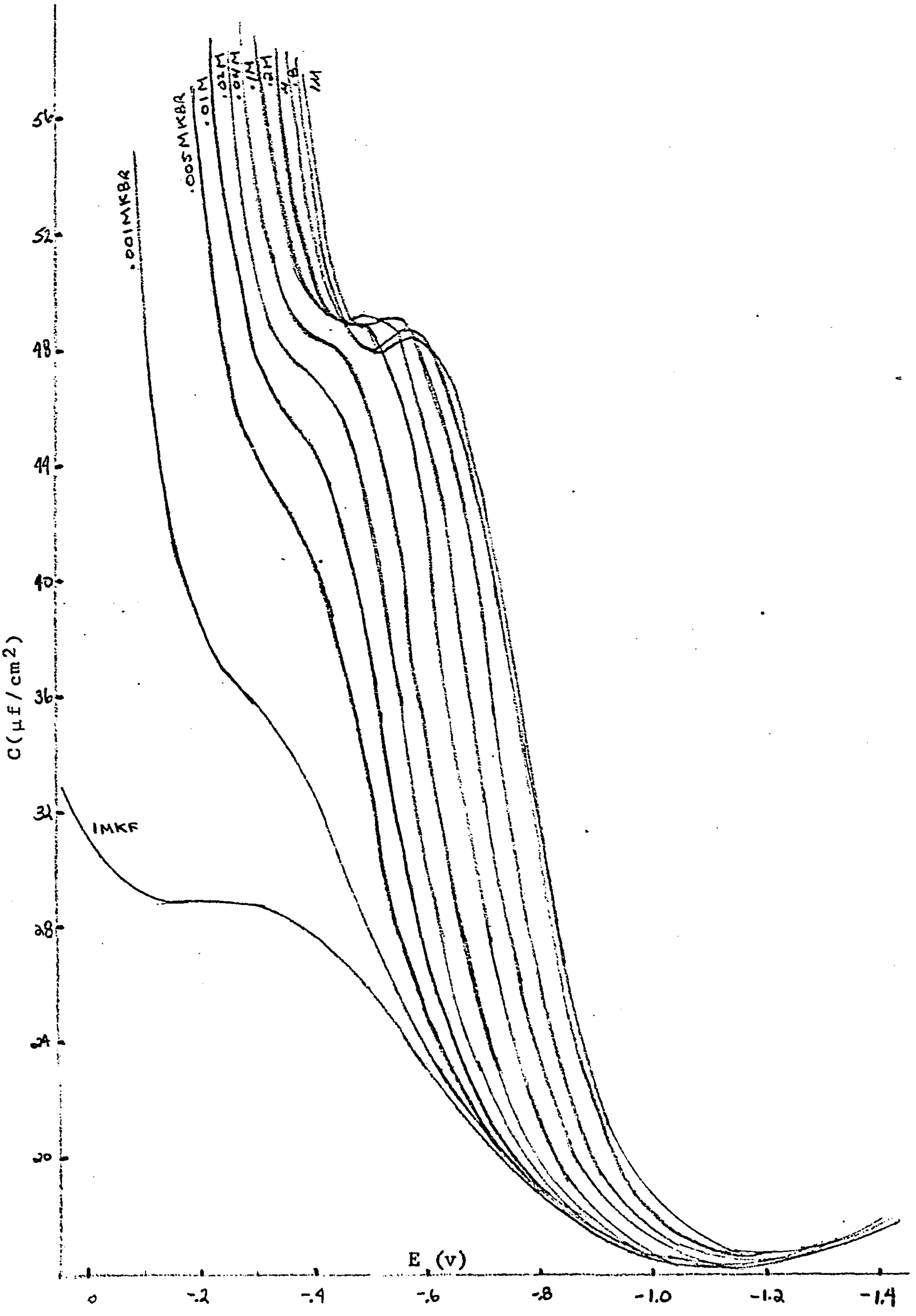

Figure 4. The Capacity of The Double Layer as a Function of Potential for xMKBr + (1-x)MKF

found for all integral values of q which occur in the range covered by the three experimental capacity points. The program then reads another experimental point and uses the determined values of the second point for the integration constants. The program is discussed in more detail in the appendix. One set of integration constants is needed to use the program. These are usually E, C, γ at E = Ez. Due to the fact that all of the curves are equivalent at large negative values of the potential, we may avoid the determination of γ. We integrate the 1MKF curve assuming $\gamma = 0$ at E = Ez, and obtain the value of γ, C, E at $q = -19$. The KBr + KF curves can now be integrated from $q = -19$ using the 1MKF data for the integration constants. If this procedure is valid, the values of Ez computed by the integration and those directly determined by the streaming electrode method must be equivalent. The two sets of values are presented in Table 1.

Table 1

Solution	Concentration x	Ez (Ex)	Ez (Com)
1	0	-.4740	-
2	.001	-.4820	-.4828
3	.005	-.4996	-.4988
4.	.01	-.5130	-.5127
5	.02	-.5295	-.5300
6	.04	-.5486	-.5486
7	.1	-.5769	-.5776
8	.2	-.6004	-.6020
9	.4	-.6245	-.6252
10	.8	-.6477	-.6472
11	1	-.6550	-.6568

The agreement is well within the acceptable limits. The second program then takes the derivative of ξ by ln x at constant q to give q^1 since

$$d\xi = E\,dq + \frac{kTN}{F}\,q^1\,d\ln x$$

The programs and data are presented in the appendix. In the course of evaluating the data, we decided not to use the .001M KBr set. It was decided that the results of the second program were more reliable if this set of data were excluded. It would be interesting to study the adsorption of KBr at low concentrations, but this would require the use of a frequency extrapolation of the capacity. The reliability of this procedure has not been demonstrated for ionic solutions. To show that the procedure was reliable, the equivalence of the twice integrated capacity curves and experimentally determined electrocapillary curves must be demonstrated. There is also the possibility that at very low concentrations the streaming electrode potential may not be the same as the potential at the point of zero charge. This will occur if equilibrium is not reached at the streaming electrode.

The specifically adsorbed charge is plotted against the surface charge at constant concentration in Figure 5 and the isotherms are plotted in Figure 6 at constant charge. The q^1 versus q curves are similar to those for KCl + KF. The major difference is that they become almost linear at lower values of the surface charges. The effect of the stronger adsorption of Br^- than Cl^- is also evident in the isotherms. The isotherms for KCl + KF and KI + KF are similar in shape to the KBr + KF isotherms for $q < 0$. In the case of KI no data was taken above $q = -4$, for KCl the amount adsorbed at any concentration and charge is almost 40% less than for KBr. The change in the curvature of the isotherms has not been previously noted and at $q > 12$ appears to indicate that saturation is being approached. An attempt was made to determine the isotherm and the charge dependence of the standard free energy. The surface pressure versus ln x curves can not be superimposed on one common curve with the same accuracy

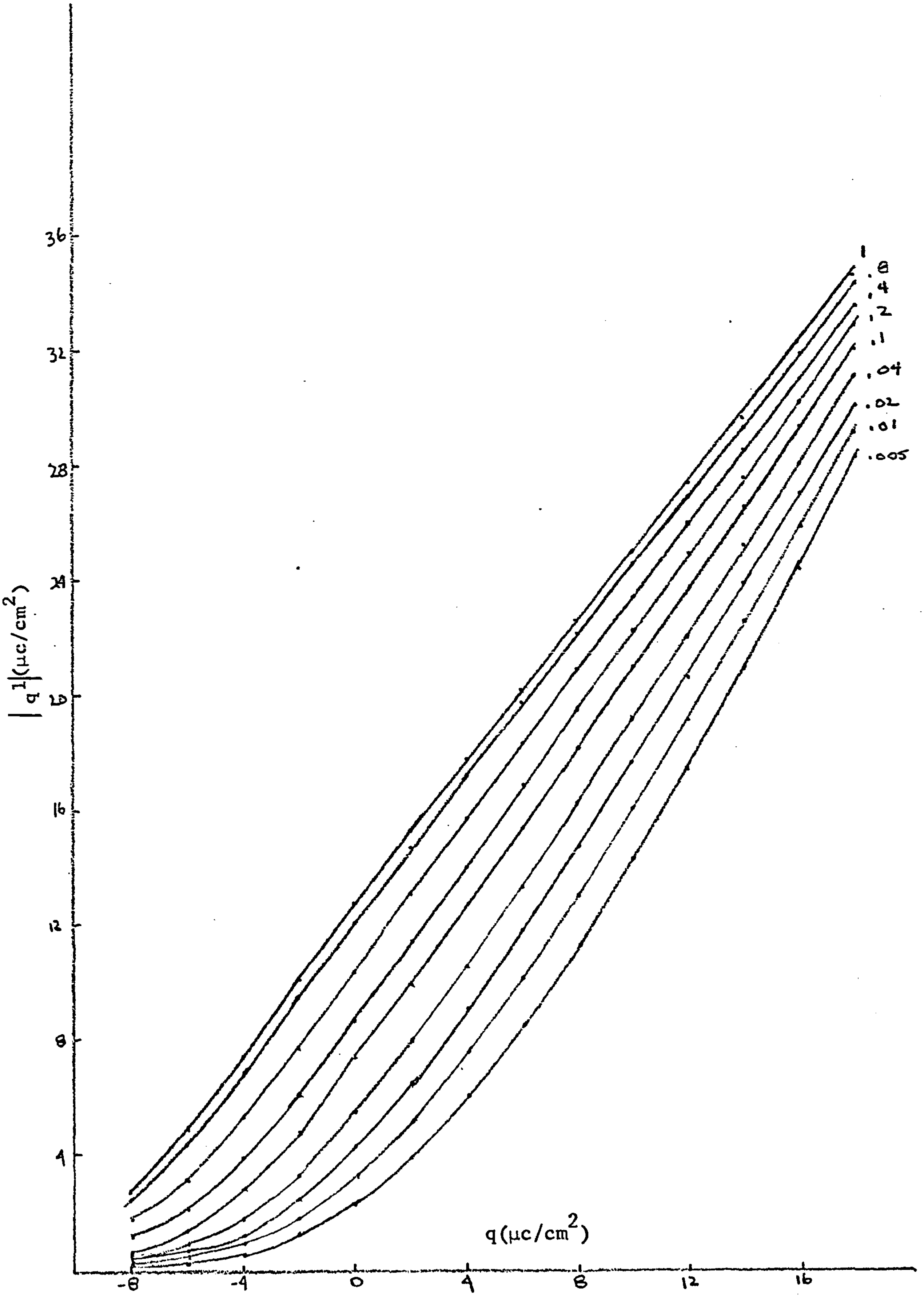

Figure 5. The Variation of The Amount Specifically Adsorbed with The Surface Charge Density at Constant Concentration for x MKBr + (1-x)MKF

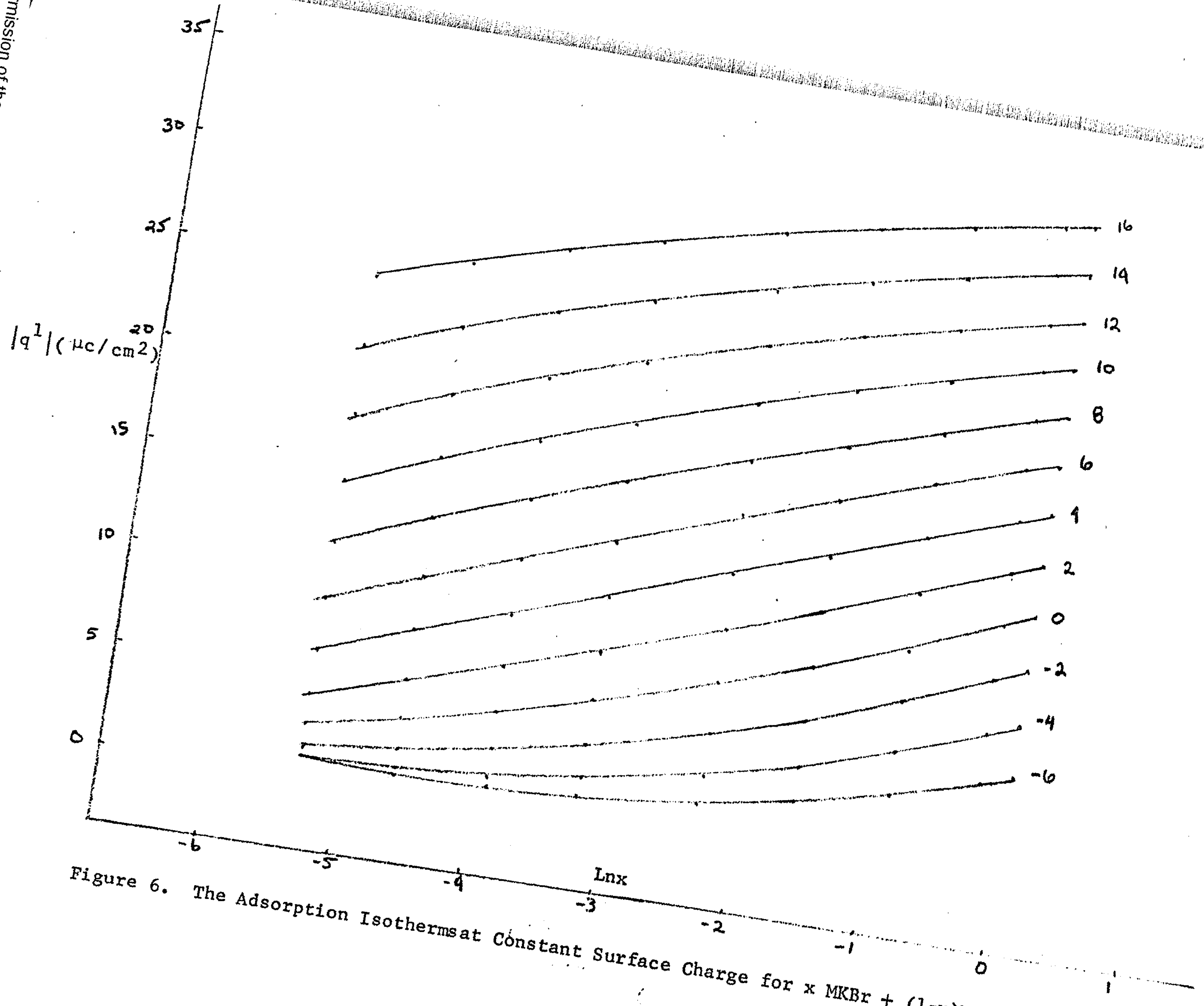

Figure 6. The Adsorption Isothermsat Constant Surface Charge for x MKBr + (1-x)MKF

as in the KCl-KF system. Payne claims that his deviations from a common curve using a virial isotherm are no greater than .2 ergs/cm^2. In this system deviations of up to 5 ergs/cm^2 occur at large $q > 8$ if the best possible curve is drawn. One explanation is that the isotherm constants are a function of the surface charge. Another is that the surface pressure method is inaccurate due to the ambiguities in chosing 1MKF as the base solution. To avoid the surface pressure problem, the virial isotherm was checked by plotting Γ_{Br^-} versus $\ln x/\Gamma_{Br^-}$ at constant q. As is evident in Figure 7, straight lines are not obtained. The low concentration values for q=-4, q=-6, can be disregarded because of the small value of q^1. If a virial isotherm were obeyed, the curves should be both linear and parallel. If one assumes that virial isotherm is obeyed but that B is not constant, it follows from Figure 7 that B is increasing with q at constant q^1 and increasing with $|q^1|$ at constant q. The increase in B with $|q^1|$ is quite reasonable and simply means that repulsion between adsorbed ions is occurring. The increase in B with increasing surface charge could only be explained by competitive adsorption of water. If it is harder for a bromide ion to displace a water molecule at large values of the surface charge than at low values, B will increase with the charge. Competitive adsorption results in a quadratic standard free energy and the fact that this system demonstrates quadratic behavior supports the above interpretation.

In Figure 8, the inner layer capacity is shown as a function of charge for several concentrations. The solutions not shown are virtually identical with the 1MKBr line. The concentration independence of C^i is also present in the KCl+KF system. In order to interpret the variation of C^i with q, the components of the capacity were determined. In Figure 9, ϕ^{m-2} is plotted against q^1 at constant q and the best straight line has been

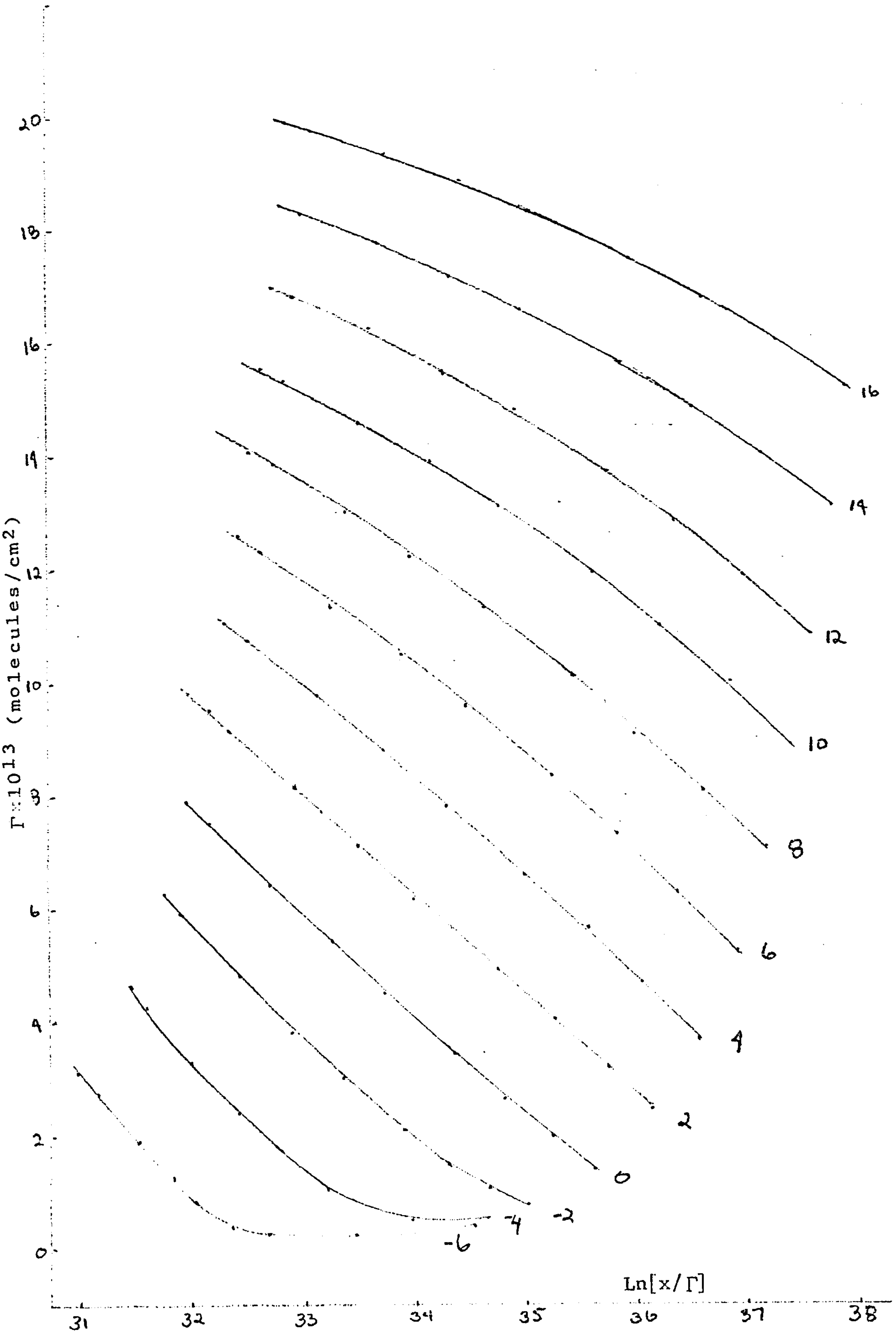

Figure 7. The Amount Specifically Adsorbed (Γ) Plotted as a Function of ln x/Γ for xMKBr + (1-x)MKF

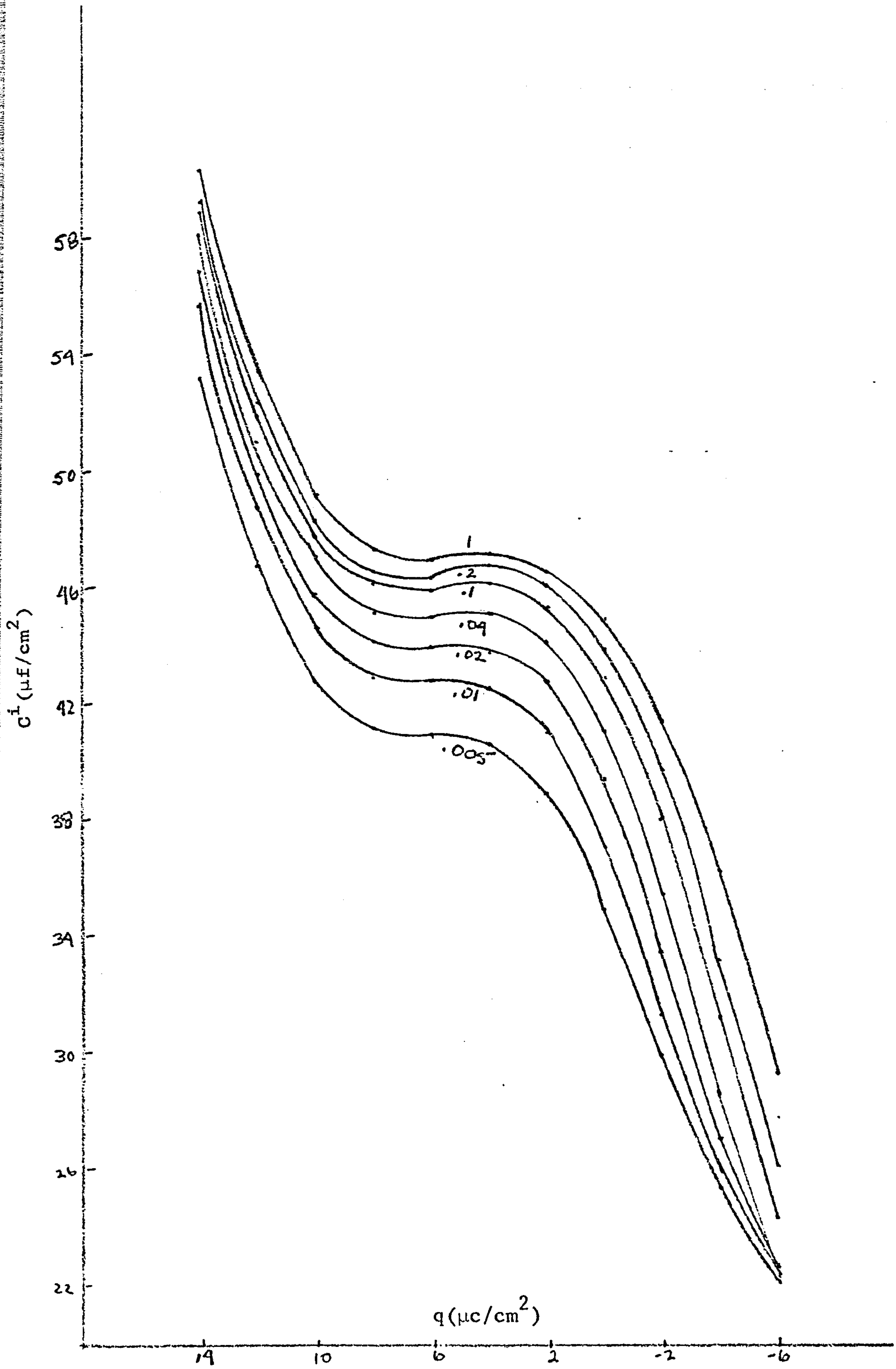

Figure 8. The Inner Layer Capacity of xMKBr + (1-x)MKF as a Function of Surface Charge Density

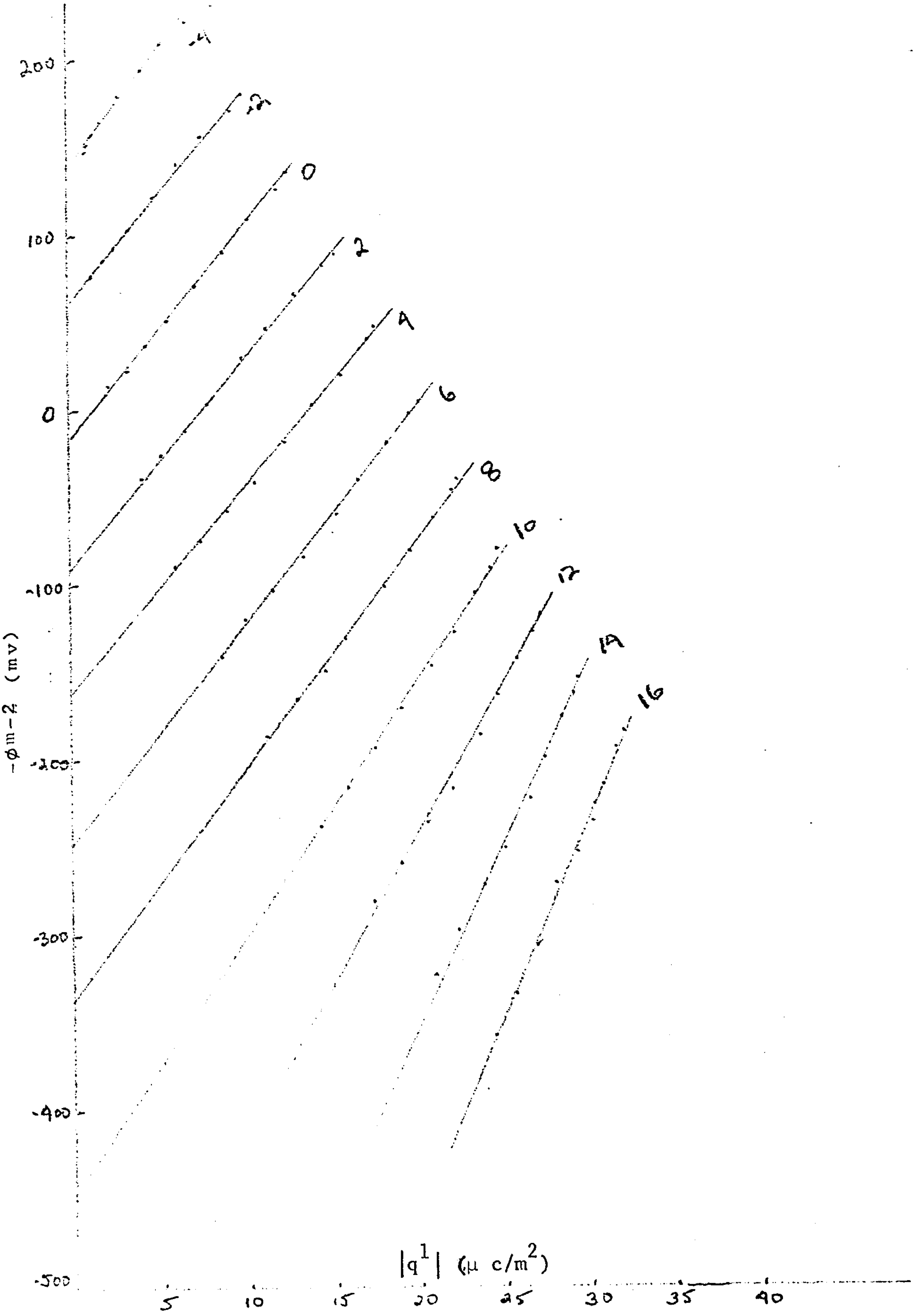

Figure 9. The Potential Across the Inner Layer Plotted as a Function of Specifically Adsorbed Cahrge for xMKBr + (1-x)MKF

drawn through the points. Though it is not apparent on this graph due to its scale, the points appear to lie on a parabola rather than a straight line. The equation for the components of the capacity is:

$$\frac{1}{C^{i}} = \frac{1}{{}_{q}C^{i}} + \frac{1}{{}^{1}_{q}C^{i}} \left(\frac{\partial q^{1}}{\partial q} \right)_{\mu}$$

$\left(\frac{\partial q^{1}}{\partial q} \right)_{\mu}$ was obtained by fitting the q^{1} versus q data to a cubic equation and obtaining its shape. These values were checked against the graphically determined values. ${}^{1}_{q}C^{i}$ is obtained either from the inverse of the slope of the lines in Figure 9, in which case it is equal to ${}^{1}_{q}K^{i}$ or from the inverse of the slope of a quadratic equation giving ϕ^{m-2} as a function of q^{1}. Both of these methods were used to evaluate ${}^{1}_{q}C^{i}$. The values of ${}^{1}_{q}K^{i}$ obtained from the Figure 8 are presented in Table 2.

Table 2

q	${}^{1}_{q}K^{i}$
-6	84.7
-4	80.0
-2	84.8
0	86.8
2	85.0
4	83.8
6	80.4
8	74.1
10	66.3
12	60.3
14	52.1

The decrease in ${}_{q}{}^{1}K^{i}$ with increasing charge would be explained by a decrease in $\epsilon/(x_2 - x_1)$ according to the present model. A decrease in either ϵ or x_1 seems perfectly reasonable, but no distinction between the two is possible. The intercept of ϕ^{m-2} at $q^1 = 0$ are not the ϕ^{m-2} values for 1MKF solution, so that if the model is valid, the lines must be curved at lower concentrations. The two sets of values for ${}_{q}{}^{1}C^{i}$ were used to obtain ${}_{q}C^{i}$. Figure 10 shows ${}_{q}C^{i}$ as a function of q for four concentrations where the linear value of ${}_{q}{}^{1}C^{i}$ were used. In Figure 11, the quadratic values were used. The most important point is that independent of the method used, ${}_{q}C^{i}$ has a distinct peak in the region $q = 0$ to $q = 4$. This peak can not be due to specific adsorption since the peak height and position are virtually independent of concentration and therefore of specific adsorption. In Figure 11, ${}_{q}C^{i}$ remains independent of the amount of specific adsorption even at large values of the surface charge whereas the curves in Figure 10 are different in this region. A peak in ${}_{q}C^{i}$ which is independent of q^1, must be due to some alteration of the interaction between the electrode and the solvent. As mentioned previously, ${}_{q}C^{i}$ is independent of concentration in KI solutions. In the KCl+KF system, ${}_{q}K^{i}$ decreases as $|q^1|$ increases at constant q. It follows that if ${}_{q}K^{i}$ is plotted against q at constant concentration, the curves at higher concentrations are lower. In the KI system, ${}_{q}K^{i}$ is independent of concentration and increases with increasing charge. In KBr+KF, ${}_{q}K^{i}$ is independent of concentration when $q < +4$. At larger values of the surface charge, ${}_{q}K^{i}$ eventually begins to increase depending on the concentration. The variation of ${}_{q}K^{i}$ with surface charge at constant concentration is shown in Figure 12 for three concentrations. The increase in ${}_{q}K^{i}$ with increasing q^1 is evident from the vertical distance between the curves in the

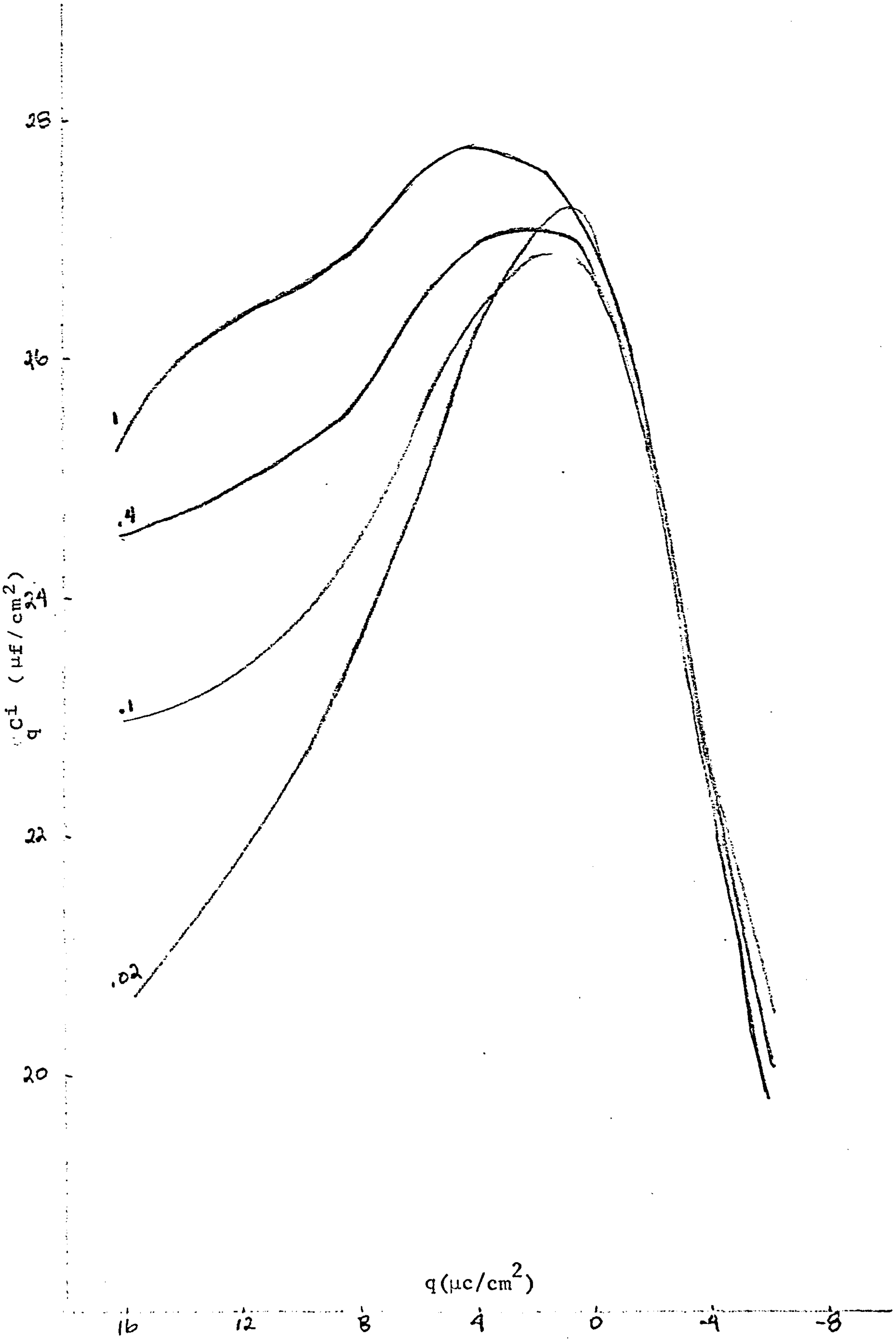

Figure 10. The Differential Capacity at Constant Amount Adsorbed as a Function of Surface Charge Density for xMKBr + (1-x)MKF Using Values of $_1C^i$ Determined from Figure 9.

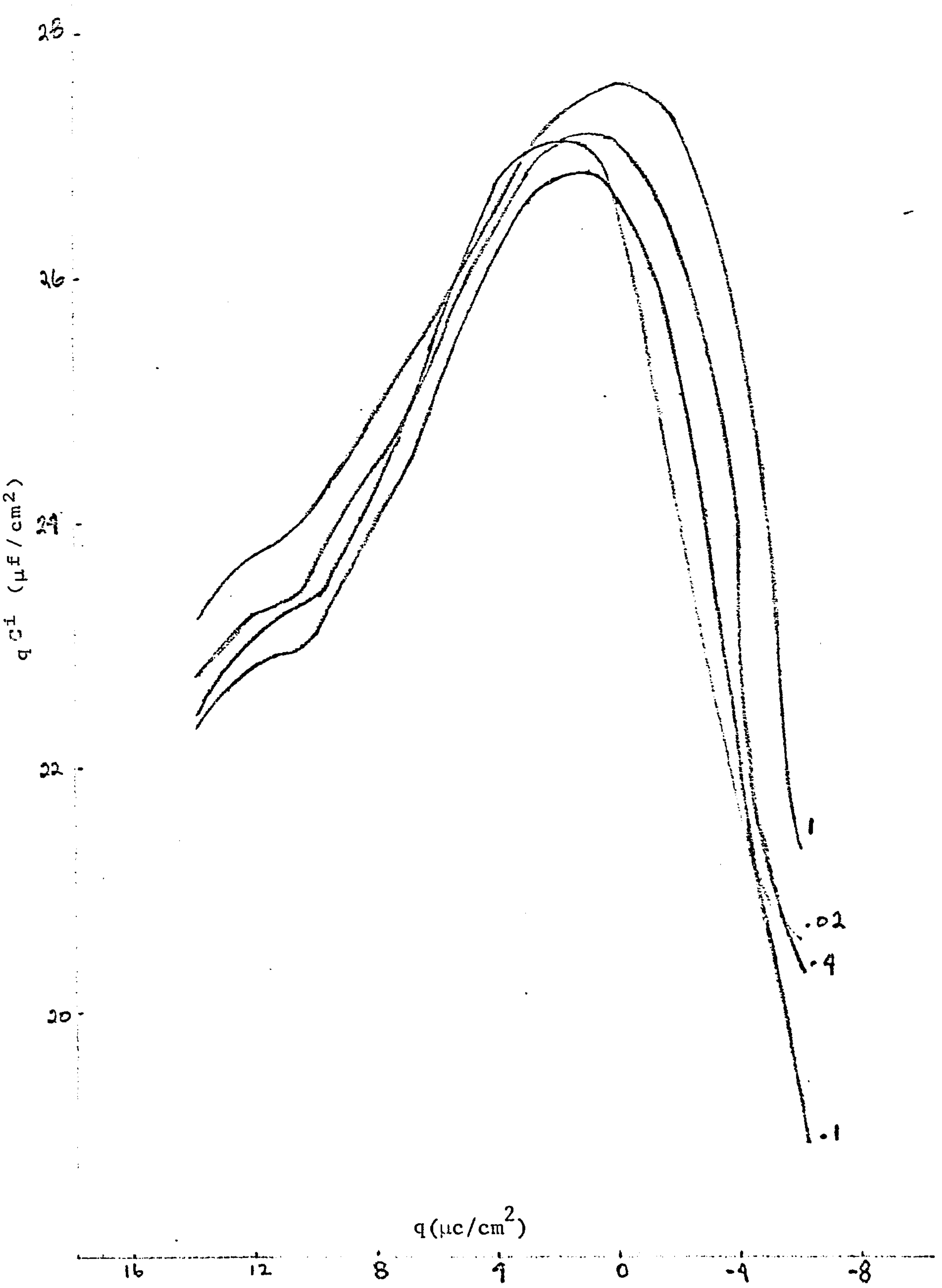

Figure 11. The Differential Capacity at Constant Amount Adsorbed as a Function of Surface Charge Density for xMKBr + (1-x)MKF Using Values of $^{1}C^{i}$ Determined by Program III

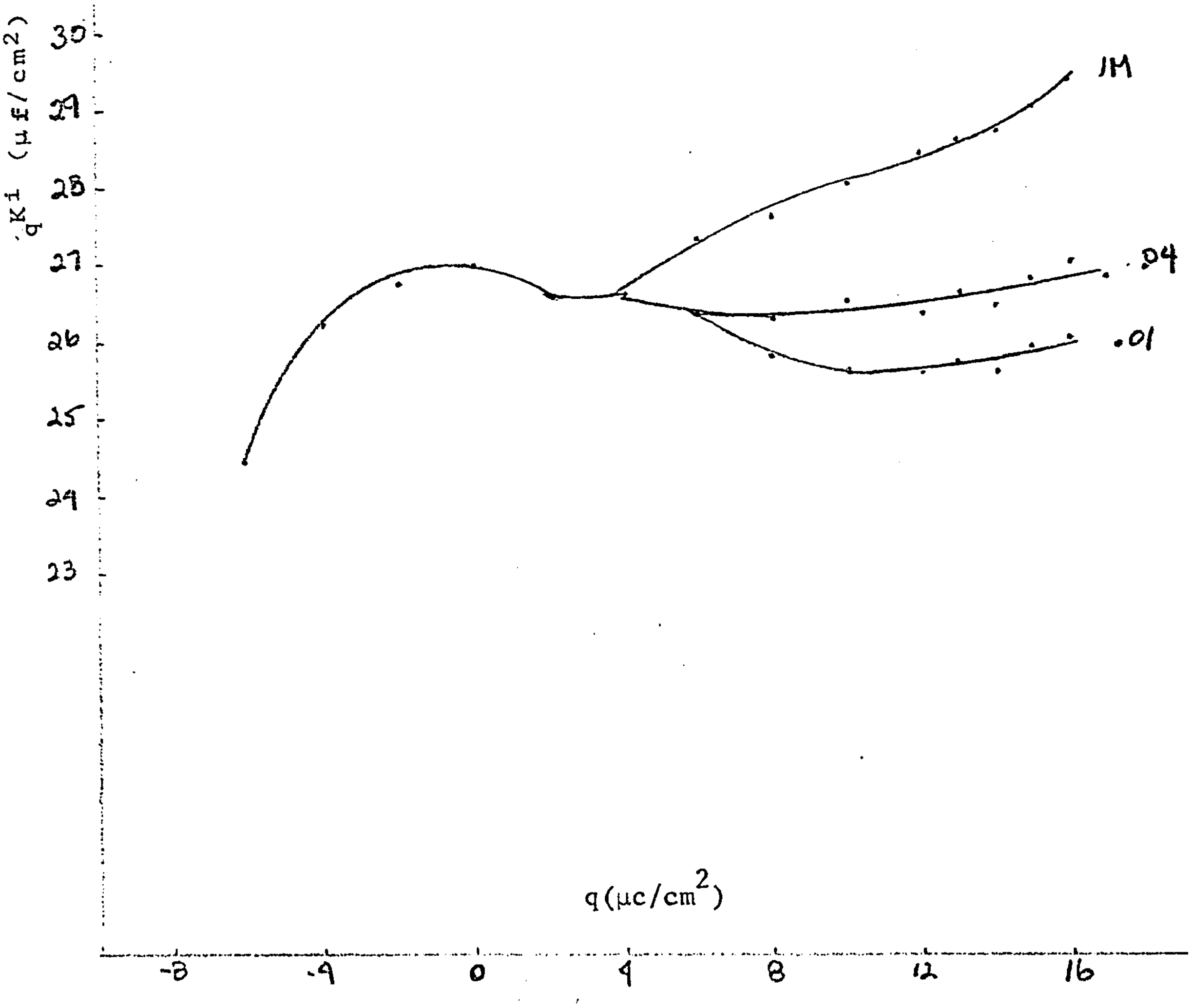

Figure 12. The Integral Capacity at a Constant Amount Adsorbed as a Function of Surface Charge Density for xMKBr + (1-x)MKF

anodic region. There is no convincing argument to explain the different behavior of the three systems.

As derived in the theoretical section, the equation relating the capacity to the isotherm is the following.

$$-\Delta \frac{1}{C^i} = -k\,T\left[\left(\frac{\partial \ln\beta}{\partial q}\right)^2 \frac{\partial|q^1|}{\partial \ln\beta} + |q^1|\,\partial^2 \frac{\ln\beta}{\partial q^2}\right]$$

We have also shown that $-\Delta \frac{1}{C}$ should reach a limiting value for large values of Γ if a virial isotherm is obeyed..In Figure 13, $-\Delta \frac{1}{C^i}$ has been plotted against $|q^1|$ at constant charge. The curves for $q > 6$ represent amounts of specific adsorption greater than those observed by Payne. Payne ascribed the decrease in the limiting value with increasing q to the neglect of the second term in the brackets which is negative. Let us assume $\ln\beta$ may be written as follows:

$$\ln\beta = \ln\beta_{max} + a\,q - \frac{b}{2}\,\delta^2$$

$$|a| \gg |b| \qquad \delta = (q - q_o)$$

Our equation for $-\Delta \frac{1}{C}$ is then

$$-\Delta \frac{1}{C^i} = k\,T\left[a^2 \frac{\partial|q^1|}{\partial \ln\beta} - b\,|q^1|\right]$$

where we have set $\frac{\partial \ln\beta}{\partial q} = a$ and q_o is a constant value of q. This equation will still give a limiting value of $-\Delta \frac{1}{C^i}$ if $|q^1|$ is not too large. The curves at higher q also appear to approach a limiting value, though now at progressively lower values of B if we assume a and b are constant. We have already shown that if a virial isotherm is assumed, B increases with increas-

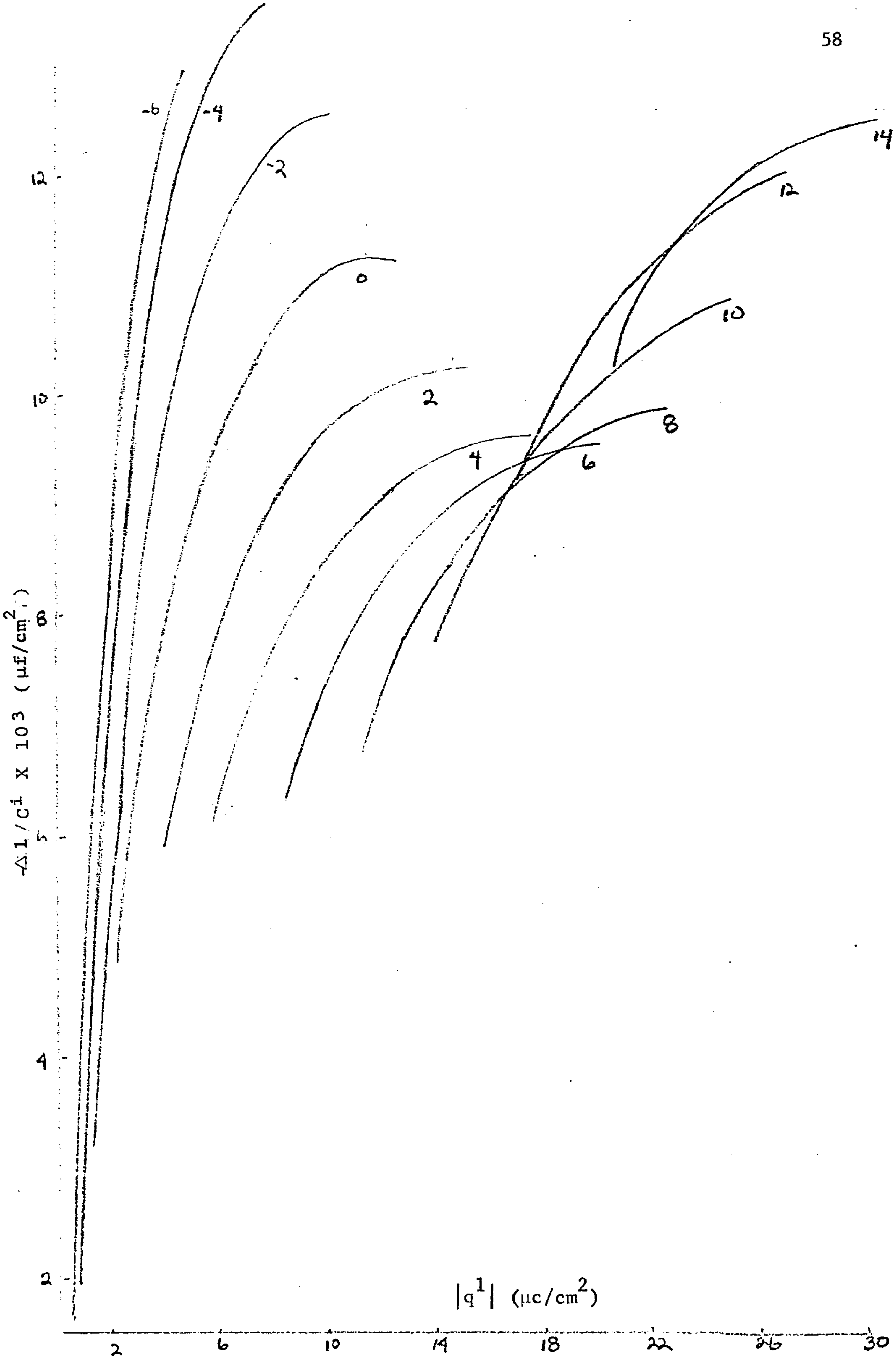

Figure 13. $-\Delta 1/C^i \times 10^3$ Plotted Against the Amount Adsorbed at Constant Surface Charge Density

ing charge. One could also assume that a increases faster with increasing charge than B which would give a higher value of $-\Delta \frac{1}{C^i}$ at the limit since

$$-\Delta \frac{1}{C^i} = \frac{k\ T\ a^2}{2B}$$

We also investigated the possibility that at high values of q, the KBr + KF system might begin to behave like the KI - KF system. In the KI+KF system, a Henry's law isotherm is obeyed. That is, if we assume the following isotherm:

$$|q^1| = \beta\ C\ K$$

C = concentration

K = constant

$$\frac{\partial \ln\beta}{\partial q} = a$$

$$-\Delta \frac{1}{C} = k\ T\ a^2\ K\ \beta\ C$$

In this case the curves are straight lines at constant charge when plotted against concentration and the slope increase with increasing charge. A plot of $-\Delta \frac{1}{C^i}$ versus concentration for this system does not give straight lines except at high concentrations. Figure 14 is a plot of $-\Delta \frac{1}{C}$ versus $|q^1|$ at constant q. It is included to demonstrate that the choice between $\Delta \frac{1}{C^i}$ and $\Delta \frac{1}{C}$ is not trivial and requires more justification than it has received. Figure 15 is a plot of $-\Delta \frac{1}{C^i}$ versus q at constant concentration and Figure 16 a plot of $-\Delta \frac{1}{C^i}$ versus $|q^1|$ at constant concentration. The KCl + KF system shows the same behavior for $q < 6$ except that the peak occurs at $0 < q < 4$ depending on the concentration whereas here it occurs

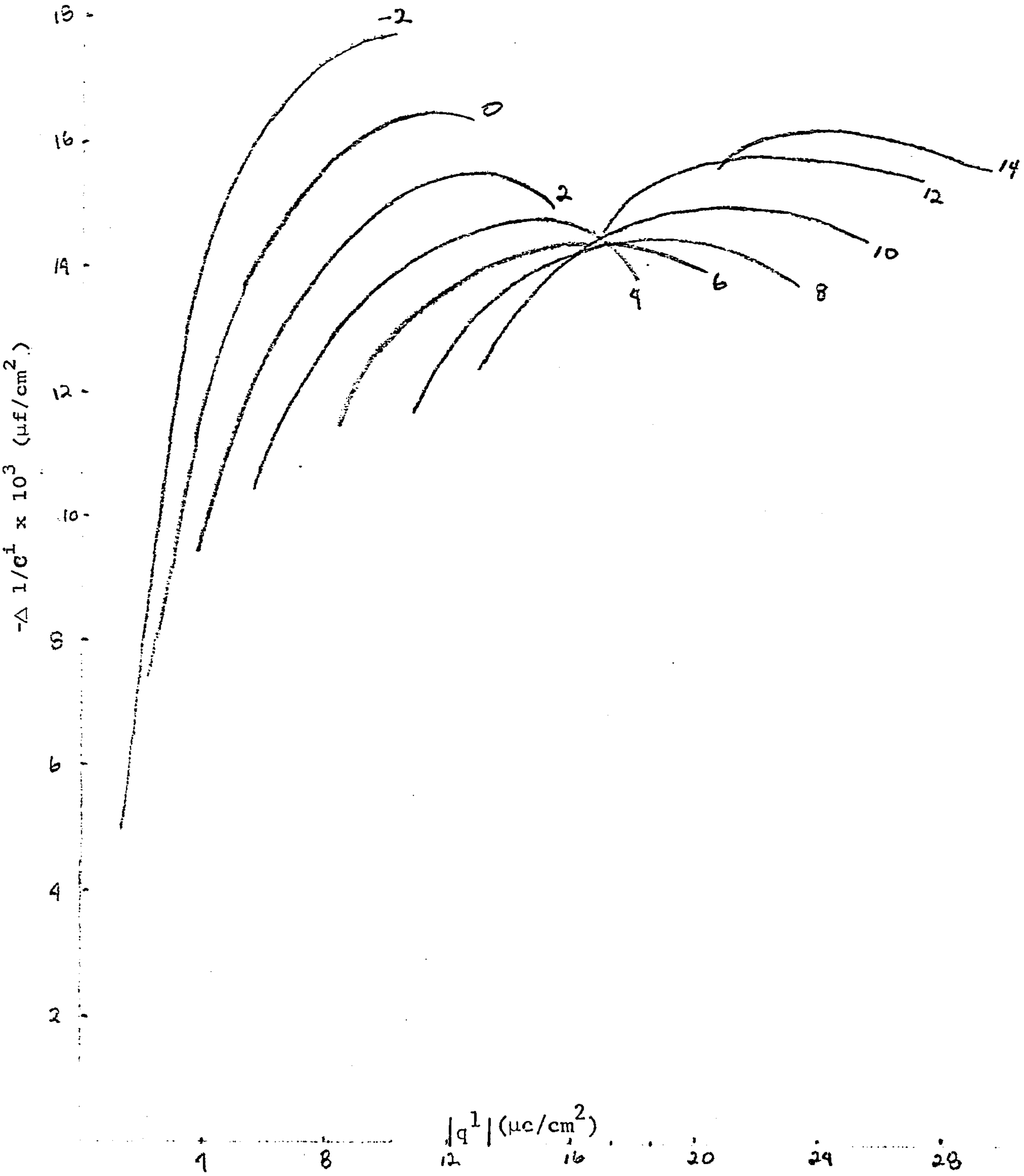

Figure 14. $-\Delta\ 1/C^i \times 10^3$ Plotted Against the Amount Adsorbed at Constant Surface Charge Density

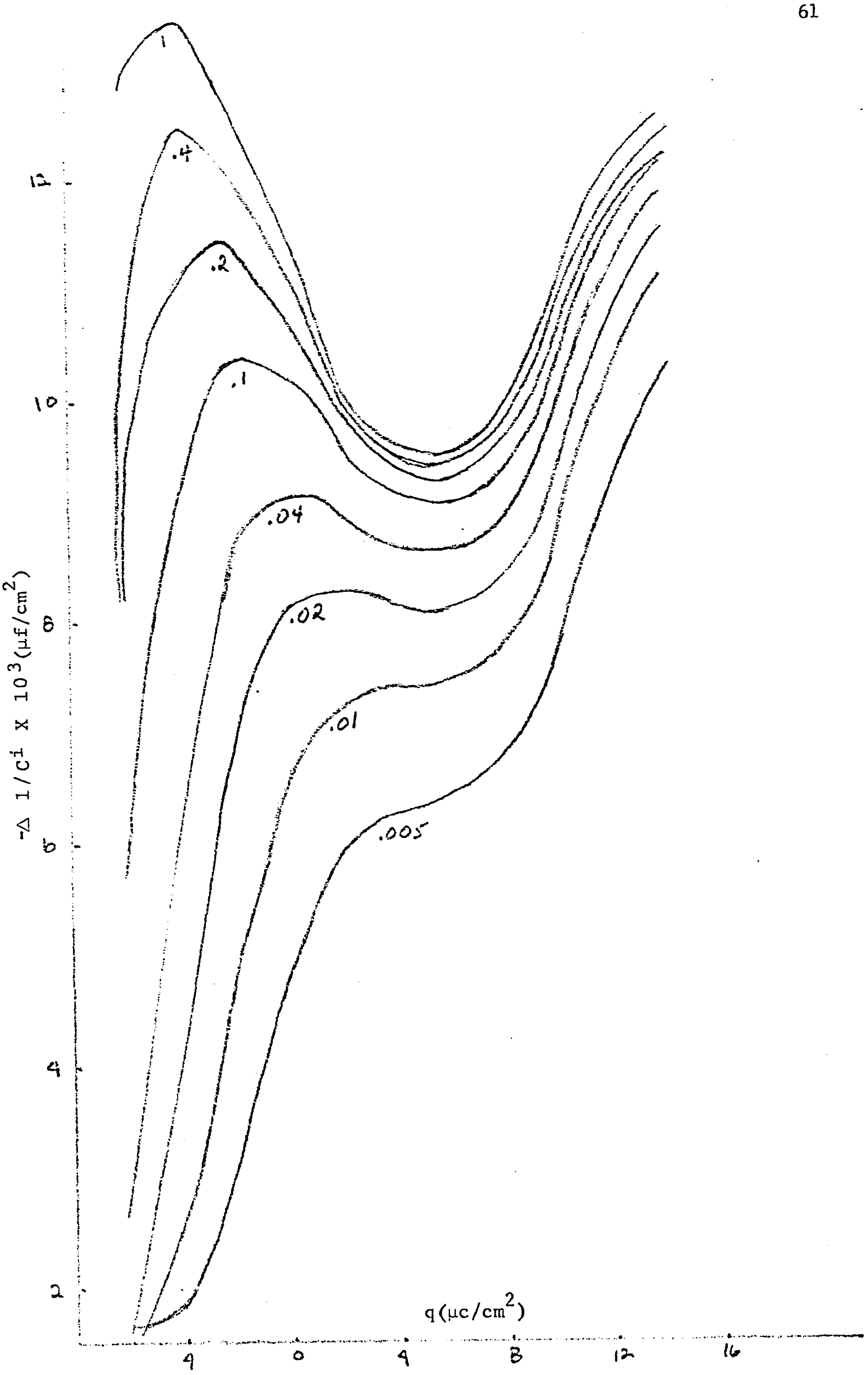

Figure 15. -Δ $1/C^i$ x 10^{-3} Plotted Against the Surface Charge Density at

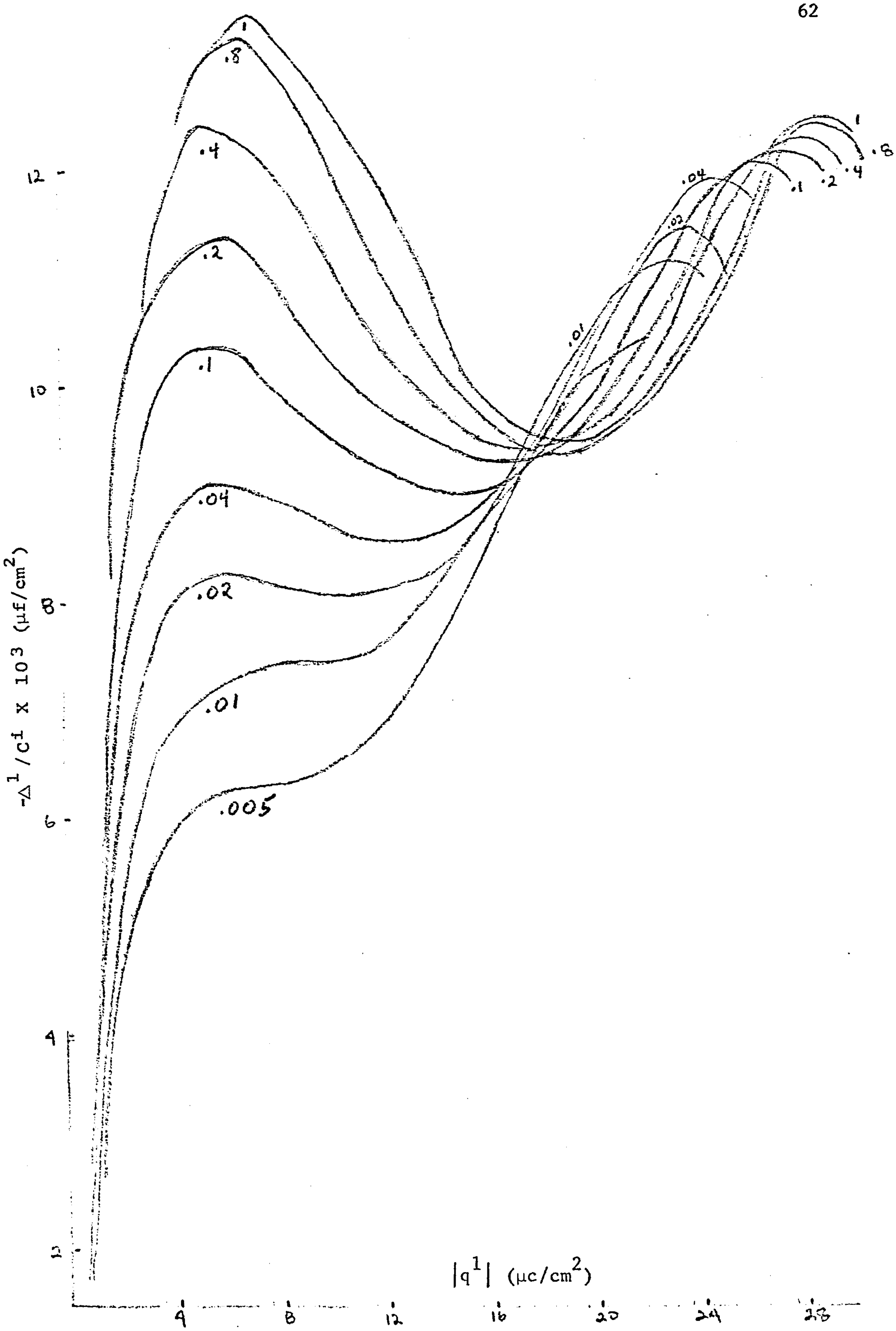

Figure 16. $-\Delta\ 1/C^i \times 10^3$ Plotted Against the Amount Specifically Adsorbed at Constant Concentration for xMKBr + (1-x)MKF

at $- 4 < q < 0$. This is no doubt due to increased adsorption. The increase for $q > 6$ or $|q^1| > 18$ is not found in KCl + KF. As discussed previously, the existence of two peaks is indicative of a quadratic standard free energy of adsorption. For a purely quadratic $\ln\beta$, $- \Delta \frac{1}{C}$ must change sign which is not the case either here or with KCl + KF. Our equation for $\ln \beta$ would result in two peaks and a minimum all at positive values of $- \Delta \frac{1}{C}$, but there really is very little justification in pushing the analysis any further.

Conclusion

The adsorption of KBr from KBr + KF has been shown to be similar to KCl from KCl + KF if the data in the same range of specifically adsorbed charge are compared. The results at large values of q^1 have not previously been observed for halide systems. They can be explained by assuming a standard free energy with both a linear and quadratic terms and variable isotherm parameters. This obviously leaves much to be desired, but nothing further can be done with the present state of the theory. The bromide and chloride results strongly imply that the simpler picture for the iodide ion is due to the limited range of surface charge which was studied.

IV. THE ADSORPTION OF 6-AMINO-HEXANOIC ACID

Introduction

The adsorption of neutral molecules with permanent dipole moments have previously been studied. The most complete investigations have been for thiourea in aqueous solution,[15,28] and in formamide.[29] The sulfur in thiourea is strongly bound to the mercury surface at all but large negative surface charges. This gives the adsorption many of the characteristics of anion adsorption. The purpose of this experiment was to study the adsorption of a permanent dipole formed by two full charges which does not have a strong chemical interaction with mercury. Three amino acids: glycine, 4-amino-butyric acid, and 6-amino-hexanoic were chosen. All are zwitterions in neutral solutions. Preliminary work indicated that glycine and 4-amino-butyric acid are virtually unadsorbed. The electrocapillary curve for .3M glycine in 1MKF and the value of Ez(-.479v) indicated that adsorption was minimal. The differential capacity curve for 4-amino butyric acid (.15M4AB + .5MKF) also indicated very slight adsorption. For this reason the only system studied in detail was 6-amino-hexanoic acid.

Experimental

Eight solutions of xM6AH + .5MKF were investigated. The amino acid was purified by dissolving it in water and precipitating it with alcohol three times. The first precipitate to appear and that remaining after total precipitation were discarded. The differential capacity, the streaming electrode potential, and the surface tension at Ez were measured for each solution. This data is recorded in Table II of the appendix.

Results

The differential capacity curves for xM6AH + .5MKF are presented in Figure 17. The inner layer capacity for .5MKF is shown in Figure 18. A comparison of Figures 2 and 18 or of Table III and IV confirms the lack of specific adsorption in KF solutions. The maximum difference in C^i is less than $.3\mu f/cm^2$. This is also the maximum difference between our values and Payne's and is probably due to using different capillaries. Programs I and II were used as discussed in the Appendix except that Program II was changed to a quadratic fit of ξ to ln x., and values of Γ are not as reliable as the value of q^1 in the previous system. This is due to the smaller total variation of ξ with ln x at constant q. Our original assumption was that this system would show two regions of maximum adsorption. One would correspond to the positive end of the dipole being adsorbed at negative surface charges and the other to the negative end being adsorbed at positive surface charges. This did not turn out to be the case; rather the maximum adsorption at each concentration occured at $q = -6$. Figure 19 shows the constant charge isotherm for several concentrations. The data do not fit a virial isotherm and the surface pressure values are too low to attempt to fit a Frumkin isotherm. The .01M values are not used in any of the figures, since Program II gave negative values of Γ for some values of q. This is due to ξ being almost constant at low concentration.

Further analysis of the data is in line with maximum adsorption occuring at $q = -6$ and with a quadratic free energy of adsorption. We will begin with the equation for $-\Delta$ 1/C.

$$-\Delta \frac{1}{C} = - kT[\Gamma b - b^2 \delta^2 \left(\frac{\partial \Gamma}{\partial \ln \beta} \right)_\mu]$$

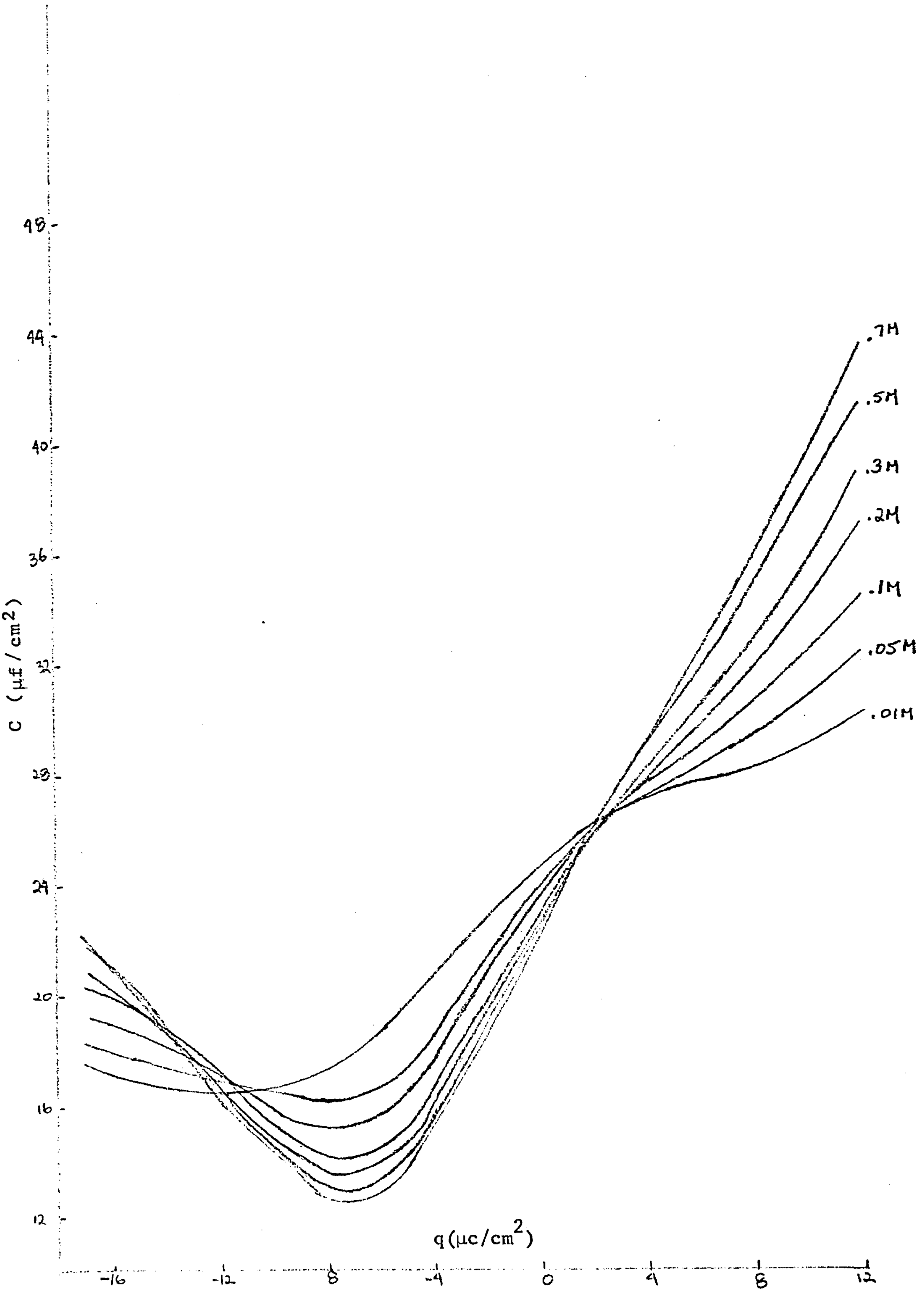

Figure 17. The Differential Capacity of x M 6-amino Hexanoic + .5MKF Acid Plotted as a Function of the Surface Charge Density

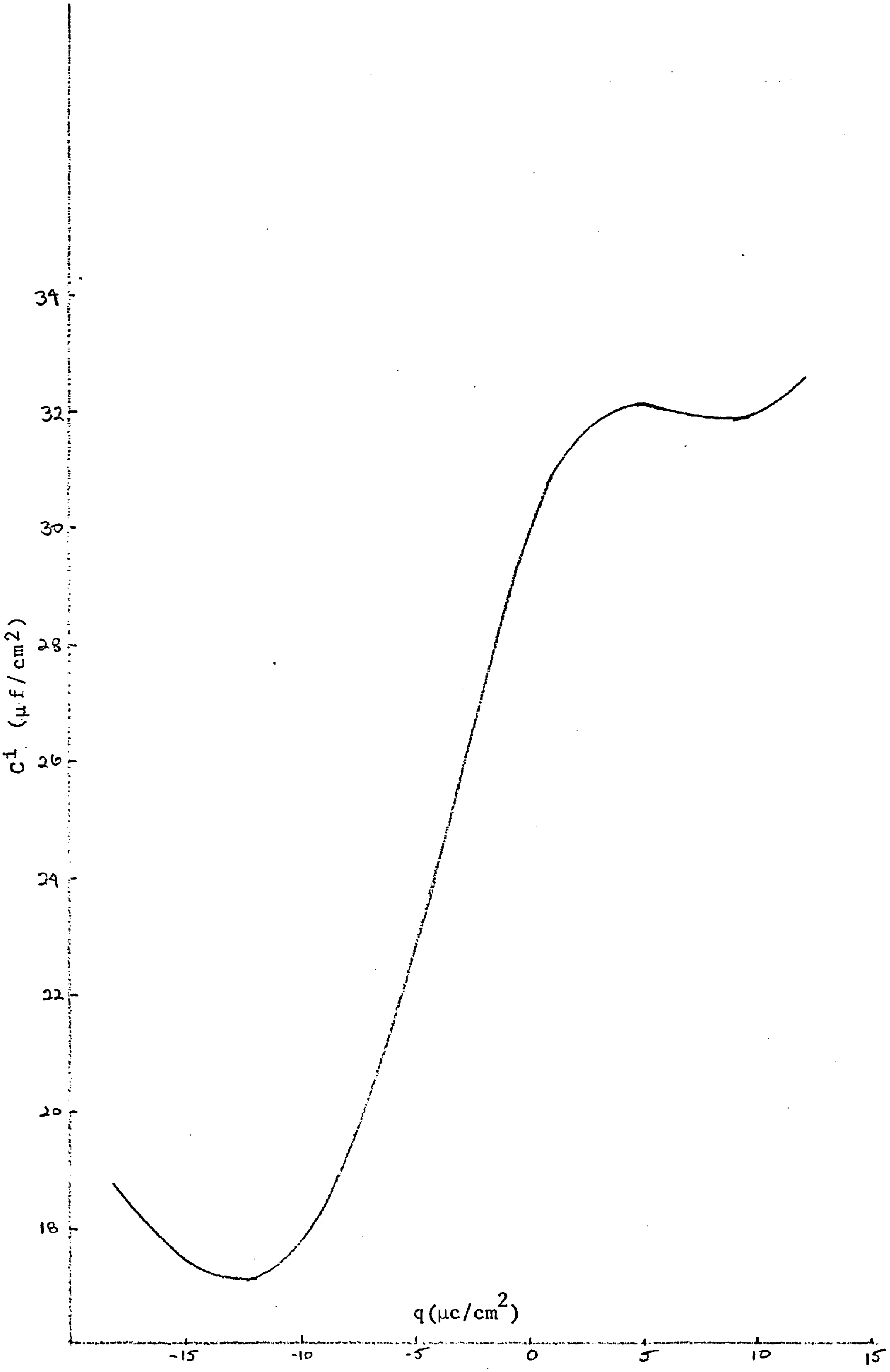

Figure 18. The Inner Layer Capacity of .5MKF Plotted as a Function of The Surface Charge Density

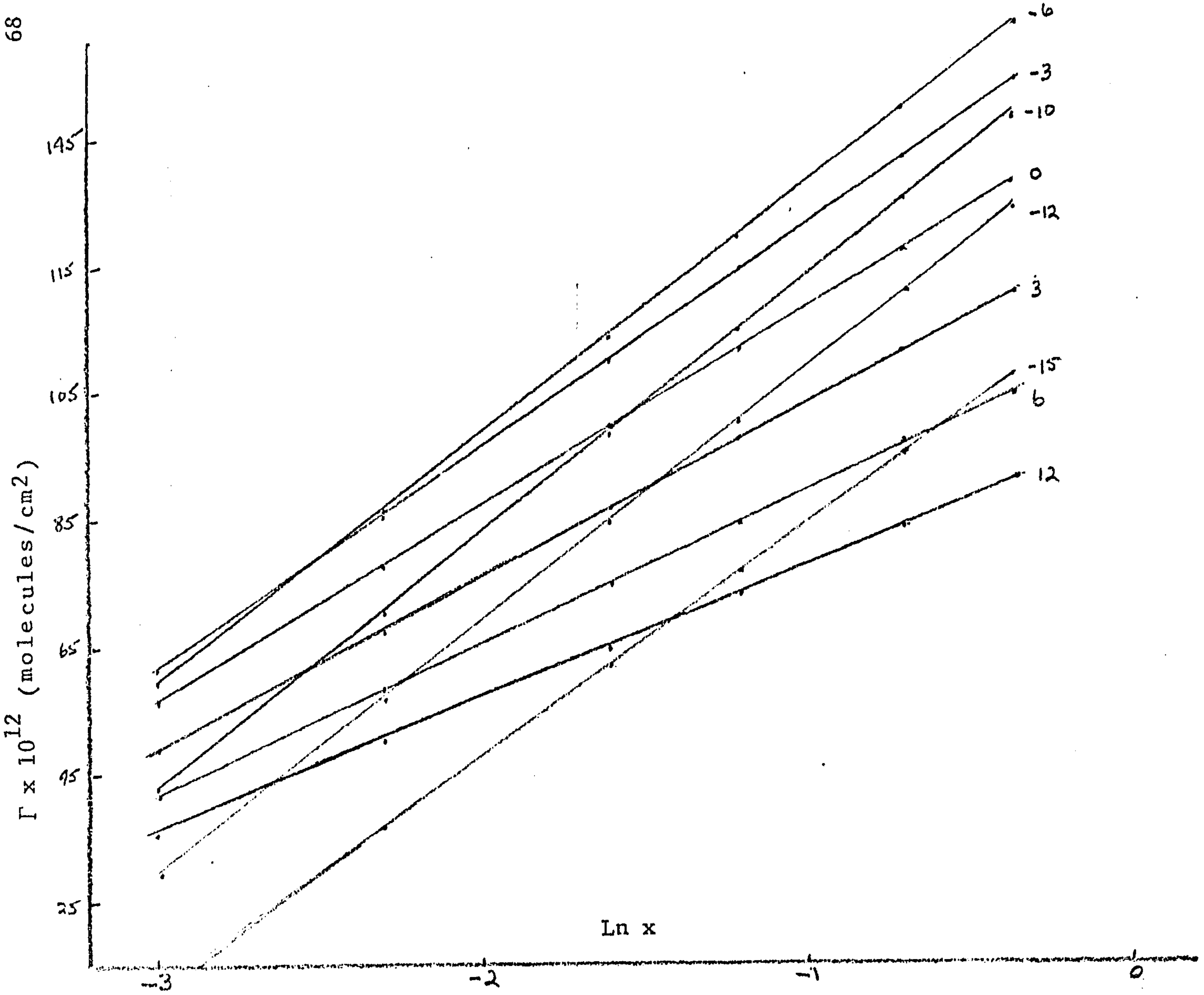

Figure 19. The Amount of xM6-Amino Hexanoic Acid ($\Gamma \times 10^{12}$) Plotted as a Function of ln x at Constant Surface Charge

assuming

$$\ln \beta = \ln \beta_{\max} - \frac{b}{2} \delta^2$$

$$\delta = q - q_{\max}$$

In Figure 20, $-\Delta\ 1/C$ is plotted against q for four different concentrations. In this system there is no ambiguity concerning C since C^d is the same in the base solution as in the mixed solution at constant q. $\Delta \frac{1}{C}$ therefore equals $\Delta\ 1/C^i$. As the equation for $\Delta\ 1/C$ predicts, the minimum occurs at $q = -6$, $\delta = 0$ and becomes more negative with increasing Γ. In the range of charge available, desorption is not complete so that the curves do not return to $\Delta \frac{1}{C} = 0$ but are still part of the desorption peaks. Figure 21 is a plot of $-\Delta\ 1/C$ versus Γ at constant. q. As expected, the curve at $q = -6$ has the minimum slope which will equal -kTb. The quadratic form of $\ln \beta$ is again supported by the plots of ϕ^{m-2} versus Γ in Figure 22. We begin by recognizing that for the adsorption of a neutral compound[30]

$$\phi^{m-2} = E - E^b \qquad q = \text{const}$$

since

$$E = \phi^{m-2} + \phi^2 - \phi^{ref}$$

$$E^b = \phi_b^{m-2} + \phi_b^2 - \phi^{ref}$$

and

$$\phi^2 = \phi_b^2$$

$$E - E^b = \phi^{m-2} - \phi_b^{m-2} \qquad q = \text{constant}$$

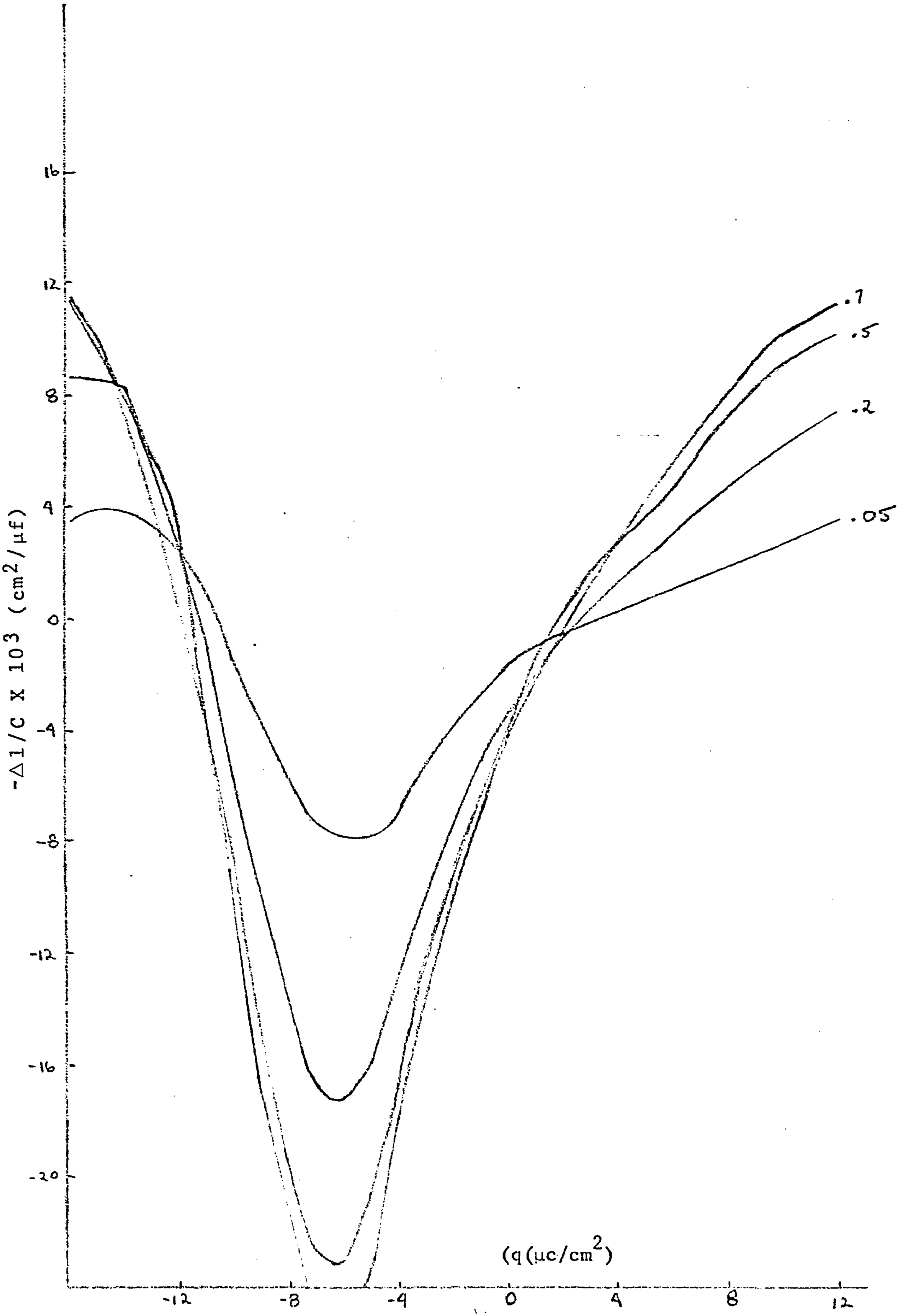

Figure 20. -Δ 1/C x 10^3 Plotted as a Function of The Surface Charge at Constant Concentration for xM 6-amino Acid + .5MKF

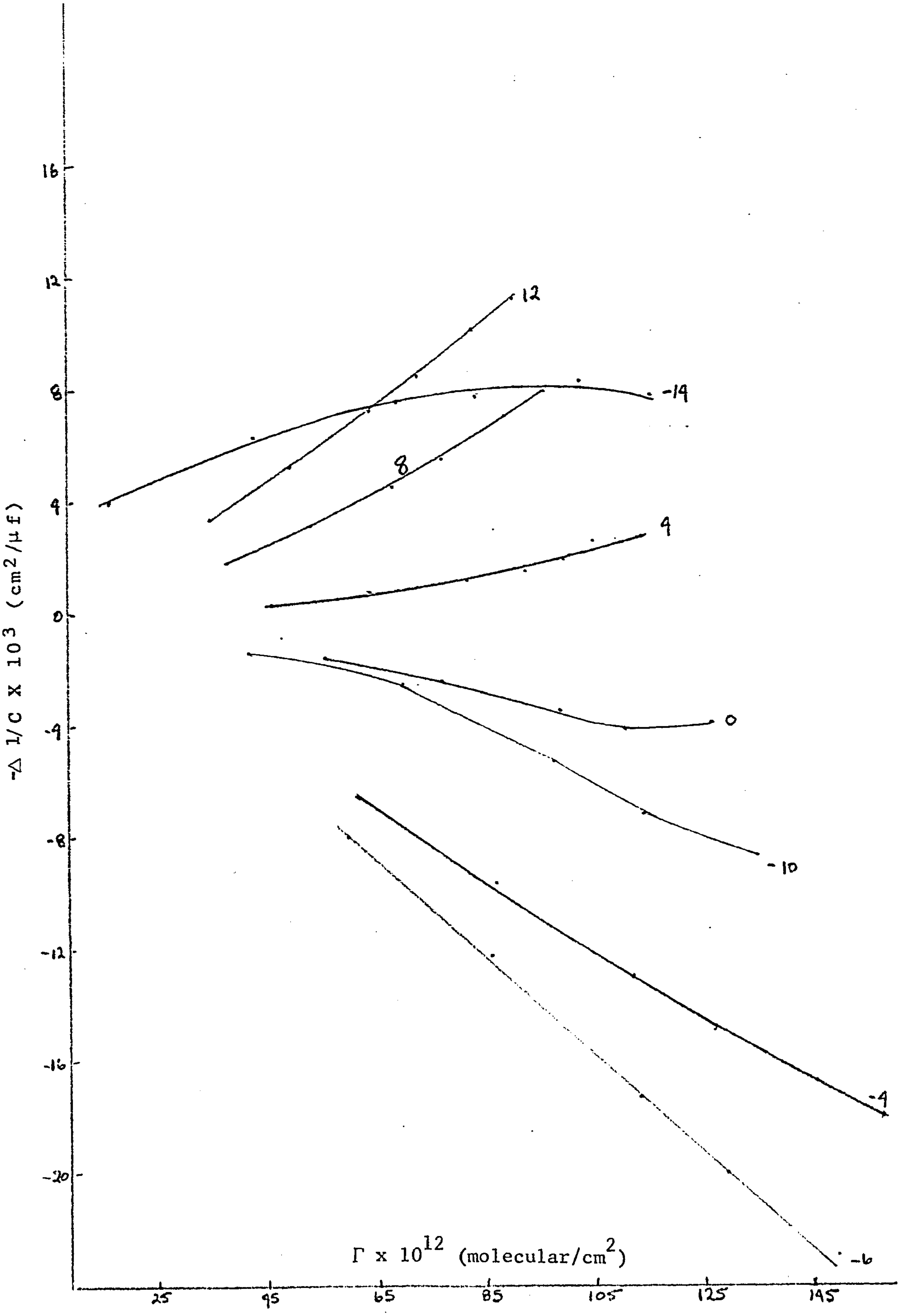

Figure 21. $-\Delta$ 1/C x 10^3 Plotted as a Function of The Amount Adsorbed at Constant Surface Charge for xM 6-amino Hexanoic Acid + .5MF

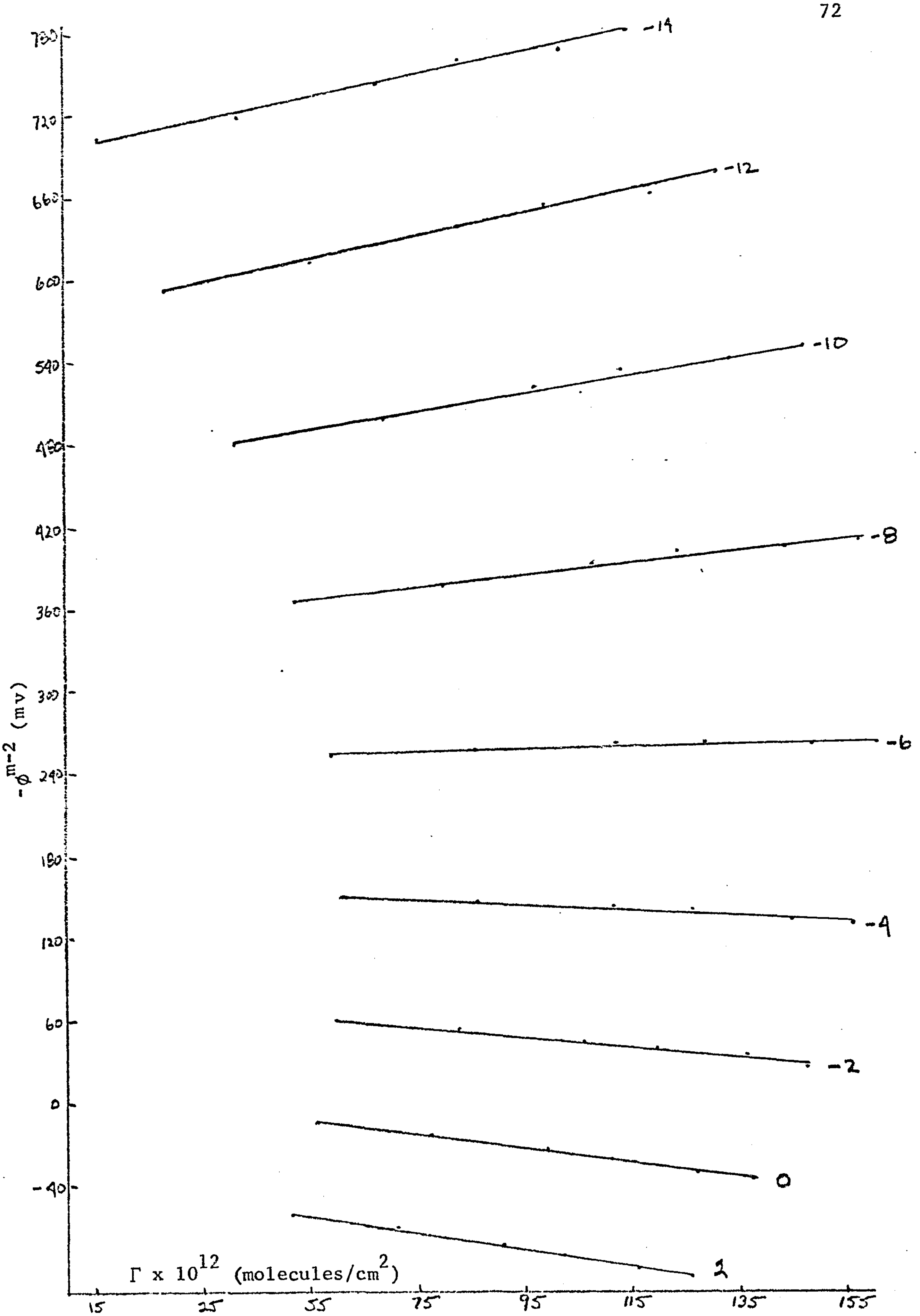

Figure 22. The Potential Across the Inner Layer ($-\phi^{m-2}$) Plotted as a Function of the Amount Adsorbed (Γ) at Constant Surface Charge

Parsons neglects ϕ_b^{m-2} which will change with q. This is justifiable if ϕ^{m-2} can be separated into two terms.

$$\phi^{m-2} = \phi_\Gamma^{m-2} + \phi_b^{m-2}$$

ϕ_Γ^{m-2} is that part of ϕ^{m-2} due to adsorption. We have previously shown that

$$\Delta E = E - E^b = -kT\Gamma \frac{\partial \ln \beta}{\partial q}$$

therefore

$$\phi^{m-2} = -kT\Gamma \frac{\partial \ln \beta}{\partial q}$$

$$\left(\frac{\partial \phi^{m-2}}{\partial \Gamma}\right)_q = -kT \frac{\partial \ln \beta}{\partial q}$$

In Figure 22, $\left(\frac{\partial \phi^{m-2}}{\partial \Gamma}\right)_q = 0$ at $q = -6$.

Assuming

$$\delta = q + 6$$

$$\left(\frac{\partial \phi^{m-2}}{\partial \Gamma}\right)_q = kTb(q + 6)$$

This model is correct except at large positive values of q where either b is getting smaller or one of the other assumptions is no longer tenable. Actually if b is notconstant, we do not have congruent isotherms and the analysis is no longer rigorous.

Conclusion

Within the range of surface charge available, 6-amino-hexanoic acid is maximally adsorbed at $q = -6$ with a quadratic standard free energy of adsorption. A quadratic standard free energy of adsorption is to be expected for a point dipole. In this case, the distance between the amino and carboxyl groups is much larger than the inner layer which is only 3-5 Å. It was therefore expected that the system would demonstrate the characteristics of ionic adsorption. It was our expectation that adsorption would be maximal at large absolute values of the surface charge density and that the molecule would reorient itself in the vicinity of the point of zero charge. The quadratic charge dependence implies that adsorption should be considered to occur in the entire double layer rather than be restricted to the inner layer for only then does the point dipole model make sense. The entire double layer for a .5MKF solution has a thickness of 40-50 Å. In line with the quadratic charge dependence, one must assume that water is preferentially adsorbed as $|q + 6|$ becomes large.

V. Bibliography

1. David M. Mohilner, "The Electrical Double Layer", Electroanalytical Chemistry, ed., A. J. Bard, (New York, Marcel Dekker Inc., 1966), Vol. 1, pp. 241-409.

2. Paul Delahay, Double Layer and Electrode Kinetics, (New York: Interscience, 1966).

3. J. A. Harrison, J. E. R. Randles, D. J. Schiffrin, J. Electroanal. Chem., Vol. 25, 1970, pp. 197-207.

4. Roger Parsons, J. Electroanal. Chem., Vol. 8, 1964, pp. 93-98.

5. E. Dutkiewicz, J. D. Garnish, R. Parsons, J. Electroanal. Chem., Vol. 16, 1968, pp. 505-515.

6. Roger Parsons, F. G. R. Zobel, J. Electroanal. Chem., Vol. 9, 1965, pp. 333-348.

7. David C. Grahame, J. Amer. Chem. Soc., Vol. 76, 1954, pp. 4819-4823.

8. David C. Grahame, J. Amer. Chem. Soc., Vol. 79, 1957, pp. 2093-2098.

9. Roger Parsons, "The Esin and Markov Effect", Proceedings of the Second International Congress on Surface Activity, ed., J. H. Schulman, (London: Butterworths, 1957), Vol. 3, pp. 38-44.

10. Roger Parsons, Trans. Faraday Soc., Vol. 55, 1959, pp. 999-1006.

11. J. M. Parry, R. Parsons, Trans. Faraday Soc., Vol. 59, 1963, pp. 241-256.

12. D. C. Grahame, R. Parsons, J. Amer. Chem. Soc., Vol. 83, 1961, pp. 1291-1296.

13. R. Payne, J. Phys. Chem., Vol. 69, 1965, pp. 4113-4123.

14. R. Payne, J. Phys. Chem., Vol. 70, 1966, pp. 4113-4123.

15. Roger Parsons, Proc. Royal Soc., Vol. 261, 1961, pp. 79-90.

16. Roger Parsons, J. Electroanal. Chem., Vol. 5, 1963, pp. 397-410.

17. Roger Parsons, J. Electroanal. Chem., Vol. 7, 1964, pp. 136-152.

18. Roger Parsons, Trans. Faraday Soc., Vol. 51, 1955, pp. 1518-1529.

19. R. Payne, J. Chem. Physics, Vol. 42, 1965, pp. 3371-3383.

20. D. C. Grahame, E. M. Coffin, J. J. Cummings, M. A. Poth, J. Amer. Chem. Soc., Vol. 74, 1952, pp. 1207-1211.

21. G. J. Hills, R. Payne, Trans. Faraday Soc., Vol. 61, 1965, pp. 316-325.

22. R. Payne, "The Electrical Double Layer in Nonaqueous Solutions", Advances in Electrochemistry and Electrochemical Engineering, ed., Paul Delahay, C. Tobias, (New York: John Wiley, Inc., 1970), Vol. 7, pp. 1-76.

23. R. Payne, J. Electrochem. Soc., Vol. 113, 1966, pp. 999-1010.

24. R. Payne, Trans Faraday Soc., Vol. 64, 1968, pp. 1638-1655.

25. J. Lawrence, R. Parsons, R. Payne, J. Electroanal. Chem., Vol. 16, 1968, pp. 193-206.

26. David Grahame, J. Amer. Chem. Soc., Vol. 80, 1958, pp. 4201-4210.

27. E. Dutkiewicz, R. Parsons, J. Electroanal. Chem., Vol. 11, 1966, pp. 100-110.

28. R. Parsons, P. C. Symons, Trans. Faraday Soc., Vol. 64, 1968, pp. 1077-1092.

29. E. Dutkiewicz, R. Parsons, J. Electroanal. Chem., Vol. 11, 1966, pp. 196-207.

30. R. Parsons, F. G. R. Zobel, Trans. Fraday Soc., Vol. 62, 1966, pp. 3511-3523.

VI. APPENDIX

Table I and Table II consist of the experimental data for the KF + KBr and .5MKF + 6-amino-hexanoic acid system respectively. The procedure for handling both sets of data is identical in all but two respects. All of the diffuse layer cards must be changed since $q^1 = 0$ in the 6-amino hexanoic system and the total ionic concentration is .5M. Care must also be taken not to exceed the maximum permissible exponent in programs where powers of Γ appear. These differences are trivial and the programs and data will be discussed only for the KBr + KF system.

The purpose of Program I is to integrate the experimental capacity versus potential curve. The input for this program consists of Table I. The first and second cards are the title. The second card was always blank since the title was short. The third card gives the initial values of q, γ, E, C, and the concentration, and indicates the direction of integration and whether specific adsorption is assumed. Provision is made to correct E values to $E^{\pm}$ if necessary. For 1MKF, this card consists of experimentally determined values. For all of the xMKBr + (1-X)MKF sets, this card consists of the $q = -19$ values for 1MKF. The following cards in each set consist of the experimentally determined potential and capacity values arranged according to the direction of integration. The program is capable of interpolating the value of C at $q = 0$, but this was not used, rather C was found directly. The program fits the first three points to a parabola and finds all integral values of q which lie between the endpoints. It then drops the first point, reads another point and repeats the process using the previously computed values of the second point as the integration constants. This procedure is repeated until all of the points have been read. The output consists of E, C, γ, ξ at integral values of q. If no specific adsorption is present, C^d, and C^i and ϕ^{m-2} are also determined. Specific adsorption is assumed absent for KF. This program is a modified version of one originally developed by Payne. Tables III and IV are the output for 1MKF and .5MKF respectively.

Table V consists of the output cards of the first program for $q = +4$. The second card is the 1MKF card and the next nine are the KBr + KF cards. With the control card, this forms the input for Program II. The second program fits ξ to a cubic equation is kTN/F ln x, the derivative of which is q^1. It also calculates Φ, C^d, $-\Delta\ 1/C$, ΔE, ϕ^2, ϕ^{m-2}. Table VI contains the printed output of Program II for $q = +4$.

Program III obtains ${}_{q}^{1}C^{i}$ from a quadratic fit of ϕ^{m-2} to q^1. Program IV obtains $\left(\frac{\partial q^1}{\partial q}\right)_{\mu}$ from a cubic fit of q^1 to q. The input cards for both programs are the output cards of Program II. In the first case they are arranged at constant charge and in the second at constant concentration. Program V evaluates C^i, ${}_{q}C^{i}$ and $-\Delta\ 1/C^i$ using the output of Programs II, III, and IV. It can be easily modified to use the constant values of ${}_{q}^{1}C^{i}$ obtained from Figure 9. The input cards for Program V are shown in Table VII. The first nine cards are the output of Program III. The next card is the 1MKF output card from Program I. The next nine cards are the output of Program IV, and the last nine are the output of Program II. All cards are for $q = +4$. Table VIII consists of the printed output of Program V.

Programs VI, VII, and VIII are used to determine whether the data will fit a Frumkin isotherm. Program VI iterates A and θ to give universal plots of ln $\Phi/kT\Gamma_S$ versus ln $a\beta/\Gamma_S$. Programs VII and VIII iterate A and Γ_S and use experimental values of Γ and a to determine the best values of A and Γ_S once a rough fit of A is made. The input cards for Programs VII and VIII consist of the output cards of Program II at constant charge (J indicates the number of such sets). The fineness of the iteration can easily be varied. Program IX simply gives Γ and ln a/Γ which are used to check for a virial isotherm. This would have been included in Program II except that there was not enough space left to print it out.

PROGRAM I

INTEGRATION OF THE CAPACTIY

```
C     INTEGRATION OF DOUBLE LAYER CAPACITY
C     L = 1 NO SPECIFIC ADSORPTION
C     K = 1 ANODIC INTEGRATION K = 2  CATHODUC
  100 READ(5,20)
   20 FORMAT (55H                                                       )
      READ(5,21)
   21 FORMAT(55H                                                        )
      READ(5,30)K,CORR,Q1,G1,E1,C1,CON,L
   30 FORMAT(I2,8X,6F10.0,12)
      WRITE(6,40)
   40 FORMAT(37H1 INTEGRATION OF DOUBLE LAYER CAPACITY//)
      WRITE(6,20)
      WRITE(6,21)
      IF(L)404,404,402
  402 WRITE(6,51)
   51 FORMAT(1H ,4HE(V),5X,9HQ(MC/CM2),2X,10HG(ERG/CM2),2X,11HXI(ERG/CM2
     1),2X,9HC(MF/CM2),4X,3HI/C,10X,2HCD,11X,2HCI,11X,4H)/CI/)
      GOTO403
  404 WRITE(6,50)
   50 FORMAT(1H,4HE(V),5X,9HQ(MC/CM2),2X,10HG(ERG/CM2),2X,11HXI(ERG/CM2
     1),2X,9HC(MF/CM2),4X,3H1/C/)
  403 IF(C1)22,22,24
   22 READ(5,70)EP,CP
   70 FORMAT(2F10.0)
      READ(5,70)E2,C2
      READ(5,70)E3,C3
      D2=E2-EP
      D3=E3-EP
      A2=C2-CP
      A3=C3-CP
      R=(A3/D3-A2/D2)/(D3-D2)
      S=(A2*D3/D2-D2*A3/D3)/(D3-D2)
      C1=R*(E1-EP)**2+(E1-EP)+CP
      GOTO23
   24 READ(5,70)E2,C2
      READ(5,70)E3,C3
   23 E=E1
      CE=C1
      QE=Q1
      GE=G1
      XN1=0.0
    1 EC=E+CORR
      CR=1./CE
      XIE=GE+QE*EC*10.0
      KE=QE
      IF(L)65,65,400
  400 F=11.72
```

```
      PH12=2.*.02569*ALOG((QE/F)+SQRT((QE/F)**2+1.))
      CD=228.5*COSH(19.46*PH12)
      CI=(CE*CD)/(CD-CE)
      B=1./CI
      PHIM2=E+0.4750-PHI2
      WRITE(6,61)E,KE,GE,XIE,CE,CR,CD,CI,B,PHIM2
   61 FORMAT(1HO,F7.4,2X,13,8X,F7.2,5X,F7.2,6X,6(E11.4,2X))
      WRITE(7,63)QE,XIE,EC,CE,CI
   63 FORMAT(F5.1,F8.2,F7.4,2E11.4)
      GOTO401
   65 WRITE(6,60)E,KE,GE,XIE,CE,CR
   60 FORMAT(1HO,F7.4,2X,I3,8X,F7.2,5X,F7.2,6X,E11.4,2X,E11.4)
      WRITE(7,62)QE,XIE,CON,EC,CE
   62 FORMAT(F5.1,F8.2,2F7.4,E11.4)
  401 IF(QE-Q1)11,2,11
    2 IF(K-1)3,3,4
    3 QE=QE+1.0
      GOTO200
    4 QE=QE-1.0
  200 D2=E2-E1
      D3=E3-E1
      A2=C2-C1
      A3=C3-C1
      R=(A3/D3-A2/D2)/(D3-D2)
      S=(A2*D3/D2-D2*A3/D3)/(D3-D2)
    5 XN=XN1+1.0/C1
      N=0
    6 XN1=XN-(R*XN**3/3.+(S*XN**2)/2.+C1*XN-(QE-Q1))/(R*XN**2+S*XN+C1)
      Y=ABS(XN1-XN)
      IF(Y.LT.0.00001)GOTO8
      XN=XN1
      N=N+1
      GOTO(6,6,6,6,6,6,6,6,6,6,6,6,6,6,6,6,6,6,6,7),N
    7 WRITE(6,80)
   25 READ(5,70)E4,C4
      IF(E4-999.99)25,15,15
    8 Z=ABS(XN1)
      Z3=ABS(D3)
      IF(Z-Z3)9,10,10
    9 E=XN1+E1
      CE=R*XN1**2+S*XN1+C1
      GE=-10.*(R*XN1**4/12.+S*XN1**3/6.+C1*XN1**2/2.+Q1*XN1)+G1
      GOTO1
   10 READ(5,70)E4,C4
      G1=-10.*(R*D2**4/12.+S*D2**3/6.+C1*D2**2/2.+Q1*D2)+G1
      Q1=R*(E2-E1)**3/3.+S*(E2-E1)**2/2.+C1*(E2-E1)+Q1
      IF(E4-999.99)300,15,15
  300 E1=E2
      E2=E3
      E3=E4
      C1=C2
      C2=C3
      C3=C4
```

```
      GOTO200
11    IF(K-1)12,12,13
12    QE=QE+1.
      GOTO14
13    QE=QE-1.
14    GOTO5
15    GOTO100
80    FORMAT(32H NO SOLUTION AFTER 20 ITERATIONS)
      END
```

II

Program II - Determination of q^1

```
$PUFFT
PUFFT VERSION 3/1/68
C       CURVE FIT FOR XI =A+BX+CX2+DX3
C       QE XIE EC CE CI  BASE SOLUTION VALUES
        DIMENSIOND(4,4),VL(6),Y(15),CON(15),X(15),E(15),DE(15),DC(15),SP(1           56437
       15),ASP(15),ACON(15),CS(15)                                                   56437
    201 READ(5,109)N,C,EZ                                                            56437
    109 FORMAT(I3,F5.1,F7.4)                                                         56451
        READ(5,402)QE,XIE,EC,CE,CI                                                   56451
    402 FORMAT(F5.1,F8.2,F7.4,2E11.4)                                                56467
    150 DO200I=1,N                                                                   56467
    200 READ(5,110)Y(I),CON(I),E(I),CS(I)                                            56500
    110 FORMAT(5X,F8.2,2F7.4,E11.4)                                                  56531
        DO8I=1,N                                                                     56531
      8 X(I)=.2569*ALOG(CON(I))                                                      56542
        AN = N                                                                       56564
        J = 1                                                                        56567
        SX = 0.0                                                                     56571
        SX2 = 0.0                                                                    56573
        SX3 = 0.0                                                                    56575
        SX4 = 0.0                                                                    56577
        SX5 = 0.0                                                                    56601
        SX6 = 0.0                                                                    56603
        SY = 0.0                                                                     56605
        SXY = 0.0                                                                    56607
        SX2Y = 0.0                                                                   56611
        SX3Y = 0.0                                                                   56613
        DO 30 L=1,N                                                                  56615
        SX = SX + X(L)                                                               56626
        SX2 = SX2 + X(L)**2                                                          56634
        SX3 = SX3 + X(L)**3                                                          56644
        SX4 = SX4 + X(L)**4                                                          56654
        SX5 = SX5 + X(L)**5                                                          56664
        SX6 = SX6 + X(L)**6                                                          56674
        SY = SY + Y(L)                                                               56704
        SXY = SXY + X(L)*Y(L)                                                        56712
        SX2Y = SX2Y + (X(L)**2) * (Y(L))                                             56722
     30 SX3Y = SX3Y + (X(L)**3) * (Y(L))                                             56736
        D(1,1) = AN                                                                  56753
        D(2,1) = SX                                                                  56755
        D(3,1) = SX2                                                                 56757
        D(4,1) = SX3                                                                 56761
        D(1,2) = SX                                                                  56763
        D(2,2) = SX2                                                                 56765
        D(3,2) = SX3                                                                 56767
        D(4,2) = SX4                                                                 56771
        D(1,3) = SX2                                                                 56773
        D(2,3) = SX3                                                                 56775
        D(3,3) = SX4                                                                 56777
        D(4,3) = SX5                                                                 57001
        D(1,4) = SX3                                                                 57003
        D(2,4) = SX4                                                                 57005
        D(3,4) = SX5                                                                 57007
        D(4,4) = SX6                                                                 57011
     35 GO TO (42,44,46,48,50),J                                                     57013
     42 VL(J) = ((D(1,1))*(D(2,2)*D(3,3)*D(4,4) + D(2,3)*D(3,4)*D(4,2) +             57025
       1D(2,4)*D(3,2)*D(4,3) - D(2,3)*D(3,2)*D(4,4) - D(4,2)*D(3,3)*D(2,4)           57042
       2-D(2,2)*D(3,4)*D(4,3))) - ((D(1,2))*(D(2,1)*D(3,3)*D(4,4) +                  57063
       3D(2,3)*D(3,4)*D(4,1) + D(2,4)*D(3,1)*D(4,3) - D(2,3)*D(3,1)*D(4,4)           57111
```

```
      4-D(2,4)*D(3,3)*D(4,1) - D(2,1)*D(3,4)*D(4,3))) + ((D(1,3))*(D(2,1)       57132
      5*D(3,2)*D(4,4) + D(2,2)*D(3,4)*D(4,1) + D(2,4)*D(3,1)*D(4,2) -           57161
      6D(2,2)*D(3,1)*D(4,4) - D(2,4)*D(3,2)*D(4,1) - D(2,1)*D(3,4)*D(4,2)       57202
      7)) - ((D(1,4))*(D(2,1)*D(3,2)*D(4,3) + D(2,2)*D(3,3)* D(4,1) +           57223
      8D(2,3)*D(3,1)*D(4,2) - D(2,2)*D(3,1)*D(4,3) - D(2,3)*D(3,2)*D(4,1)       57251
      9- D(2,1)*D(3,3)*D(4,2)))                                                 57272
       J = J + 1                                                                57317
       IF (J-6) 35,52,52                                                        57322
   44 D(1,1) = SY                                                               57327
      D(2,1) = SXY                                                              57331
      D(3,1) = SX2Y                                                             57333
      D(4,1) = SX3Y                                                             57335
      GO TO 42                                                                  57337
   46 D(1,2) = SY                                                               57340
      D(2,2) = SXY                                                              57342
      D(3,2) = SX2Y                                                             57344
      D(4,2) = SX3Y                                                             57346
      D(1,1) = AN                                                               57350
      D(2,1) = SX                                                               57352
      D(3,1) = SX2                                                              57354
      D(4,1) = SX3                                                              57356
      GO TO 42                                                                  57360
   48 D(1,3) = SY                                                               57361
      D(2,3) = SXY                                                              57363
      D(3,3) = SX2Y                                                             57365
      D(4,3) = SX3Y                                                             57367
      D(1,2) = SX                                                               57371
      D(2,2) = SX2                                                              57373
      D(3,2) = SX3                                                              57375
      D(4,2) = SX4                                                              57377
      GO TO 42                                                                  57401
   50 D(1,4) = SY                                                               57402
      D(2,4) = SXY                                                              57404
      D(3,4) = SX2Y                                                             57406
      D(4,4) = SX3Y                                                             57410
      D(1,3) = SX2                                                              57412
      D(2,3) = SX3                                                              57414
      D(3,3) = SX4                                                              57416
      D(4,3) = SX5                                                              57420
      GO TO 42                                                                  57422
   52 CONTINUE                                                                  57423
      A = VL(2) / VL(1)                                                         57423
      B = VL(3) / VL(1)                                                         57426
      C = VL(4) / VL(1)                                                         57431
      P=VL(5)/VL(1)                                                             57434
      WRITE(6,300)Q                                                             57437
  300 FORMAT(8H1CHARGE=,F5.1)                                                   57445
      WRITE(6,301)A,B,C,P                                                       57445
  301 FORMAT(5H0XI=(,E11.4,3H)+(,E11.4,4H)X+(,E11.4,5H)X2+(,E11.4,3H)X3)        57461
      WRITE(6,303)                                                              57461
  303 FORMAT(1H0,3HCON,6X,5HLNCON,4X,3HQSA,5X,2HSP,7X,3HLSP,6X,2HXI,7X,4        57465
     1HDIFF,5X,2HCD,11X,2HDC,11X,2HDE,7X,4HPHI2,5X,6HPHIM-2)                    57465
      IF(EC)400,501,400                                                         57465
  501 DO502I=1,N                                                                57471
      DE(I)=0.0                                                                 57502
      DC(I)=0.0                                                                 57507
      SP(I)=0.0                                                                 57514
      ASP(I)=0.0                                                                57521
  502 CONTINUE                                                                  57526
      GOTO500                                                                   57527
```

```
 400 DO403I=1,N                                                        57530
     DE(I)=EC-E(I)                                                     57541
     DC(I)=(1./CF)-(1./CS(I))                                          57547
     SP(I)=XIE-Y(I)                                                    57562
     IF(SP(I)-.005)403,403,404                                         57570
 404 ASP(I)=ALOG(SP(I))                                                57600
 403 CONTINUE                                                          57615
 500 DO302I=1,N                                                        57616
     XIC=A+B*X(I)+C*X(I)**2+P*X(I)**3                                  57627
     QSA=B+2.0*C*X(I)+3.0*P*X(I)**2                                    57661
     F=11.72                                                           57706
     PHI2=2.*.02569*ALOG(((Q+QSA)/F)+SQRT(((Q+QSA)/F)**2+1.))          57710
     PHIM=E(I)-EZ-PHI2                                                 57741
     DIFF=XIC-Y(I)                                                     57750
     CD=228.5*COSH(19.46*PHI2)                                         57756
     ACON(I)=ALOG(CON(I))                                              57771
     WRITE(6,304)CON(I),ACON(I),QSA,SP(I),ASP(I),Y(I),DIFF,CD,DC(I),DE(60006
    1I),PHI2,PHIM,X(I)                                                 60055
 304 FORMAT(1H0,2(F7.4,2X),F6.2,2X,F7.2,2X,F7.4,2X,2(F7.2,2X),2(E11.4,2 60074
    1X),4(F7.4,2X))                                                    60074
     WRITE(7,406)CON(I),QSA,SP(I),CD,DC(I),DE(I),CS(I),Q,PHIM          60074
 406 FORMAT(F7.4,F6.2,F7.2,2E11.4,F7.4,E11.4,F5.1,E11.4)              60141
 302 CONTINUE                                                          60141
     GOTO201                                                           60142
     END                                                               60143


 **0**       EXECUTION
```

Program III - Determination of $\left(\frac{\partial q^1}{\partial \phi}m\text{-}2\right)_q$

```
$ID             CHM2[illegible]-2701,[illegible]                 [illegible]
$[illegible]
C       LEAST SQUARES CURVE FIT FOR QUADRATIC EQUATION Y = A + BX + CX2
        DIMENSIOND(3,3),VL(5),X(30),Y(30),OSA(30),PHIM(20),CONC(20)
    201 READ(5,105)N,W
    105 FORMAT(I3,F5.1)
        DO200I=1,N
        READ(5,110)CONC(I),OSA(I),PHIM(I)
    110 FORMAT(F7.4,F6.2,52X,E11.4)
        X(I)=OSA(I)
        Y(I)=PHIM(I)
    200 CONTINUE
        AN = N
        J = 1
        SX=0.0
        SX2=0.0
        SX3=0.0
        SX4 = 0.0
        SY=0.0
        SXY=0.0
        SX2Y=0.0
        DO 30 L=1,N
        SX = SX + X(L)
        SX2 = SX2 + X(L)**2
        SX3 = SX3 + X(L)**3
        SX4 = SX4 + X(L)**4
        SY = SY + Y(L)
        SXY = SXY + X(L)*Y(L)
     30 SX2Y = SX2Y + (X(L)**2) * (Y(L))
        D(1,1)=AN
        D(2,1)=SX
        D(3,1)=SX2
        D(1,2)=SX
        D(2,2)=SX2
        D(3,2)=SX3
        D(1,3)=SX2
        D(2,3)=SX3
        D(3,3)=SX4
     35 GO TO (42,44,46,48),J
     42 VL(J) = (D(1,1)*D(2,2)*D(3,3)) + (D(1,2)*D(2,3)*D(3,1)) + (D(1,3)
       1*D(2,1)*D(3,2)) - (D(3,1)*D(2,2)*D(1,3)) - (D(3,2)*D(2,3)*D(1,1))
       2) - (D(3,3)*D(2,1)*D(1,2))
        J = J + 1
        IF (J-5) 35,36,36
     44 D(1,1)=SY
        D(2,1)=SXY
        D(3,1)=SX2Y
        GO TO 42
     46 D(1,2)=SY
        D(2,2)=SXY
        D(3,2)=SX2Y
        D(1,1)=AN
        D(2,1)=SX
        D(3,1)=SX2
        GO TO 42
     48 D(1,3)=SY
        D(2,3)=SXY
        D(3,3)=SX2Y
        D(1,2)=SX
        D(2,2)=SX2
```

```
      D(3,2)=SX3
      GO TO 42
   52 CONTINUE
      A = VL(2)/VL(1)
      B = VL(3)/VL(1)
      C = VL(4)/VL(1)
      WRITE(6,300)Q
  300 FORMAT(1H1,2HQ=,F5.1)
      WRITE(6,301)A,B,C
  301 FORMAT(1H0,5HPHIM=,E11.4,1H+,E11.4,3HOSA,1H+,E11.4,6HOSA**2)
      WRITE(6,302)
  302 FORMAT(1H0,3HCON,6X,3HOSA,5X,4HPHIM,9X,5HPHIMC,8X,6HDOSPHI)
      DO303J=1,N
      PHIMC=A+B*OSA(J)+C*(OSA(J)**2)
      DPHIM=B+2.0*C*OSA(J)
      DOSPHI=1.0/DPHIM
      WRITE(6,304)CON(J),OSA(J),PHIM(J),PHIMC,DOSPHI
  304 FORMAT(1H0,F7.4,2X,F6.2,2X,3(E11.4,2X))
      WRITE(7,305)CON(J),Q,DOSPHI
  305 FORMAT(F7.4,F5.1,F6.2)
  303 CONTINUE
      GO TO 201
      END
$DATA
```

Program IV - Determination of $\left(\frac{\partial q^{1}}{\partial q}\right)_{\mu}$

IV

```
$ID               CHM201-2701,30S,3000,1000       SEARS
$DUFFT
C         OSA=A+BX+CX2+PX3
          DIMENSIONOSA(30),Q(30),X(30),Y(30),D(4,4),VL(10)
      201 READ(5,800)N,CON
      800 FORMAT(I3,F7.4)
          DO801I=1,N
          READ(5,802)OSA(I),Q(I)
      802 FORMAT(7X,F6.2,47X,F5.1)
          X(I)=Q(I)
          Y(I)=OSA(I)
      801 CONTINUE
          AN = N
          J = 1
          SX = 0.0
          SX2 = 0.0
          SX3 = 0.0
          SX4 = 0.0
          SX5 = 0.0
          SX6 = 0.0
          SY = 0.0
          SXY = 0.0
          SX2Y = 0.0
          SX3Y = 0.0
          DO 30 L=1,N
          SX = SX + X(L)
          SX2 = SX2 + X(L)**2
          SX3 = SX3 + X(L)**3
          SX4 = SX4 + X(L)**4
          SX5 = SX5 + X(L)**5
          SX6 = SX6 + X(L)**6
          SY = SY + Y(L)
          SXY = SXY + X(L)*Y(L)
          SX2Y = SX2Y + (X(L)**2) * (Y(L))
       30 SX3Y = SX3Y + (X(L)**3) * (Y(L))
          D(1,1) = AN
          D(2,1) = SX
          D(3,1) = SX2
          D(4,1) = SX3
          D(1,2) = SX
          D(2,2) = SX2
          D(3,2) = SX3
          D(4,2) = SX4
          D(1,3) = SX2
          D(2,3) = SX3
          D(3,3) = SX4
          D(4,3) = SX5
          D(1,4) = SX3
          D(2,4) = SX4
          D(3,4) = SX5
          D(4,4) = SX6
       35 GO TO (42,44,46,48,50),J
       42 VL(J) = ((D(1,1))*(D(2,2)*D(3,3)*D(4,4) + D(2,3)*D(3,4)*D(4,2) +
         1D(2,4)*D(3,2)*D(4,3) - D(2,3)*D(3,2)*D(4,4) - D(4,2)*D(3,3)*D(2,4)
         2-D(2,2)*D(3,4)*D(4,3))) - ((D(1,2))*(D(2,1)*D(3,3)*D(4,4) +
         3D(2,3)*D(3,4)*D(4,1) + D(2,4)*D(3,1)*D(4,3) - D(2,3)*D(3,1)*D(4,4)
         4-D(2,4)*D(3,3)*D(4,1) - D(2,1)*D(3,4)*D(4,3))) + (((D(1,3))*(D(2,1)
         5*D(3,2)*D(4,4) + D(2,2)*D(3,4)*D(4,1) + D(2,4)*D(3,1)*D(4,2) -
         6D(2,2)*D(3,1)*D(4,4) - D(2,4)*D(3,2)*D(4,1) - D(2,1)*D(3,4)*D(4,2)
         7)) - ((D(1,4))*(D(2,1)*D(3,2)*D(4,3) + D(2,2)*D(3,3)* D(4,1) +
```

```
     8D(2,3)*D(3,1)*D(4,2) - D(2,2)*D(3,1)*D(4,3) - D(2,3)*D(3,2)*D(4,1)
     9- D(2,1)*D(3,3)*D(4,2)))
      J = J + 1
      IF (J-6) 35,52,52
   44 D(1,1) = SY
      D(2,1) = SXY
      D(3,1) = SX2Y
      D(4,1) = SX3Y
      GO TO 42
   46 D(1,2) = SY
      D(2,2) = SXY
      D(3,2) = SX2Y
      D(4,2) = SX3Y
      D(1,1) = AN
      D(2,1) = SX
      D(3,1) = SX2
      D(4,1) = SX3
      GO TO 42
   48 D(1,3) = SY
      D(2,3) = SXY
      D(3,3) = SX2Y
      D(4,3) = SX3Y
      D(1,2) = SX
      D(2,2) = SX2
      D(3,2) = SX3
      D(4,2) = SX4
      GO TO 42
   50 D(1,4) = SY
      D(2,4) = SXY
      D(3,4) = SX2Y
      D(4,4) = SX3Y
      D(1,3) = SX2
      D(2,3) = SX3
      D(3,3) = SX4
      D(4,3) = SX5
      GO TO 42
   52 CONTINUE
      A = VL(2) / VL(1)
      B = VL(3) / VL(1)
      C = VL(4) / VL(1)
      P=VL(5)/VL(1)
      WRITE(6,803)CON
  803 FORMAT(1H1,4HCON=,F7.4)
      WRITE(6,301)A,B,C,P
  301 FORMAT(5HOY1=(,E11.4,3H)+(,E11.4,4H)X+(,E11.4,5H)X2+(,E11.4,3H)X3)
      WRITE(6,804)
  804 FORMAT(1H0,1HQ,6X,3HQSA,5X,4HQSAC,4X,5HDQSAC)
      DO805I=1,N
      QSAC=A+B*Q(I)+C*Q(I)**2+P*Q(I)**3
      DQSAC=B+2.0*C*Q(I)+3.0*P*Q(I)**2
      WRITE(7,806)DQSAC,Q(I),CON
  806 FORMAT(F7.4,F5.1,F7.4)
      WRITE(6,807)Q(I),QSA(I),QSAC,DQSAC
  807 FORMAT(1H0,F5.1,2X,3(F6.2,2X))
  805 CONTINUE
      GOTO201
      END
$DATA
```

Program V - Determination of the Components of Capacity

```
      $PUFFT
      PUFFT VERSION 3/1/68
      C     COMPONENTS OF CAPACITY
            DIMENSIONDQSA(9),CON(9),CD(9),CS(9),DQSPHI(9)                    56437
         12 DO100N=1,9                                                       56437
            READ(5,11)Q,DQSPHI(N)                                            56450
         11 FORMAT(7X,F5.1,F6.2)                                             56463
        100 CONTINUE                                                         56463
            READ(5,50)CIB                                                    56464
         50 FORMAT(31X,E11.4)                                                56472
            DO1I=1,9                                                         56472
            READ(5,2)DQSA(I)                                                 56503
          2 FORMAT(F7.4)                                                     56514
          1 CONTINUE                                                         56514
            DO3J=1,9                                                         56515
            READ(5,4)CON(J),CD(J),CS(J)                                      56526
          4 FORMAT(F7.4,13X,E11.4,18X,E11.4)                                 56551
          3 CONTINUE                                                         56551
            WRITE(6,5)Q                                                      56552
          5 FORMAT(1H1,2HQ=,F5.1)                                            56560
            WRITE(6,6)                                                       56560
          6 FORMAT(1H0,3HCON,6X,1HC,12X,2HCD,11X,4HDQSA,9X,2HCI,11X,5HDQPHI,8X 56564
           1,6HDQSPHI,7X,3HDCI)                                              56564
            DO10K=1,9                                                        56564
            R=1.0/CS(K)-(1.0/CD(K))*(1.0+DQSA(K))                            56575
            CI=1.0/R                                                         56614
            T=1.0/CIB-R                                                      56617
            P=R-(1.0/DQSPHI(K))*DQSA(K)                                      56624
            S=1.0/P                                                          56634
            WRITE(6,8)CON(K),CS(K),CD(K),DQSA(K),CI,S,DQSPHI(K),T            56637
          8 FORMAT(1H0,F7.4,2X,7(E11.4,2X))                                  56702
         10 CONTINUE                                                         56702
            GOTO12                                                           56703
            END                                                              56704

  **0**     EXECUTION
```

Program VI

```
$ID               CHM201-2701,30S,3000,200  SEARS
$PUFFT
C FRUMKIN ISOTHERM
          READ(5,1)A,N
        1 FORMAT(F5.1,I3)
          DO6J=1,N
          THETA=0.0
          IF(J.EQ.1)GOTO13
          A=A+0.5
       13 WRITE(6,4)
        4 FORMAT(1H1,16HFRUMKIN ISOTHERM)
          WRITE(6,5)A
        5 FORMAT(1H0,2HA=,F5.1)
          WRITE(6,7)
        7 FORMAT(1H0,5HTHETA,2X,3HPHI,6X,4HAPHI,5X,1HB)
          DO3I=1,23
          IF(I.GE.5)GOTO14
          IF(THETA-0.07)8,14,14
        8 GOTO(9,10,11),I
        9 THETA=0.01
          GOTO12
       10 THETA=0.03
          GOTO12
       11 THETA=0.07
          GOTO12
       14 D=I
          THETA=(D-3.0)*0.05
       12 PHI=-1.0*ALOG(1.0-THETA)+(A/2.0)*(THETA**2)
          APHI=ALOG(PHI)
          B=ALOG((THETA)/(1.0-THETA))+A*THETA
          WRITE(6,2)THETA,PHI,APHI,B
        2 FORMAT(1H0,F5.2,2X,3(F7.2,2X))
        3 CONTINUE
        6 CONTINUE
          END
$DATA
                                                     CARD COUNT 0037
```

Program VII

```
$ID            CHM201-2701,30S,3000,200  SEARS
$PUFFT
C FRUMKIN ISOTHERM
      DIMENSIONCON(10),QSA(10),SP(10),Q(10),GAM(10),ASP(10)
      DO12J=1,2
      DO14I=1,9
      READ(5,1)CON(I),QSA(I),SP(I),Q(I)
    1 FORMAT(F7.4,F6.2,F7.2,40X,F5.1)
   14 GAM(I)=(-1.0)*QSA(I)*0.60232E+24/0.964935E+11
      DO18L=1,5
      P=L
      A=7.5+0.1*P
      DO15K=1,21
      R=K
      GAMS=0.1480E+15+0.0020E+15*R
      F=Q(1)
      WRITE(6,6)A,GAMS,F
    6 FORMAT(1H1,2HA=,F5.1,5X,5HGAMS=,E11.4,5X,2HQ=,F5.1)
      WRITE(6,7)
    7 FORMAT(1H0,3HCON,6X,3HGAM,10X,3HQSA,6X,2HSP,7X,4HDIFF,5X,3HSPC,6X,
     14HASPC,5X,3HASP,6X,3HPER)
      DO16M=1,9
      THETA=GAM(M)/GAMS
      IF(THETA.GE.1.0)GOTO9
      GOTO8
    9 PHI=0.0
      APHI=0.0
      ASP(M)=ALOG(SP(M))
      GOTO10
    8 PH=-1.0*ALOG(1.0-THETA)+(A/2.0)*(THETA**2)
      PHI=0.138045E-15*298.15*GAMS*PH
      ASP(M)=ALOG(SP(M))
      APHI=ALOG(PHI)
   10 DIFF=SP(M)-PHI
      PER=DIFF/SP(M)*100.0
      WRITE(6,2)CON(M),GAM(M),QSA(M),SP(M),DIFF,PHI,APHI,ASP(M),PER
    2 FORMAT(1H0,F7.4,2X,E11.4,2X,7(F7.2,2X))
   16 CONTINUE
   15 CONTINUE
   18 CONTINUE
   13 CONTINUE
      END
$DATA
                                                  CARD COUNT 0044
```

Program VIII

```
$ID              CHM201-2701,305,3000,200  SEARS
$PUFFT
C FRUMKIN ISOTHERM
      DIMENSIONCON(10),QSA(10),SP(10),Q(10),GAM(10),ASP(10)
      DO13J=1,1
      DO14I=1,9
      READ(5,1)CON(I),QSA(I),SP(I),Q(I)
    1 FORMAT(F7.4,F6.2,F7.2,40X,F5.1)
   14 GAM(I)=(=1.0)*QSA(I)*0.60232E+24/0.964935E+11
      DO18L=1,15
      P=L
      A=4.6+0.2*P
      DO15K=1,16
      R=K
      GAMS=0.1600E+15+0.0020E+15*R
      F=Q(1)
      WRITE(6,6)A,GAMS,F
    6 FORMAT(1H1,2HA=,F5.1,5X,5HGAMS=,E11.4,5X,2HQ=,F5.1)
      WRITE(6,7)
    7 FORMAT(1H0,3HCON,6X,3HGAM,10X,3HQSA,6X,5HABETA)
      DO16M=1,9
      THETA=GAM(M)/GAMS
      IF(THETA.GE.1.0)GOTO9
      GOTO8
    9 ABETA=0.0
      GOTO10
    8 ABETA=-1.0*ALOG(CON(M))+ALOG(GAMS)+ALOG(THETA/(1.0-THETA))+A*THETA
   10 WRITE(6,2)CON(M),GAM(M),QSA(M),ABETA
    2 FORMAT(1H0,F7.4,2X,E11.4,2X,F7.2,2X,E11.4)
   16 CONTINUE
   15 CONTINUE
   18 CONTINUE
   13 CONTINUE
      END
$DATA
                                                      CARD COUNT 0036
```

Program IX

```
$PUFFT
PUFFT VERSION 3/1/68
C      VIRIAL ISOTHERM
   12 WRITE(6,1)                                                         56437
    1 FORMAT(1H1,15HVIRIAL ISOTHERM)                                     56443
      WRITE(6,2)                                                         56443
    2 FORMAT(1H0,3HCON,6X,3HQSA,5X,3HGAM,10X,1HQ,6X,12HL(CON)/(GAM))     56447
      DO11I=1,9                                                          56447
      READ(5,3)CON,QSA,Q                                                 56460
    3 FORMAT(F7.4,F6.2,47X,F5.1)                                         56472
      GAM=(-1.0*QSA)*(0.6023E+24)/(0.9549E+11)                           56472
      IF(GAM)4,4,6                                                       56507
    4 GOTO9                                                              56513
    6 F=ALOG(CON)-ALOG(GAM)                                              56514
    9 WRITE(6,10)CON,QSA,GAM,Q,F                                         56524
   10 FORMAT(1H0,F7.4,2X,F6.2,2X,F11.4,2X,F5.1,2X,F8.3)                  56542
   11 CONTINUE                                                           56542
      GOTO12                                                             56543
      END                                                                56544



**0**      EXECUTION
```

Table I: Experimental Data for xMKBr + (1-x)MKF Arranged

As Used For Input of Program I.

```
    1MKF  25  DEG

    1                                   -.4750     26.38      1.0        1
   -0.4413      27.01
   -0.4119      27.61
   -0.3815      28.01
   -0.3516      28.35
   -0.3214      28.58
   -0.2905      28.69
   -0.2606      28.76
   -0.2307      28.77
   -0.2007      28.81
   -0.1703      28.60
   -0.1404      28.90
   -0.1106      29.04
   -0.0608      29.48
   -0.0124      30.44
   +0.0347      32.33
   +0.0599      33.96
   999.99
    1MKF  25  DEG

    2                                   -0.4750    26.38      1.0        1
   -0.5025      25.77
   -0.5526      24.41
   -0.6034      23.03
   -0.6533      21.69
   -0.7041      20.47
   -0.7514      19.42
   -0.8012      18.55
   -0.8487      17.83
   -0.8977      17.24
   -0.9491      16.80
   -1.0014      16.52
   -1.0514      16.37
   -1.1022      16.30
   -1.1504      16.34
   -1.2015      16.46
   -1.2517      16.88
   -1.3007      16.89
   -1.3511      17.18
   -1.4021      17.53
   -1.4525      17.93
   -1.4971      18.35
   999.99
   .001M KBR  25  DEG

    1                    -19.0      -103.053  -1.4914    16.293     .001
   -1.4546      18.04
   -1.4047      17.59
   -1.3542      17.25
   -1.3045      16.95
   -1.2540      16.70
   -1.2043      16.50
   -1.1528      16.39
   -1.1041      16.35
   -1.0535      16.29
   -1.0039      16.54
   -0.9537      16.81
   -0.9040      17.23
```

```
        -0.8537     17.79
        -0.8040     18.53
        -0.7535     19.46
        -0.7040     20.61
        -0.6539     21.96
        -0.6042     23.52
        -0.5526     25.45
        -0.5030     27.62
        -0.4724     29.08
        -0.4426     30.67
        -0.4127     32.18
        -0.3821     33.61
        -0.3524     34.69
        -0.3225     35.45
        -0.2720     36.20
        -0.2227     37.37
        -0.1727     40.41
        -0.1230     47.61
        -0.0732     64.80
        -0.0496     99.63
        999.99
         .005M  KBR  25  DEG

         1                  -19.0    -103.053  -1.4914    16.293    .005
        -1.4515     17.97
        -1.4021     17.55
        -1.3518     17.20
        -1.3024     16.91
        -1.2520     16.66
        -1.2023     16.46
        -1.1520     16.34
        -1.1023     16.30
        -1.0519     16.35
        -1.0023     16.52
        -0.9518     16.80
        -0.9023     17.23
        -0.8521     17.63
        -0.8029     18.65
        -0.7526     19.68
        -0.7030     21.04
        -0.6527     22.86
        -0.6031     25.31
        -0.5526     28.64
        -0.5228     31.19
        -0.4922     33.91
        -0.4625     36.69
        -0.4329     39.13
        -0.4030     41.09
        -0.3719     42.39
        -0.3422     43.28
        -0.3127     44.12
        -0.2825     45.43
        -0.2326     50.12
        -0.1817     61.35
        -0.1324    +87.87
        -0.0836    179.00
        999.99
         .01 M  KBR  IKDEG

         1                  -19.0    -103.053  -1.4914   +16.293    .01
```

```
        -1.4520    17.97
        -1.4018    17.59
        -1.3511    17.22
        -1.3011    16.92
        -1.2503    16.68
        -1.2003    16.48
        -1.1507    16.37
        -1.1008    16.33
        -1.0502    16.38
        -1.0004    16.55
        -0.9506    16.85
        -0.9005   +17.31
        -0.8496    17.96
        -0.8016    18.82
        -0.7513    20.04
        -0.7013    21.67
        -0.6507    24.06
        -0.6009    27.47
        -0.5509    32.04
        -0.5150    35.96
        -0.4840    39.15
        -0.4539    41.93
        -0.4239    43.90
        -0.3837    45.34
        -0.3340    46.55
        -0.2835    49.44
        -0.2338    57.08
        -0.1834    74.39
        -0.1341   118.40
        999.99
          .02M  KBR  25 DEG

        1                    -19.0      -103.053  -1.4914   +18.293    .02
        -1.4538    16.06
        -1.4041    17.65
        -1.3537    17.29
        -1.3041    16.98
        -1.2537    16.73
        -1.2039    16.53
        -1.1535    16.37
        -1.1039    16.34
        -1.0534    16.39
        -1.0035    16.57
        -0.9529    16.86
        -0.9030    17.38
        -0.8513    18.12
        -0.8012    19.13
        -0.7506    20.62
        -  .7006    22.64
        -0.6501    26.14
        -0.6022    30.68
        -0.5761    33.81
        -0.5517    36.59
        -0.5251    39.92
        -0.5019    42.25
        -0.4504    45.91
        -0.4006    47.12
        -0.3501    48.00
        -0.3024    51.09
```

```
     -0.2521    59.51
     -0.2025    78.65
     -0.1525    126.5
     999.99
      .04M  KBR  25 DEG
      1                     -19.0      -103.053  -1.4914     16.293     .04
     -1.4501       18.01
     -1.4018       17.61
     -1.3512       17.24
     -1.3013       16.96
     -1.2507       16.70
     -1.2019       16.53
     -1.1515       16.40
     -1.1018       16.37
     -1.0513       16.43
     -1.0019       16.64
     -0.9513       17.00
     -0.9015       17.56
     -0.8512       18.41
     -0.8014       19.70
     -0.7509       21.64
     -0.7013       24.67
     -0.6512       29.14
     -0.6016       35.08
     -0.5793       37.62
     -0.5513       41.40
     -0.5299       43.70
     -0.5018       46.02
     -0.4798       47.14
     -0.4515       48.05
     -0.4303       48.23
     -0.4020       48.49
     -0.3802       48.87
     -0.3524       49.96
     -0.3031       55.04
     -0.2532       67.29
     -0.2043       93.64
     999.99
      .1 M KBR  25  DEG

      1                     -19.0      -103.053  -1.4914    +18.293    +.1
     -1.4546       16.12
     -1.4046       17.05
     -1.3543       17.27
     -1.3044       16.96
     -1.2541       16.72
     -1.2042       16.52
     -1.1536       16.43
     -1.1038       16.41
     -1.0535       16.52
     -1.0035       16.78
     -0.9533     +17.22
     -0.9035       17.99
     -0.8532       19.20
     -0.8034       21.14
     -0.7532       24.21
     -0.7035       28.56
     -0.6532       34.47
     -0.6276       38.29
```

```
          -0.6036      41.54
          -0.5747      44.46
          -0.5534      45.55
          -0.5280      46.03
          -0.5048      46.78
          -0.4777      46.93
          -0.4536      46.98
          -0.4279      47.02
          -0.4040      47.50
          -0.3776      50.64
          -0.3541      52.80
          -0.3261      56.40
          -0.2779      69.48
          -0.2284      87.54
          999.99
          .2M KBR  25 DEG

          1                      -19.0      -103.053  -1.4914   16.293    0.2
          -1.4541      16.11
          -1.4025      17.60
          -1.3515      17.29
          -1.3016      17.03
          -1.2513      16.78
          -1.2016      16.61
          -1.1513      16.53
          -1.1016      16.53
          -1.0512      16.69
          -1.0015      17.03
          -0.9572      17.69
          -0.9017      18.78
          -0.8515      20.55
          -0.8019      23.41
          -0.7516      27.67
          -0.7022      33.56
          -0.6529      40.11
          -0.6266      43.07
          -0.6034      45.67
          -0.5767      47.51
          -0.5533      48.66
          -0.5291      49.13
          -0.5038      49.23
          -0.4790      49.07
          -0.4538      49.06
          -0.4296      49.44
          -0.4044      50.55
          -0.3796      52.56
          -0.3304      60.84
          -0.2806      76.35
          -0.2317     114.70
          999.99
            .4M  KBR  25 DEG

          1                      -19.0      -103.053  -1.4914   16.293    0.4
          -1.4526    16.20
          -1.4021    17.69
          -1.3517    17.35
          -1.3013    17.05
          -1.2506    16.80
          -1.2013    16.67
          -1.1510    16.52
```

```
-1.1009   16.66
-1.0504   16.94
-1.0023   17.42
-0.9517   18.36
-0.9013   19.92
-0.8512   22.58
-0.8010   26.51
-0.7512   32.01
-0.7013   38.38
-0.6691   42.26
-0.6394   45.37
-0.6093   47.54
-0.5792   48.75
-0.5493   49.07
-0.5193   48.99
-0.4894   48.72
-0.4600   48.94
-0.4020   52.28
-0.3523   60.60
-0.3026   77.60
999.99
.5% KBR  25 DEG

1                      -19.0     -103.053  -1.4914  +18.293    .8
-1.4518       18.07
-1.4020       17.70
-1.3524       17.36
-1.3029       17.08
-1.2529       16.88
-1.2035       16.79
-1.1536       16.81
-1.1042       16.96
-1.0544       17.36
-1.0048       18.09
-0.9549       19.43
-0.9058       21.60
-0.8559       24.90
-0.8065       29.57
-0.7567       35.33
-0.7072       41.19
-0.6814       43.83
-0.6573       45.81
-0.6317       47.36
-0.6080       48.12
-0.5815       48.47
-0.5579       48.42
-0.5320       48.19
-0.5084       48.12
-0.4818       48.31
-0.4584       49.19
-0.4093       53.67
-0.3593       63.94
-0.3096       83.52
999.99
  1%KBR  25 DEG

1                      -19.0     -103.053  -1.4914  +18.293    1.0
-1.4637   18.30
-1.4573   18.21
-1.4149   17.90
```

```
-1.4032   17.83
-1.3578   17.51
-1.3165   17.27
-1.3062   17.19
-1.2642   17.05
-1.2577   17.00
-1.2061   16.91
-1.1552   16.94
-1.1051   17.17
-1.0543   17.63
-1.0040   18.52
-0.9530   20.11
-0.9029   22.62
-0.8524   26.37
-0.8023   31.44
-0.7518   37.33
-0.7019   42.96
-0.6730   46.42
-0.6514   46.81
-0.6227   47.33
-0.6016   46.32
-0.5736   46.39
-0.5512   46.25
-0.5226   46.09
-0.5015   48.20
-0.4731   48.64
-0.4513   50.06
-0.4034   55.66
-0.3530   67.83
-0.3035   91.06
999.99

                              CARD COUNT 0390
```

Table II: Experimental Data for xM6-Amino Hexanoic Acid

Arranged as Used for Input of Program I.

```
      .5M  KF
    1                           425.7     -0.4740   25.10       1
     -0.4515   25.56
     -0.4018   26.35
     -0.3513   26.92
     -0.3016   27.34
     -0.2514   27.58
     -0.2018   27.81
     -0.1516   28.04
     -0.1020   28.42
     -0.0518   28.97
     -0.0024   29.76
     999.99
      .5M  KF
    2                           425.7     -0.4740   25.10       1
     -0.5019   24.61
     -0.5515   23.54
     -0.6017   22.42
     -0.6515   21.30
     -0.7024   20.20
     -0.7523   19.23
     -0.8046   18.37
     -0.8549   17.67
     -0.9042   17.13
     -0.9537   16.71
     -1.0038   16.42
     -1.0534   16.26
     -1.1036   16.21
     -1.1532   16.24
     -1.2033   16.35
     -1.2528   16.52
     -1.3028   16.78
     -1.3522   17.08
     -1.4022   17.43
     -1.4575   17.98
     999.99
      .01M  6AH
    1                           424.1     -0.4656   24.96     0.01
     -0.4516   25.14
     -0.4018   26.05
     -0.3518   26.72
     -0.3020   27.20
     -0.2520   27.57
     -0.2022   27.93
     -0.1523   28.39
     -0.1025   28.95
     -0.0525   29.76
     -0.0031   30.95
     999.99
      .01M  6AH
    2                           424.1     -0.4656   24.96     0.01
     -0.5016   24.06
     -0.5516   22.57
     -0.6044   21.64
     -0.6543   20.46
```

```
    -0.7042   19.45
    -0.7542   18.59
    -0.8041   17.81
    -0.8540   17.34
    -0.9041   16.94
    -0.9540   16.65
    -1.0041   16.49
    -1.0537   16.42
    -1.1038   16.41
    -1.1537   16.47
    -1.2037   16.59
    -1.2537   16.78
    -1.3038   17.05
    -1.3538   17.32
    -1.4039   17.62
    -1.4652   18.13
    999.99
     0.05M   6AH

    1                        421.6     -0.4597   24.13     0.05
    -0.4515   24.17
    -0.4016   25.48
    -0.3515   26.54
    -0.3015   27.41
    -0.2514   28.12
    -0.2014   28.80
    -0.1513   29.61
    -0.1014   30.59
    -0.0516   31.97
    -0.0019   33.82
    999.99
      .05M   6AH

    2                        421.6     -0.4597   24.13     0.05
    -0.5017   22.74
    -0.5516   21.24
    -0.6021   19.84
    -0.6522   18.63
    -0.6994   17.66
    -0.7506   16.89
    -0.8008   16.42
    -0.8509   16.12
    -0.9010   16.05
    -0.9512   16.09
    -1.0013   16.27
    -1.0464   16.49
    -1.1001   16.77
    -1.1505   17.05
    -1.2008   17.29
    -1.2510   17.56
    -1.3015   17.78
    -1.3506   18.04
    -1.4011   18.30
    -1.4493   18.61
    -1.4890   18.95
    999.99
      0.1M   6AH

    1                        421.3     -0.4506   23.60     0.1
    -0.4023   25.12
```

```
       -0.3519   26.46
       -0.3020   27.62
       -0.2518   28.60
       -0.2022   29.56
       -0.1520   30.69
       -0.1023   32.06
       -0.0522   33.79
       -0.0033   36.04
       999.99
          .1M 6AH

        2                          421.3     -0.4506   23.60     0.1
       -0.4519   23.59
       -0.5024   21.96
       -0.5521   20.33
       -0.6028   18.21
       -0.6525   17.57
       -0.7030   16.53
       -0.7500   15.83
       -0.8006   15.38
       -0.8458   15.17
       -0.9039   15.18
       -0.9470   15.35
       -1.0016   15.74
       -1.0512   16.19
       -1.1016   16.69
       -1.1513   17.21
       -1.2015   17.72
       -1.2512   18.17
       -1.3015   18.54
       -1.3512   18.87
       -1.4017   19.17
       -1.4514   19.44
       -1.4797   19.81
       999.99
        0.2M  6AH

        1                          416.4     -0.4393   23.07     0.2
       -0.4040   24.38
       -0.3537   26.01
       -0.3043   27.49
       -0.2540   28.83
       -0.2047   30.16
       -0.1544   31.80
       -0.1050   33.68
       -0.0549   35.92
       -0.0058   38.79
       999.99
         .2M  6AH

        2                          416.4     -0.4393   23.07     0.2
       -0.4534   22.67
       -0.5037   20.89
       -0.5532   19.29
       -0.6034   17.80
       -0.6528   16.47
       -0.7030   15.41
       -0.7538   14.70
       -0.8040   14.28
       -0.8535   14.09
```

```
     -0.9036   14.14
     -0.9530   14.37
     -1.0031   14.77
     -1.0535   15.31
     -1.1037   15.97
     -1.1533   16.71
     -1.2036   17.48
     -1.2530   18.25
     -1.3033   18.95
     -1.3528   19.24
     -1.4030   19.99
     -1.4525   20.46
     -1.4811   20.50
     999.99
       0.3M  6AH

      1                                  416.3     -0.4317    22.72      0.3
     -0.4012   24.03
     -0.3509   25.81
     -0.3011   27.54
     -0.2508   29.04
     -0.2009   30.70
     -0.1506   32.63
     -0.1009   34.99
     -0.0508   37.69
     -0.0016   40.91
     999.99
       .3M  6AH

      2                                  416.3     -0.4317    22.72      0.3
     -0.4510   22.19
     -0.5015   20.41
     -0.5511   18.78
     -0.6015   17.26
     -0.6512   15.91
     -0.7014   14.86
     -0.7513   14.16
     -0.8015   13.70
     -0.8514   13.52
     -0.9016   13.54
     -0.9517   13.74
     -1.0022   14.14
     -1.0520   14.70
     -1.1025   15.38
     -1.1525   16.13
     -1.2031   17.00
     -1.2500   17.66
     -1.3013   18.77
     -1.3512   19.62
     -1.4016   20.33
     -1.4517   20.94
     -1.4760   21.16
     999.99
       .5M  6AH

      1                                  413.1     -0.4219    22.85      0.5
     -0.4003   23.66
     -0.3523   25.65
     -0.3022   27.97
     -0.2519   29.64
```

```
   -0.2017   31.89
   -0.1517   34.43
   -0.1018   37.30
   -0.0520   40.50
   -0.0022   44.23
   999.99
     0.5M   6AH

   2                       413.1     -0.4215   22.65     0.5
   -0.4504   21.87
   -0.5007   19.93
   -0.5506   18.20
   -0.6011   16.61
   -0.6510   15.29
   -0.7010   14.27
   -0.7511   13.58
   -0.8013   13.18
   -0.8513   13.03
   -0.9015   13.09
   -0.9515   13.33
   -1.0017   13.74
   -1.0520   14.30
   -1.1004   14.98
   -1.1508   15.79
   -1.2010   16.73
   -1.2516   17.74
   -1.3001   18.75
   -1.3507   19.82
   -1.4014   20.85
   -1.4518   21.71
   -1.4825   22.17
   999.99
     .7M   6AH

   1                       411.7     -0.4153   22.59     0.7
   -0.4013   23.24
   -0.3513   25.32
   -0.3012   27.57
   -0.2512   29.82
   -0.2012   32.11
   -0.1512   35.03
   -0.1016   38.46
   -0.0517   42.25
   -0.0021   46.79
   999.99
     0.7M   6AH

   2                       411.7     -0.4153   22.59     0.7
   -0.4512   21.24
   -0.5012   19.35
   -0.5512   17.68
   -0.6012   16.21
   -0.6511   14.85
   -0.7010   13.83
   -0.7510   13.17
   -0.8012   12.80
   -0.8511   12.67
   -0.9011   12.65
   -0.9510   12.87
   -1.0010   13.30
```

```
-1.0509   13.83
-1.1008   14.48
-1.1508   15.27
-1.2010   16.13
-1.2510   17.14
-1.3012   18.24
-1.3513   19.39
-1.4015   20.54
-1.4523   21.68
-1.4927   22.78
999.99

                              CARD COUNT 0311
```

Table III: INTEGRATION OF DOUBLE LAYER CAPACITY For 1MKF

1MKF 25 DEG

E	q	γ	ξ	C	$1/C$	C^d	C^i	$1/C^i$	ϕ^{m-2}
E(V)	C(MC/CM2)	G(ERG/CM2)	XI(ERG/CM2)	C(MF/CM2)	1/C	CD	CI	1/CI	PHIM2
-0.4750	-0	-0.	0.	0.2638E 02	0.3791E-01	0.2285E 03	0.2982E 02	0.3353E-01	0.
-0.4376	1	-0.19	-4.56	0.2708E 02	0.3692E-01	0.2293E 03	0.3071E 02	0.3256E-01	0.3304E-01
-0.4012	2	-0.73	-8.76	0.2778E 02	0.3600E-01	0.2318E 03	0.3156E 02	0.3169E-01	0.6510E-01
-0.3654	3	-1.62	-12.59	0.2820E 02	0.3546E-01	0.2359E 03	0.3203E 02	0.3122E-01	0.9655E-01
-0.3302	4	-2.86	-16.07	0.2852E 02	0.3506E-01	0.2414E 03	0.3235E 02	0.3092E-01	0.1276E 00
-0.2953	5	-4.43	-19.19	0.2868E 02	0.3487E-01	0.2484E 03	0.3242E 02	0.3084E-01	0.1584E 00
-0.2604	6	-6.34	-21.97	0.2876E 02	0.3477E-01	0.2567E 03	0.3239E 02	0.3087E-01	0.1893E 00
-0.2257	7	-8.60	-24.40	0.2877E 02	0.3475E-01	0.2661E 03	0.3226E 02	0.3100E-01	0.2202E 00
-0.1909	8	-11.21	-26.48	0.2881E 02	0.3471E-01	0.2766E 03	0.3216E 02	0.3109E-01	0.2513E 00
-0.1562	9	-14.16	-28.22	0.2883E 02	0.3468E-01	0.2881E 03	0.3204E 02	0.3121E-01	0.2824E 00
-0.1216	10	-17.45	-29.61	0.2898E 02	0.3450E-01	0.3004E 03	0.3208E 02	0.3117E-01	0.3136E 00
-0.0873	11	-21.06	-30.65	0.2921E 02	0.3423E-01	0.3134E 03	0.3222E 02	0.3104E-01	0.3447E 00
-0.0532	12	-24.97	-31.36	0.2960E 02	0.3379E-01	0.3270E 03	0.3254E 02	0.3073E-01	0.3757E 00
-0.0197	13	-29.15	-31.72	0.3026E 02	0.3305E-01	0.3412E 03	0.3321E 02	0.3012E-01	0.4061E 00
0.0128	14	-33.55	-31.75	0.3134E 02	0.3191E-01	0.3559E 03	0.3436E 02	0.2910E-01	0.4358E 00
0.0441	15	-38.08	-31.47	0.3289E 02	0.3041E-01	0.3711E 03	0.3609E 02	0.2771E-01	0.4643E 00

```
INTEGRATION OF DOUBLE LAYER CAPACITY

 1MKF   25  DEG
 E(V)      W(MC/CM2)  G(ERG/CM2)  XI(ERG/CM2)  C(MF/CM2)     1/C           CD           CI           1/CI         PHIM2

 -0.4750   -0           -0.           0.          0.2638E 02   0.3791E-01   0.2285E 03   0.2982E 02   0.3353E-01   0.
 -0.5135   -1           -0.19         4.94        0.2550E 02   0.3922E-01   0.2293E 03   0.2869E 02   0.3486E-01  -0.3415E-01
 -0.5537   -2           -0.80        10.28        0.2438E 02   0.4101E-01   0.2318E 03   0.2725E 02   0.3670E-01  -0.6993E-01
 -0.5957   -3           -1.85        16.02        0.2324E 02   0.4303E-01   0.2359E 03   0.2578E 02   0.3879E-01  -0.1076E 00
 -0.6398   -4           -3.40        22.20        0.2205E 02   0.4535E-01   0.2414E 03   0.2427E 02   0.4121E-01  -0.1476E 00
 -0.6865   -5           -5.50        28.83        0.2088E 02   0.4790E-01   0.2484E 03   0.2279E 02   0.4387E-01  -0.1902E 00
 -0.7357   -6           -8.21        35.93        0.1976E 02   0.5061E-01   0.2567E 03   0.2141E 02   0.4671E-01  -0.2354E 00
 -0.7377   -7          -11.59        43.55        0.1376E 02   0.5330E-01   0.2661E 03   0.2018E 02   0.4954E-01  -0.2836E 00
 -0.8422   -8          -15.68        51.70        0.1792E 02   0.5580E-01   0.2766E 03   0.1916E 02   0.5218E-01  -0.3344E 00
 -0.8992   -9          -20.53        60.40        0.1722E 02   0.5806E-01   0.2881E 03   0.1832E 02   0.5459E-01  -0.3878E 00
 -0.9581   -10         -26.13        69.69        0.1674E 02   0.5974E-01   0.3004E 03   0.1773E 02   0.5641E-01  -0.4434E 00
 -1.0184   -11         -32.46        79.57        0.1646E 02   0.6077E-01   0.3134E 03   0.1737E 02   0.5758E-01  -0.5004E 00
 -1.0795   -12         -39.48        90.06        0.1632E 02   0.6127E-01   0.3270E 03   0.1718E 02   0.5821E-01  -0.5583E 00
 -1.1408   -13         -47.15       101.16        0.1632E 02   0.6126E-01   0.3412E 03   0.1714E 02   0.5833E-01  -0.6167E 00
 -1.2019   -14         -55.39       112.87        0.1646E 02   0.6075E-01   0.3559E 03   0.1726E 02   0.5794E-01  -0.6749E 00
 -1.2616   -15         -64.05       125.19        0.1691E 02   0.5912E-01   0.3711E 03   0.1772E 02   0.5643E-01  -0.7319E 00
 -1.3209   -16         -73.24       138.11        0.1697E 02   0.5892E-01   0.3866E 03   0.1775E 02   0.5633E-01  -0.7885E 00
 -1.3791   -17         -82.84       151.61        0.1736E 02   0.5759E-01   0.4025E 03   0.1815E 02   0.5510E-01  -0.8441E 00
 -1.4360   -18         -92.80       165.68        0.1779E 02   0.5620E-01   0.4197E 03   0.1858E 02   0.5381E-01  -0.8986E 00
 -1.4914   -19        -103.05       180.32        0.1829E 02   0.5466E-01   0.4352E 03   0.1910E 02   0.5237E-01  -0.9517E 00
 **0**      EOF READ ON UNIT 00005 --- EXECUTION TERMINATED
```

Table IV: Integration of Double-Layer-Capacity For .5 MKF

.5M KF

E E(V)	q Q(MC/CM2)	γ G(ERG/CM2)	ξ XI(ERG/CM2)	C C(MF/CM2)	1/C 1/C	C^d CD	C^i CI	$1/C^i$ 1/CI	ϕ^{m-2} PHIM2
-0.4740	-0	425.70	425.70	0.2510E 02	0.3984E-01	0.1616E 03	0.2972E 02	0.3365E-01	0.
-0.4348	1	425.51	421.15	0.2588E 02	0.3854E-01	0.1627E 03	0.3078E 02	0.3249E-01	0.3301E-01
-0.3966	2	424.93	417.00	0.2642E 02	0.3785E-01	0.1662E 03	0.3141E 02	0.3183E-01	0.5516E-01
-0.3590	3	423.99	413.22	0.2685E 02	0.3725E-01	0.1718E 03	0.3182E 02	0.3143E-01	0.9676E-01
-0.3220	4	422.70	409.82	0.2718E 02	0.3679E-01	0.1794E 03	0.3204E 02	0.3121E-01	0.1281E 00
-0.2854	5	421.05	406.78	0.2744E 02	0.3645E-01	0.1887E 03	0.3211E 02	0.3115E-01	0.1592E 00
-0.2490	6	419.05	404.11	0.2759E 02	0.3624E-01	0.1995E 03	0.3202E 02	0.3123E-01	0.1904E 00
-0.2129	7	416.70	401.80	0.2776E 02	0.3602E-01	0.2115E 03	0.3195E 02	0.3130E-01	0.2217E 00
-0.1770	8	414.01	399.85	0.2792E 02	0.3581E-01	0.2246E 03	0.3189E 02	0.3136E-01	0.2530E 00
-0.1413	9	410.97	398.25	0.2811E 02	0.3558E-01	0.2385E 03	0.3186E 02	0.3139E-01	0.2844E 00
-0.1059	10	407.61	397.03	0.2839E 02	0.3523E-01	0.2532E 03	0.3197E 02	0.3128E-01	0.3157E 00
-0.0708	11	403.93	396.14	0.2874E 02	0.3479E-01	0.2685E 03	0.3219E 02	0.3107E-01	0.3469E 00
-0.0363	12	399.96	395.61	0.2920E 02	0.3425E-01	.2843E 03	0.3254E 02	0.3073E-01	0.3778E 00

```
INTEGRATION OF DOUBLE LAYER CAPACITY

 .5M  KF
 E(V)     Q(MC/CM2)  G(ERG/CM2)  XI(ERG/CM2)  C(MF/CM2)    1/C          CD           CI           1/CI         PHIM2

 -0.4740   -0         425.70      425.70      0.2510E 02   0.3984E-01   0.1616E 03   0.2972E 02   0.3365E-01   0.
 -0.5144   -1         425.50      430.64      0.2436E 02   0.4104E-01   0.1627E 03   0.2865E 02   0.3490E-01  -0.3423E-01
 -0.5543   -2         424.87      435.99      0.2344E 02   0.4267E-01   0.1662E 03   0.2728E 02   0.3665E-01  -0.6999E-01
 -0.5998   -3         423.78      441.77      0.2246E 02   0.4452E-01   0.1718E 03   0.2584E 02   0.3870E-01  -0.1076E 00
 -0.6454   -4         422.18      448.00      0.2144E 02   0.4665E-01   0.1794E 03   0.2435E 02   0.4107E-01  -0.1475E 00
 -0.6932   -5         420.03      454.69      0.2039E 02   0.4903E-01   0.1887E 03   0.2287E 02   0.4373E-01  -0.1899E 00
 -0.7435   -6         417.26      461.87      0.1939E 02   0.5157E-01   0.1995E 03   0.2148E 02   0.4655E-01  -0.2350E 00
 -0.7964   -7         413.82      469.57      0.1849E 02   0.5407E-01   0.2115E 03   0.2027E 02   0.4934E-01  -0.2830E 00
 -0.8517   -8         409.67      477.81      0.1771E 02   0.5646E-01   0.2246E 03   0.1923E 02   0.5201E-01  -0.3336E 00
 -0.9092   -9         404.78      486.61      0.1708E 02   0.5854E-01   0.2385E 03   0.1840E 02   0.5435E-01  -0.3868E 00
 -0.9686   -10        399.13      496.00      0.1661E 02   0.6020E-01   0.2532E 03   0.1778E 02   0.5625E-01  -0.4422E 00
 -1.0294   -11        392.75      505.98      0.1633E 02   0.6124E-01   0.2685E 03   0.1739E 02   0.5752E-01  -0.4991E 00
 -1.0909   -12        385.68      516.59      0.1621E 02   0.6169E-01   0.2843E 03   0.1719E 02   0.5817E-01  -0.5570E 00
 -1.1525   -13        377.97      527.80      0.1624E 02   0.6158E-01   0.3005E 03   0.1717E 02   0.5825E-01  -0.6152E 00
 -1.2139   -14        369.69      539.64      0.1638E 02   0.6105E-01   0.3171E 03   0.1727E 02   0.5789E-01  -0.6733E 00
 -1.2745   -15        360.90      552.08      0.1662E 02   0.6016E-01   0.3341E 03   0.1749E 02   0.5717E-01  -0.7309E 00
 -1.3341   -16        351.67      565.12      0.1697E 02   0.5894E-01   0.3512E 03   0.1783E 02   0.5610E-01  -0.7875E 00
 -1.3924   -17        342.05      578.75      0.1736E 02   0.5761E-01   0.3687E 03   0.1822E 02   0.5490E-01  -0.8430E 00
 -1.4492   -18        332.11      592.97      0.1739E 02   0.5591E-01   0.3863E 03   0.1876E 02   0.5332E-01  -0.8972E 00
 **0**      EOF READ ON UNIT 00005 --- EXECUTION TERMINATED
```

Table V: Input Cards for Program II.

```
+9 +4.0-0.4750
4.0  -16.07-0.3302 0.2852E 02 0.3245E 02
4.0  -18.26-0.0050-0.3932 0.4158E 02
4.0  -19.47 0.0100-0.4147 0.4435E 02
4.0  -21.05-0.0200-0.4381-0.4642E 02
4.0  -22.63 0.0400-0.4606 0.4782E 02
4.0  -25.36 0.1000-0.4931 0.4892E 02
4.0  -27.95 0.2000-0.5189 0.4922E 02
4.0  -30.52 0.4000-0.5424 0.4909E 02
4.0  -33.15 0.8000-0.5638 0.4846E 02
4.0  -34.57 1.0000-0.5732 0.4859E 02
                                          CARD COUNT 0024
```

Table VI: Output of the Program II.

```
CHARGE=  4.0
XI=(-0.3441E 02)+(-0.1771E 02)X+(-0.4309E 01)X2+(-0.4577E-02)X3
                                                                  d                  1            b       2          m-2
  X          ln X      q^r      Φ        ln Φ      ξ                 C                -Δ-           E-E         φ          φ
                                                                                       C
  CON        LNCON     QSA      SP       LSP       XI        DIFF    CD               DC            DE          PHI2       PHIM-2     X(I)
   0.0050   -5.2983    -6.00     2.19    0.7839   -18.26    -0.02    0.2318E 03    0.1101E-01    0.0630    -0.0087     0.0905   -1.3611
   0.0100   -4.6052    -7.53     3.40    1.2238   -19.47    -0.01    0.2386E 03    0.1252E-01    0.0845    -0.0153     0.0756   -1.1831
   0.0200   -3.9120    -9.06     4.96    1.6014   -21.03     0.07    0.2489E 03    0.1352E-01    0.1079    -0.0216     0.0585   -1.0050
   0.0400   -3.2189   -10.59     6.56    1.8810   -22.63    -0.08    0.2621E 03    0.1415E-01    0.1304    -0.0276     0.0420   -0.8269
   0.1000   -2.3026   -12.62     9.29    2.2289   -25.36    -0.08    0.2836E 03    0.1462E-01    0.1629    -0.0350     0.0169   -0.5915
   0.2000   -1.6094   -14.15    11.88    2.4749   -27.95     0.12    0.3022E 03    0.1475E-01    0.1887    -0.0402    -0.0037   -0.4135
   0.4000   -0.9163   -15.68    14.45    2.6707   -30.52     0.04    0.3226E 03    0.1469E-01    0.2122    -0.0452    -0.0222   -0.2354
   0.8000   -0.2231   -17.21    17.12    2.8402   -33.19    -0.22    0.3443E 03    0.1443E-01    0.2336    -0.0498    -0.0390   -0.0573
   1.0000    0.       -17.71    18.50    2.9178   -34.57     0.16    0.3516E 03    0.1440E-01    0.2430    -0.0512    -0.0470    0.
 **0**          EOF READ ON UNIT 00005 --- EXECUTION TERMINATED
```

Table VII: Input Cards for Program V.

```
0.0050 4.0 94.39
0.0100 4.0 91.60
0.0200 4.0 88.97
0.0400 4.0 86.48
0.1000 4.0 83.39
0.2000 4.0 81.21
0.4000 4.0 79.14
0.6000 4.0 77.16
1.0000 4.0 76.54
 4.0  -16.07-0.3302 0.2852E 02 0.3235E 02
-1.1335 4.0 0.0050
-1.2290 4.0 0.0100
-1.2990 4.0 0.0200
-1.3448 4.0 0.0400
-1.3671 4.0 0.1000
-1.3552 4.0 0.2000
-1.3182 4.0 0.4000
-1.2566 4.0 0.8000
-1.2309 4.0 1.0000
 0.0050 -6.00   2.19 0.2318E 03 0.1101E-01 0.0630 0.4158E 02  4.0 0.9054E-01
 0.0100 -7.53   3.40 0.2386E 03 0.1252E-01 0.0845 0.4435E 02  4.0 0.7556E-01
 0.0200 -9.06   4.96 0.2489E 03 0.1352E-01 0.1079 0.4642E 02  4.0 0.5845E-01
 0.0400-10.59   6.56 0.2621E 03 0.1415E-01 0.1304 0.4782E 02  4.0 0.4196E-01
 0.1000-12.62   9.29 0.2836E 03 0.1462E-01 0.1629 0.4892E 02  4.0 0.1690E-01
 0.2000-14.15  11.88 0.3022E 03 0.1475E-01 0.1867 0.4922E 02  4.0-0.3657E-02
 0.4000-15.68  14.45 0.3226E 03 0.1469E-01 0.2122 0.4909E 02  4.0-0.2224E-01
 0.8000-17.21  17.12 0.3443E 03 0.1443E-01 0.2336 0.4846E 02  4.0-0.3903E-01
 1.0000-17.71  18.50 0.3516E 03 0.1440E-01 0.2430 0.4839E 02  4.0-0.4701E-01
                                                                CARD COUNT 0041
```

Table VIII Printed Output of Program V.

c^d $\left(\frac{\partial q^1}{\partial q}\right)_\mu$ c^1 $\left(\frac{\partial q}{\partial \phi_{m-2}}\right)_q^1$ $\left(\frac{\partial q^1}{\partial \phi_{m-2}}\right)_q$ $-\Delta \frac{1}{c^1}$

```
Q=  4.0
CON       C            CD           DQSA          CI           DQPHI        DQSPHI       DCI
 0.0050   0.4158E 02   0.2318E 03   -0.1133E 01   0.4061E 02   0.2730E 02   0.9439E 02   0.6286E-02
 0.0100   0.4435E 02   0.2386E 03   -0.1229E 01   0.4254E 02   0.2708E 02   0.9160E 02   0.7404E-02
 0.0200   0.4642E 02   0.2489E 03   -0.1299E 01   0.4397E 02   0.2678E 02   0.8897E 02   0.8168E-02
 0.0400   0.4782E 02   0.2621E 03   -0.1345E 01   0.4499E 02   0.2647E 02   0.8648E 02   0.8685E-02
 0.1000   0.4892E 02   0.2836E 03   -0.1367E 01   0.4601E 02   0.2623E 02   0.8339E 02   0.9176E-02
 0.2000   0.4922E 02   0.3022E 03   -0.1355E 01   0.4653E 02   0.2619E 02   0.8121E 02   0.9420E-02
 0.4000   0.4909E 02   0.3226E 03   -0.1318E 01   0.4682E 02   0.2631E 02   0.7914E 02   0.9555E-02
 0.8000   0.4846E 02   0.3443E 03   -0.1257E 01   0.4677E 02   0.2655E 02   0.7716E 02   0.9530E-02
 1.0000   0.4839E 02   0.3516E 03   -0.1231E 01   0.4690E 02   0.2674E 02   0.7654E 02   0.9590E-02
**0**     EOF READ ON UNIT 00005 --- EXECUTION TERMINATED
```